MARCH
5-7
2023

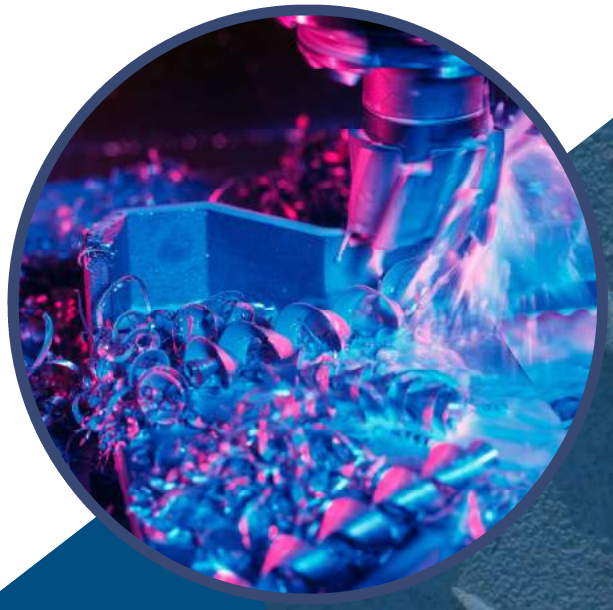

PROCEEDINGS

OF THE INTERNATIONAL CONFERENCE ON INDUSTRY, ENGINEERING & MANAGEMENT SYSTEMS

IEMS
2023
#29

ISSN 2690-3210 (Print)
ISSN 2690-3229 (online)

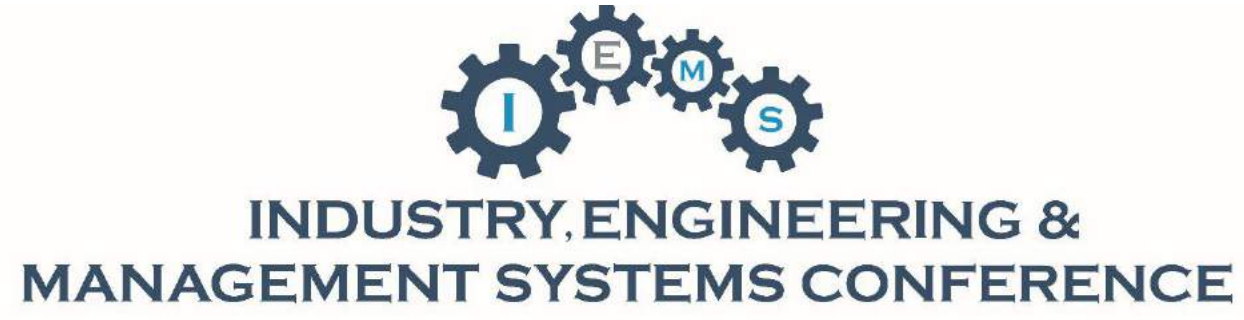

March 5 - 7, 2023

Dear Conference Participants:

It is with pleasure that we present to you the Proceedings of the 29th International Conference on Industry, Engineering and Management Systems (IEMS). The papers presented this year consistently represented high quality scholarship in the authors' respective fields. The papers covered a wide range of topics in the business and engineering disciplines, integrating concepts that further the mission of the IEMS Conference.

We present these Proceedings to you to enable your own thought leadership so that you may share your presentations and papers in the future at our IEMS conference.

These proceedings would not have been made possible without the valuable contributions of our Track Chairs and reviewers for the time and effort they spent reviewing the papers.

We look forward to seeing you virtually at IEMS 2024! Warm Regards,

Wilfredo Moscoso- Kingsley, PhD
Proceedings Editor

2023 IEMS Officers

Gamal Weheba, Conference Chair
Wichita State University

Hesham Mahgoub, Program Chair
Erigeosciences, Inc

Dalia Mahgoub, Technical Director
Lockheed Martin, Florida

Ed Sawan, Publications Editor
Wichita State University

Wilfredo Moscoso, Proceedings Editor
Wichita State University

Abdulaziz G. Abdulaziz, Associate Editor
Wichita State University

Track Chairs

Additive Manufacturing
Krishna Krishnan, Wichita State University

Artificial Intelligence and Machine Learning
Hongsheng He, Wichita State University

Automation, Modeling and Simulation
Andrzej Gapinski, Penn State University

Business Analytics
John Wang, Montclair State University
Sue Abdinnour, Wichita State University

Complex Systems- Performance Assessment & Improvement
Wilfredo Moscoso-Kingsley, Wichita State University

Education Leadership
Abdelnasser Hussein, University of Houston-Downtown

Education & Training
Abdulaziz G. Abdulaziz, Wichita State University

Human Factors & Cognitive Engineering
Deborah Carstens, Florida Institute of Technology

Track Chairs

Innovation Management
Abram Walton & Darrel Sandall, Florida Institute of Technology

Lean Systems
Deepak Gupta, Wichita State University

Management of Technology
Arpita Jadav, Jacksonville University

Marketing
Scott Swain, Clemson University

Nanomaterials & Nanoengineering
Eylem Asmatulu, Wichita State University

Quality Planning & Process Improvement
Roger Merriman, Wichita State University

Supply Chain Management & Logistics
Ewa Rudnicka, University of Pittsburgh

Sustainability & Industry 4.0
Mehmet Yildirim, Wichita State University

Reviewers

Junyong Ahn
Mohammed Ali
Gordon Arbogast
Ramazan Asmatulu
LuAnn Bean
Roelof deVries
Roelof deVries
Amelia Falcon
Andrzej Gapinski
Byul Hur
Abdelnasser Hussein
Xiaochun (Steven) Jiang
Robert Keyser
Krishna Krishnan
Jingyun Li
Ti Lin Liu
Adam Lynch
Holger Mauch
Roger Merriman
Narasimha Nagaiah
Dennis Ridley
Scott Swain
Dennis Tribby
Rick Wallace
Abram Walton
Gwen White
Xun Xu

Table of Contents

Finding Relationship Between Alzheimer's Disease and Noise in Electroencephalogram (EEG) Data Using Novel Machine Learning (ML) Algorithms

Nihar Mudigonda[1]
[1]*Rocklin High School*
5301 Victory Lane, Rocklin, CA 95765
nihar.mudigonda@gmail.com

Abstract

Alzheimer's disease (AD) is a neurodegenerative disease affecting an estimated 6.5 million Americans and is expected to double in the next thirty years. The only treatments that patients can receive for the disease are to slow the disease progression, which is more effective if the disease is diagnosed early. A popular form of early diagnosis used by doctors is to analyze the brain's electroencephalogram (EEG). EEG measures electrical activity by placing electrodes on the scalp or surgically placing electrodes inside the brain. Given the electrical activity measurements of the brain, high and low-frequency signals are traditionally filtered during preprocessing as previously believed to be noise or irrelevant information. However, we believe this filtered data contains valuable information that can help doctors diagnose Alzheimer's patients earlier. We use novel machine learning models, such as transformers, and additionally use metrics such as accuracy, precision, recall, and F1 score to evaluate the model performance. Our methods result in higher accuracy compared to current machine learning methods. Our best-performing transformer resulted in an accuracy of 0.846, while the best-performing non-transformer model resulted in an accuracy of 0.564.

Keywords:.

1. Introduction

Alzheimer's disease (AD) is the sixth leading cause of death and the most prevalent kind of dementia. The disease affects over 50 million people worldwide and over 6 million in the United States alone[1]. Care for Alzheimer's disease patients in the US costs $321 Billion and is on track to be over $1 trillion by 2050[11]. Despite the current heavy costs, the number of people affected by Alzheimer's disease is expected to triple in thirty years if no new innovations are created[26].

Alzheimer's disease interferes with the transmission of electrical signals between neurons, causing cells to die and lose function. Some of the hallmarks of Alzheimer's disease are plaques of beta-amyloid, tangles of tau proteins, and a compromised blood-brain barrier.

The first hallmark, beta-amyloid, is a protein that is naturally found in the brain; however, its normal function is not well understood[2]. The beta sheets found in the beta-amyloid molecule often form together, and over time, these small formations become plaques connecting to nerve cell receptors.

Submitted: March 21, 2023
Revised: December 12, 2023

These plaques destroy the communication of nerve cells, hindering all critical brain functions. The second hallmark of Alzheimer's disease involves finding tangles of tau proteins. Inside neurons, a structure called microtubules transports substances to other parts of the neurons. Usually, tau proteins stabilize the microtubules by attaching to them[27]. When there is a large amount of beta-amyloid plaques, tau proteins start to remove themselves from microtubules and attach to themselves. These tangles obstruct communication between neurons[23]. The third hallmark of Alzheimer's disease involves a compromised blood-brain barrier. One of the genes known as TREM2 instructs microglial cells to clean unnecessary substances and clumps of protein, such as beta-amyloid. Patients with Alzheimer's have dysfunctional TREM2, which causes glial cells to clean the brain improperly. The malfunctioning glial cells cause additional plaque buildup and excretion of damaging chemicals that lead to inflammation[3].

Beyond studying the hallmarks, scientists are researching new ways to cure Alzheimer's. Varesi et al. published a review that examined claims that restoring gut microbiota with probiotics or other interventions will help stop the neurodegenerative effects of Alzheimer's. The current results are inconclusive for effective treatment[14]. Johri states that restoring mitochondrial bioenergetics via antioxidants will reduce the amount of beta-amyloid. This form of therapy can potentially be used to treat Alzheimer's disease[4].

One way that scientists are able to diagnose the early onset of Alzheimer's is by analyzing a patient's EEG data. We select the EEG dataset from the THINGS database as a baseline. Due to the volume and diversity of the individuals, the THINGS dataset serves as good data for pre-training to compare against individuals with known diseases. Additionally, it is assumed that all individuals who participated in data collection are healthy individuals[8].

In order to evaluate our experiment in diagnosing Alzheimer's, we use the Data from: Quantile Graphs for EEG-Based Diagnosis of Alzheimer's Disease dataset. This dataset is good for training and testing as the patients in the dataset have been organized based on mental disorders and provide easy-to-use data. The authors analyzed Alzheimer's patients with open and closed eyes, as well as how well quantile graphs, perform to discriminate which electrode placement gives the most information. Beyond that, the authors also analyzed the alpha, beta, delta, and theta waves to show the distinction between Alzheimer's and healthy patients[9]. We will compare our results to their quantile graphs.

It is essential that patients are diagnosed early so they have a higher chance of receiving a successful treatment. We summarize a few works whose aims are to diagnose Alzheimer's disease.

An early work using machine learning methods is from Kumar, Sharma, and Tsunoda. They use an LSTM model with Linear Discriminant Analysis (LDA) for feature reduction and Constraint satisfaction problems for classifying different motor movements, such as left vs. right-hand movements[5]. Constraint satisfaction problems (CSP) gather data that satisfy certain constraints, which reduces the amount of data available to be inputted. However, a large dataset is required to generalize to a diverse population of patients. The experiment's highest accuracy on a single dataset is 82.52%, and the dataset only contained four human subjects.

One of the earliest studies which combined deep learning on EEG was done by Lawhern et al., who

proposed EEGNet: a discriminative deep learning model that uses a Convolutional Neural Network (CNN) to classify EEG signals. The study extracts well-known features from the EEG data collected through various Brain-Computer Interface (BCI) paradigms[6]. Our experiment uses raw EEG data as input, which is different since CNNs need well-cleaned data to perform well.

Meghdadi et al. investigate the relationship between Alzheimer's disease and features in resting-stage EEG. The authors claim that as the disease generally occurs in older individuals, we must consider the brain changes that come with old age. This is why patients with Alzheimer's, mild cognitive impairment (MCI), and healthy patients ranging from age 18-90 were used for EEG data collection. However, there are a few key caveats in this study. The patients with Alzheimer's and MCI in the dataset were diagnosed at various labs, and each location has a different criterion for diagnosis. In addition, it is unsure whether the MCI patients developed Alzheimer's later on. The EEG data was analyzed for abnormalities that correlate to Alzheimer's. But, the data may have a similar relationship with other forms of dementia, which was not assessed in this study[7].

It is very difficult to get data in this domain because we want to ensure patient privacy however, that privacy comes at the cost of the reproducibility of research. It is difficult to verify, repeat, or even progress on other disease-based research if all patient data is kept private. We use datasets where all patient information has been scrubbed to develop this ethically.

While other machine learning models have been previously used, such as LSTMs and CNNs, a difficulty with all of them has to do with the sheer size of the input. Transformers are one of the latest machine learning models with superior capabilities compared to the previous models, but they also face similar difficulties in processing long inputs. To overcome this issue, we propose several methods, such as processing overlapping input sequences and long signals in a compressed Fourier domain. Ultimately, we decided to use the transformer, specifically DistilBERT. We plan to pre-train the model on 50 patients from the THINGS dataset before fine-tuning it for Alzheimer's disease detection. We have also adapted a novel pre-training scheme for EEG data, whereby the model is trained to predict the next X seconds of EEG. We experiment with different values of X, such as 1, 2, and 5 seconds. We expect the model to significantly outperform the current state of the art for Alzheimer's disease detection.

2. Hypothesis

This experiment is guided by multiple hypotheses:

(1) If we use transformers, we will be better able to predict the onset of Alzheimer's compared to other machine learning algorithms.
(2) If we analyze EEG data abnormalities, then we will find deeper and more meaningful relationships to Alzheimer's when compared to filtered EEG data.

3. Materials List

3.1. Datasets

The baseline EEG dataset we use is from the THINGS database, which is a collection of various brain datasets and enjoys the benefit of being collaborated on by multiple scientists worldwide. The THINGS database uses the dataset Human electroencephalography recordings from 50 subjects for 22,248

images from 1,854 object concepts (OpenNeuro Accession Number ds003825). In the dataset, 50 people were presented with images of various objects, and their brain responses were recorded via Electroencephalogram (EEG)[8].

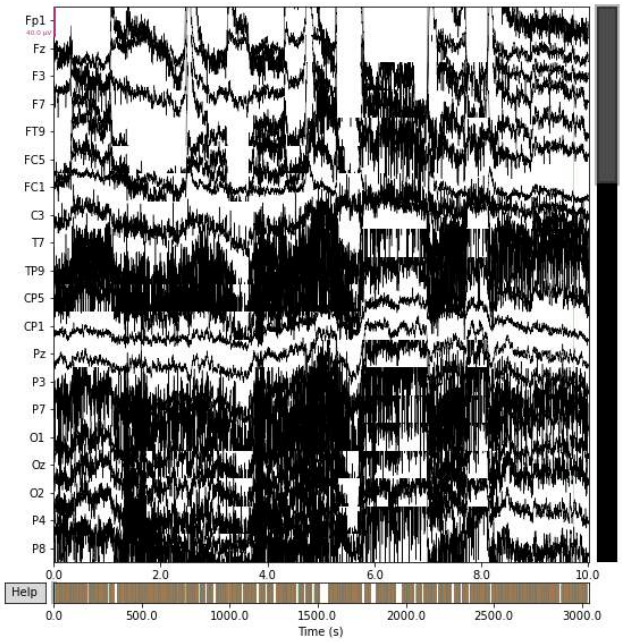

Figure 1: Raw EEG data for User 1 for the duration of the experiment[8]

The dataset Data from: Quantile Graphs for EEG-Based Diagnosis of Alzheimer's Disease is used to measure the experiment's success since it contains EEG from Alzheimer's patients. The database is designed by Florida State University scientists and contains four sets of data: Set A and Set B are considered control groups and contain EEG data from twenty-four senior citizens with no neurological disorders. In contrast, Set C and Set D contain EEG data from twenty-four individuals who potentially have Alzheimer's disease based on a few criteria[9].

3.2. Hardware

The computer used in this experiment is a Lenovo Yoga C940-15IRH (product number: 81TE0000US) with Microsoft Windows 11 Pro as the OS. The internals include an Intel Core i7-9750H @ 2.60GHz with 16GB of DDR4 physical memory and 512GB solid-state drive (SSD). The computer also has NVIDIA GeForce GTX 1650 with Max-Q Design as the graphics card.

3.3. Software

The programming for the experiment is done on the cloud via Google Colab. The datasets and code will be easily integrated as they are both connected through Google Suite.

The programming language of choice is Python 3.9.2. More specifically, we will use the Numerical Python (NumPy), PyTorch, TensorFlow, MNE, Matplotlib, Sci-Kit Learn, and SciPy libraries during the experiment. Each library used allows the code to execute faster or work with the dataset in ways that weren't possible before:

- The NumPy library is used to work with numerical data. The library is used to create multi-dimensional arrays and matrices, which are faster and more compact than the standard Python equivalent.
- The MNE library contains all of the functions needed to work with Brainvision data and graph it. The EEG data is imported and worked on via this library.
- The PyTorch, TensorFlow, and Sci-Kit Learn libraries are used to build this experiment's various novel machine-learning models. Some examples of machine learning models that are implemented include K-Nearest Neighbors (KNN), Neural Networks, Linear Regression, and Long Short-Term Memory (LSTM).

4. Procedural Steps

4.1. Loading

First, the entire baseline and Alzheimer's dataset is downloaded and stored online on Google Drive. The datasets are then loaded from the cloud to Google Colab for pre-training the models. Then, we the model with the baseline dataset and part of the Alzheimer's dataset. From the Alzheimer's dataset, Sets A and B have data from mentally healthy patients, and Sets C and D have data from potential Alzheimer's patients. We train the model with Set A and Set C. We test our model with Set B and Set D since there is no overlap between the four sets.

4.2. Cleaning

We perform minimal data pre-processing such as normalization of the dataset, so that large values aren't given a higher weightage when the model is training. We experiment with compressing the data before inputting, which saves space and time when running the program. We choose to minimally pre-process the data as it may remove valuable information that will benefit our model. Instead, we feed raw data into the model to let the algorithm decide the weight of each feature in the dataset.

4.3. Algorithms Selection

We use a pre-trained DistilBERT model[19] before fine-tuning on the Alzheimer's dataset. Then, we implement other machine learning algorithms to serve as baselines, such as LSTM, logistic regression, and other standard models.

(1) Transformers

(a) Overview

Transformers are a novel deep-learning algorithm that has not been previously used on EEG data for Alzheimer's disease detection. The model we will be using will be pre-trained with the EEG data, and the training task is to predict what will happen next in the EEG. Then, the model is fine-tuned for the classification of Alzheimer's disease. This model adopts the mechanism of self-attention, differentially weighting the significance of each part of the input data. Self-attention is a mechanism by which models learn to focus (or pay more attention) on some signals and ignore others[18].

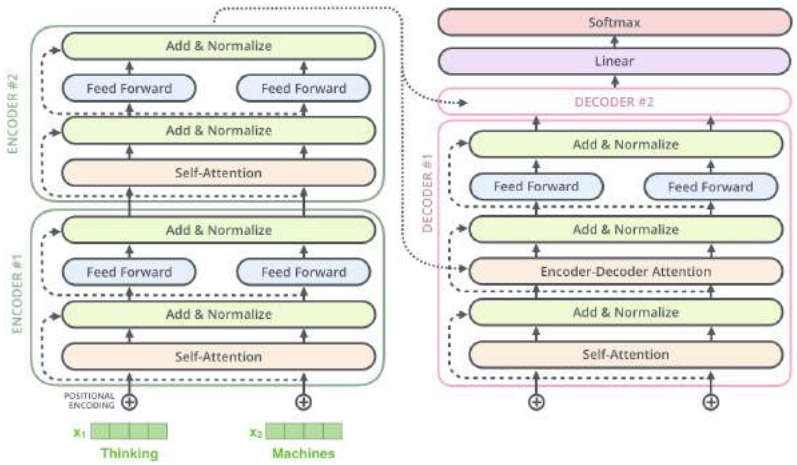

Figure 2: Architecture of Transformer[20]

(b) Neurons

Transformers are a type of neural network, and their basic unit is a neuron. Paola and Schowengerdt state that a neural network has processing nodes where the values of its inputs are processed, and an output is given. At the beginning of the network, there is an input layer where the data is inputted into the neural network. This data is passed onto a new layer of nodes to be processed, and so on. The end of a neural network, where the output is given, is called the output layer. The processing layers between the input and output layers are called hidden layers [15].

Inside the nodes, the input values are added together and passed to an activation function. The result from this activation function is the output of that node. Each connection between nodes has a weight, and inputs are multiplied by the weight.

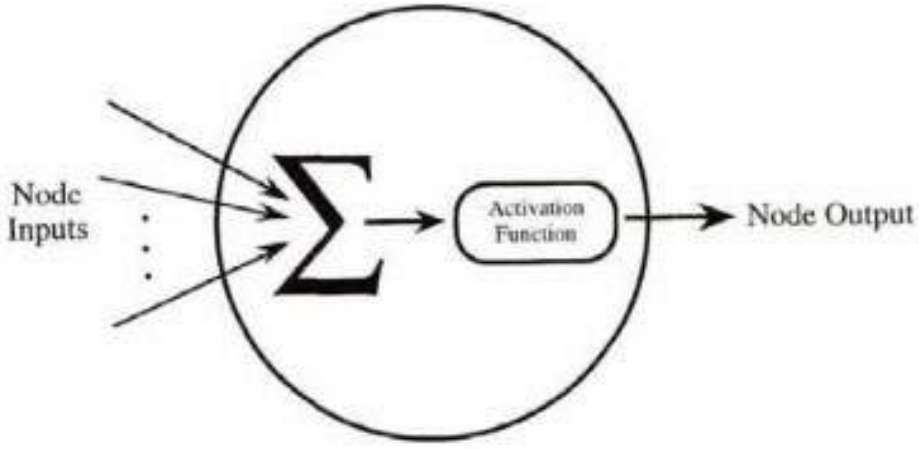

Figure 3: Inside a processing node [15]

In our transformer, we will be using an activation function. An activation function is an equation that is attached to each neuron and gives an output. It is used when many inputs to a neuron must be turned into an output. In this experiment, we will use a GeLU (Gaussian Error Linear Unit), which is a function

that approximates a normal distribution with the function of $x \cdot P(X \leq x)$, where P is the probability of x compared to the normal distribution. More formally, the equation can be expanded as the following $x \cdot 1/2\ [\ 1 + \text{erf}(x/\sqrt{2})]$ where erf is known as the error function, it can be computed by integrating the standard normal function[16].

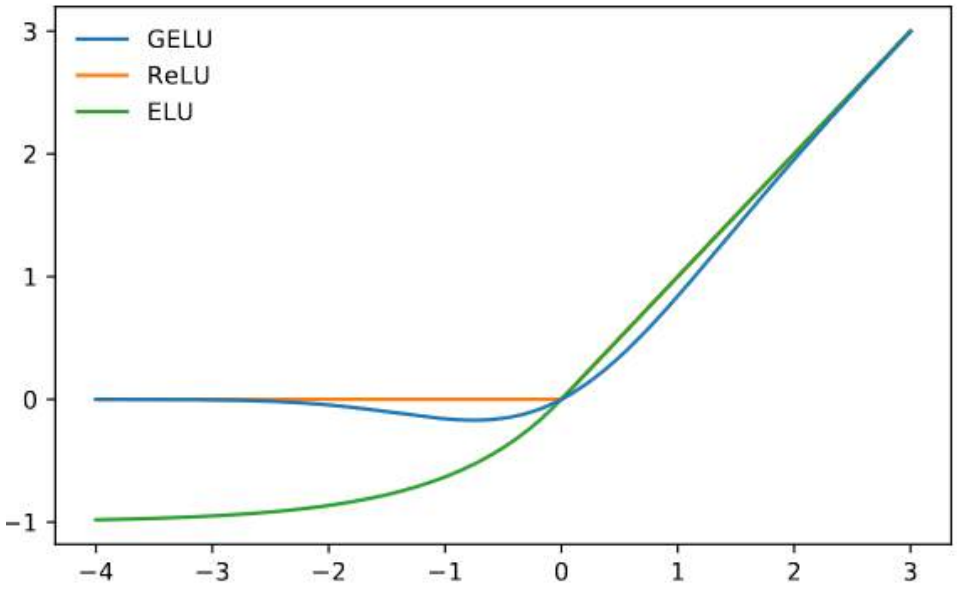

Figure 4: GeLU, ReLU, and ELU Function[16]

The GeLU activation function tends to outperform the rectified linear unit (ReLU) function and the exponential linear unit (ELU) function when used for deep learning classification tasks, such as our experiment [16].

(c) Self-Attention

Given the basic units described above, the only basic building block missing is how the input is processed before sending it through each layer of neurons. The formula for "self-attention" is as follows x^T @ (Q @ K^T) @ x where x is the input, K and Q are learnable neurons, @ is matrix multiplication and ^T is the transpose function. K and Q are referred to as key and query matrices, respectively[10]. Part of the intuition behind this is that neural networks perform best on discrete data, and this works to convert the continuous functions into discrete representations.

(d) Layers

(i) Encoder

The initial layer in the transformer is composed of a self-attention module, followed by the addition of the outputs with the inputs. The result of that addition is normalized. After applying the normalization, we then apply a linear layer which is a layer of neurons that perform the dot product. A linear layer corresponds to a set of neurons, all of which receive the same inputs, and each neuron contains its own independent set of learnable weights. The result from 1 neuron is 1 output, so to keep

the dimensionality consistent between inputs and outputs, we use the same number of neurons as inputs. Thus, the length of the linear layer is equal to the length of the input.

For the subsequent layers following the initial layer, the only difference is that input being used does not come from the initial data. Instead, the input will be from the previous layer, i.e., the previous encoder. The remaining operations in the encoder are the same even as you increase in layers of encoders.

(ii) Decoder

The decoder portion of the module is very similar to the encoder. The key differences in the decoder are that instead of taking in information from the input data, the information comes in from the encoder. The other main difference involves masking. Given a whole sequence, the decoder masks out "future" information when making its prediction about what comes next in the signal.

(e) Classification

The outputs of a neural network can sometimes be negative or greater than one, which makes them hard to interpret. This is why the raw output values are sent to a softmax layer. We will use the softmax function, as seen in Formula 1, to convert the output to a valid probability distribution where all values are between zero and one. The sum of all probabilities is equal to one. Probabilities are easier to interpret as well, which is a useful feature.

$$\sigma(\vec{z})_i = \frac{e^{z_i}}{\sum_{j=1}^{K} e^{z_j}}$$

Formula 1: Softmax Function

Here are definitions of some machine learning models we will be using:

Long Short-Term Memory (LSTM): a deep-learning algorithm that passes data through parts of the algorithm in a recursive manner. EEG data will be approximated into one dimension and then inputted into the model[12]. The three best-performing LSTM models from Hong et al.'s paper are replicated in this experiment[22]. The specification of each model is shown in Table 1. Each LSTM is named based on the number of fully connected nodes and the number of LSTM layers.

	Fully Connected	LSTM Cell Number	LSTM Layer Number
LSTM_512_2	512	128	2
LSTM_1024_2	1024	128	2
LSTM_512_4	512	128	4

Table 1: Specifications of Each LSTM Model

Logistic Regression: a simple machine-learning algorithm that predicts the binary output value based on given input variables. In this experiment, key features of the EEG data, such as range, frequency, and other statistical values, will be extracted for input [13].

4.4. Results Collection

In order to measure the success of our experiment, we use multiple performance metrics and visualization tools. Each classification done by the model can be labeled as true positive (TP), true negative (TN), false positive (FP), and false negative (FN). Various combinations of these values are used to calculate performance metrics. Each metric has a specific benefit and provides a unique insight into how the model is performing.

- Accuracy: this performance metric measures the number of correct classifications versus the total number of classifications. This metric may not be the best choice if the dataset is heavily imbalanced.

$$Accuracy = \frac{TN + TP}{TN + TP + FN + FP}$$

Formula 2: Accuracy Formula

- Precision: this performance metric measures the number of correct class classifications to the number of times an input was labeled that specific class. This metric provides insight into each class and is useful in assessing imbalanced datasets.

$$Precision = \frac{TP}{TP + FP}$$

Formula 3: Precision Formula

- Recall: this performance metric measures how often a specific class is classified correctly. This metric provides insight into the overlap between the detection of different classes.

$$Recall = \frac{TP}{TP + FN}$$

Formula 4: Recall Formula

- F1 Score: this performance metric takes the harmonic mean of precision and recall. It is more sensitive to accurately represent model performance in an imbalanced dataset.

$$F1\ Score = 2 \cdot \frac{Precision \cdot Recall}{Precision + Recall}$$

Formula 5: F1 Score Formula

- Confusion Matrix: A matrix where both the rows and columns entries are the classes and the entries represent for a given class what the model predicts. It shows where the model gets confused between different classes. In our case, it would be a two-by-two matrix highlighting the type 1 and type 2 errors. Type 1 and 2 refer to how often the model misclassified Alzheimer's as healthy and vice-versa.

In addition, we will compare our results to other explored machine learning models to validate the significance of our model. We will also compare the success of our model when changing parameters in the transformer, such as activation function, number of encoders/decoders, and normalization techniques. The runtime will also be noted to check for our model's efficiency.

5. Results

Here is a table with each model's accuracy, precision, recall, F1 score, and mAUC:

	Accuracy	Precision	Recall	F1 Score	mAUC
DistilBERT	0.846	0.778	0.846	0.845	0.804
LSTM_512_2	0.564	0.536	0.564	0.563	0.572
LSTM_1024_2	0.496	0.498	0.496	0.349	0.565
LSTM_512_4	0.522	0.512	0.522	0.504	0.552
Logistic Regression	0.542	0.522	0.542	0.521	0.553

Table 2: Results of Each Model

The most accurate DistilBERT had an accuracy of 0.846. Figure 5 is the confusion matrix for this transformer. Precision was the lowest metric, with the model having a sizable false positive rate.

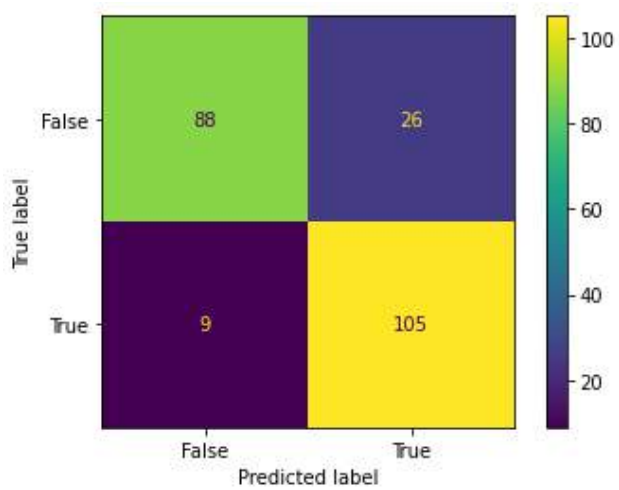

Figure 5: Confusion Matrix of DistilBERT

The most accurate LSTM model had an architecture of 512, 512, 128, 128, and 1 node in each layer, respectively. The accuracy of this neural network was 0.564. Figure 6 is the confusion matrix for this LSTM. The model was not very precise, with a high false negative rate.

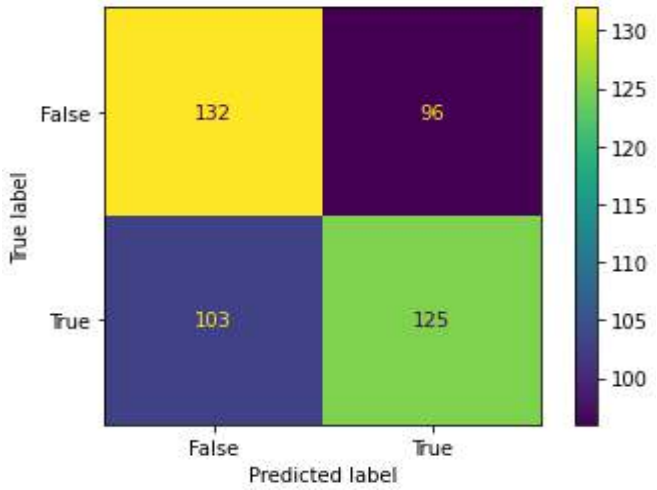

Figure 6: Confusion Matrix of Most Accurate LSTM Model

The logistic regression model had an accuracy of 0.542, which was the lowest of all models used in this experiment. Figure 7 is the confusion matrix for the logistic regression. The model had a high false positive rate.

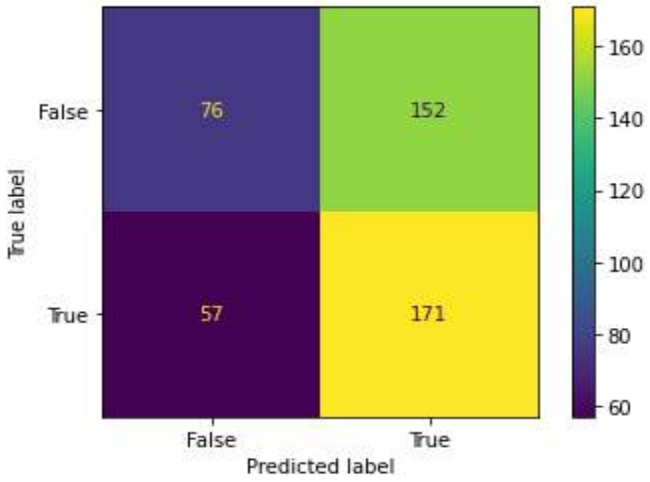

Figure 7: Confusion Matrix of Logistic Regression

6. Discussion and Conclusions

Using transformers for early diagnosis of Alzheimer's disease results in significantly higher performant across all metrics when compared to models in similar works.[23]. LSTM uses hidden state and cell state vectors to generate the output of the model given an input sequence. In contrast, transformers use a self-attention mechanism to process sequences as a whole. LSTM processes data in

order; however, we hypothesize that the ordering of the data is less important in how Alzheimer's symptoms present themselves in EEG data. This is why we predict transformers are a better fit for diagnosis.

This research can be expanded to diagnose other forms of dementia, such as Parkinson's Disease, Korsakoff Syndrome, and Huntington's Disease. Additionally, other forms of body data, such as heart rate and blood pressure, can be included in future experiments [24].

EEG collection devices are often expensive and difficult to operate. This creates a gap in accessible devices that consumers can operate. Affordable EEG collection devices available to consumers are not as accurate as medical-grade devices[25]. In the future, we propose creating an Arduino-based EEG collection device that is able to process accurate and precise data from twelve brain channels. This device is inspired by Dhillon et al.'s device[21]. This will allow EEG research to be conducted outside a lab, broadening the scope of EEG-based research.

Our novel experiment tests how effectively each algorithm is diagnosing Alzheimer's Disease using EEG data. Our findings show that transformers outperform algorithms that other research papers have used. The accuracy at which DistilBERT can diagnose Alzheimer's is 0.846, enabling Alzheimer's patients to be diagnosed more accurately and giving more time for prevention before the disease noticeably progresses.

7. Bibliography

1. Alzheimer's Association. 2022 Alzheimer's Disease Facts and Figures. Alzheimers Dement 2022;18.
2. Hiltunen M, van Groen T, Jolkkonen J (2009). "Functional roles of amyloid-beta protein precursor and amyloid-beta peptides: evidence from experimental studies". Journal of Alzheimer's Disease. 18 (2): 401–12. doi:10.3233/JAD-2009-1154. PMID 19584429
3. National Institute on Aging. (2017). What Happens to the Brain in Alzheimer's Disease?
4. Johri A. (2021). Disentangling Mitochondria in Alzheimer's Disease. International journal of molecular sciences, 22(21), 11520. https://doi.org/10.3390/ijms222111520
5. Kumar, S., Sharma, A. & Tsunoda, T. Brain wave classification using long short-term memory network based OPTICAL predictor. Sci Rep 9, 9153 (2019). https://doi.org/10.1038/s41598-019-45605-1
6. Lawhern, V. J., Solon, A. J., Waytowich, N. R., Gordon, S. M., Hung, C. P., & Lance, B. J. (2018). EEGNet: a compact convolutional neural network for EEG-based brain-computer interfaces. Journal of neural engineering, 15(5), 056013. https://doi.org/10.1088/1741-2552/aace8c
7. Meghdadi, A. H., Stevanović Karić, M., McConnell, M., Rupp, G., Richard, C., Hamilton, J., ... & Berka, C. (2021). Resting state EEG biomarkers of cognitive decline associated with Alzheimer's disease and mild cognitive impairment. PloS one, 16(2), e0244180.
8. Grootswagers, T., Zhou, I., Robinson, A.K. et al. Human EEG recordings for 1,854 concepts presented in rapid serial visual presentation streams. Sci Data 9, 3 (2022). https://doi.org/10.1038/s41597-021-01102-7
9. Pineda, A. M., Ramos, F. M., Betting, L. E., & Campanharo, A. S. (2020). Quantile graphs for EEG-based diagnosis of Alzheimer's disease. Plos one, 15(6), e0231169.
10. Weng, Lilian. "Attention? Attention!" Lil'Log (Alt + H), 24 June 2018, https://lilianweng.github.io/posts/2018-06-24-attention/.
11. Committee, U. S. J. E. (2022, July 6). Joint Economic Committee Democrats chairman - rep. Don Beyer (D-VA). The Economic Costs of Alzheimer's Disease - The Economic Costs of Alzheimer's Disease - United States Joint Economic Committee. Retrieved January 27, 2023, from https://www.jec.senate.gov/public/index.cfm/democrats/issue-briefs?id=02F4CADC-954F-4E3B-8409-A4213E3C0759

12. Altaheri, H., Muhammad, G., Alsulaiman, M., Amin, S. U., Altuwaijri, G. A., Abdul, W., ... & Faisal, M. (2021). Deep learning techniques for classification of electroencephalogram (EEG) motor imagery (MI) signals: a review. Neural Computing and Applications, 1-42.
13. Guerrero, M. C., Parada, J. S., & Espitia, H. E. (2021). EEG signal analysis using classification techniques: Logistic regression, artificial neural networks, support vector machines, and convolutional neural networks. Heliyon, 7(6), e07258.
14. Varesi, A., Pierella, E., Romeo, M., Piccini, G. B., Alfano, C., Bjørklund, G., Oppong, A., Ricevuti, G., Esposito, C., Chirumbolo, S., & Pascale, A. (2022). The Potential Role of Gut Microbiota in Alzheimer's Disease: From Diagnosis to Treatment. Nutrients, 14(3), 668. https://doi.org/10.3390/nu14030668
15. Paola, J. D., & Schowengerdt, R. A. (1997). The effect of neural-network structure on a multispectral land-use/land-cover classification. Photogrammetric Engineering and Remote Sensing, 63(5), 535-544.
16. Hendrycks, D., & Gimpel, K. (2016). Gaussian error linear units (gelus). arXiv preprint arXiv:1606.08415.
17. Swets, J. A. (1996). Signal detection theory and ROC analysis in psychology and diagnostics: Collected papers. Psychology Press.
18. Vaswani, A., Shazeer, N., Parmar, N., Uszkoreit, J., Jones, L., Gomez, A. N., ... & Polosukhin, I. (2017). Attention is all you need. Advances in neural information processing systems, 30.
19. He, P., Liu, X., Gao, J., & Chen, W. (2020). Deberta: Decoding-enhanced bert with disentangled attention. arXiv preprint arXiv:2006.03654.
20. Alammar, J. (n.d.). The illustrated transformer. The Illustrated Transformer – Jay Alammar – Visualizing machine learning one concept at a time. Retrieved November 2, 2022, from https://jalammar.github.io/illustrated-transformer/
21. Dhillon, N. S., Sutandi, A., Vishwanath, M., Lim, M. M., Cao, H., & Si, D. (2021). A Raspberry Pi-based traumatic brain injury detection system for single-channel electroencephalogram. Sensors, 21(8), 2779.
22. Hong, Xin, et al. "Predicting Alzheimer's Disease Using LSTM." IEEE Access, vol. 7, May 2019, pp. 80893–80901., https://doi.org/10.1109/access.2019.2919385.
23. Iqbal, K., Liu, F., Gong, C. X., & Grundke-Iqbal, I. (2010). Tau in Alzheimer disease and related tauopathies. Current Alzheimer Research, 7(8), 656-664.
24. Babayan, A., Erbey, M., Kumral, D. et al. A mind-brain-body dataset of MRI, EEG, cognition, emotion, and peripheral physiology in young and old adults. Sci Data 6, 180308 (2019). https://doi.org/10.1038/sdata.2018.308
25. LaRocco, John, et al. "A Systemic Review of Available Low-Cost EEG Headsets Used for Drowsiness Detection." Frontiers in Neuroinformatics, vol. 14, 15 Oct. 2020, https://doi.org/10.3389/fninf.2020.553352.
26. Matthews, K.A., Xu, W., Gaglioti, A.H., Holt, J.B., Croft, J.B., Mack, D. and McGuire, L.C. (2019), Racial and ethnic estimates of Alzheimer's disease and related dementias in the United States (2015–2060) in adults aged ≥65 years. Alzheimer's & Dementia, 15: 17-24. https://doi.org/10.1016/j.jalz.2018.06.3063
27. Kadavath, H., Hofele, R. V., Biernat, J., Kumar, S., Tepper, K., Urlaub, H., ... & Zweckstetter, M. (2015). Tau stabilizes microtubules by binding at the interface between tubulin heterodimers. Proceedings of the National Academy of Sciences, 112(24), 7501-7506.

Decision-Making Factors in Selecting a Collegiate Flight School

Onur Abdullah Tunc[1]
David J. Leitz[1]
Ezequiel Finkielman[1]
Deborah S. Carstens, Ph.D., PMP[1]
[1]*Florida Institute of Technology*
Melbourne, FL. 32901
niOtunc2016@my.fit.edu; Dleitz2019@my.fit.edu; Efinkielmanb2021@my.fit.edu; carstens@fit.edu*

Abstract

Choosing a university is a major decision for those seeking an aviation degree. Choosing to major in flight increases the total educational cost. Past studies discuss students' decision-making factors in choosing universities, but little research has been conducted specifically for flight majors. The study methodology utilized surveys and interviews with 31 participants. Using Spradley's (1979) domain analysis to categorize common themes and patterns, the domains that emerged were university reputation, past family enrollment, funding mechanism to pay for student's education, campus tour, aircraft availability, and interactions with university staff and faculty. The findings are discussed along with the implications and recommendations for practice and research.

Keywords:.

1. Introduction

The decision-making process on a selecting a career can be tough and with 66% of high school graduates seeking a college degree, it is important to understand the decision-making factors that influence young minds to attend specific aviation colleges and universities (NCES, 2021). This research aims to understanding these factors, which could help colleges, families, and individual students across the nation to better tailor the processes and information available for prospective students.

2. Literature Review

Choosing an academic major is usually the first step in a career decision. The range of factors that students consider when choosing a university vary according to students' financial, geographical, social, and cultural backgrounds as well as the reputation of the college, location, cost, potential job opportunities, and influence from parents and teachers (Allen & Barnhart, 2006; Edmonds, 2012; Mustafa et al., 2018). The total costs of attending a college or university in the United States fluctuate. However, regardless of the chosen university, enrolling in a flight degree program substantially increases the costs because of fuel costs, type of aircraft flown, flight instruction, and course costs. A past survey suggests the top three reasons for choosing a college or university were good academic reputation, graduates get good jobs, and size of the college (Steckel et al., 2010). Another reason for studying flight can also include a lifelong passion for flying, the desire to travel, the prestige associated with a position

Submitted: April 28, 2023
Revised: July 17, 2023

as an airline pilot, or to appease their parents who have found career success in the aviation industry (Daku, 2021). To fill certain gaps in the literature, the current study investigated decision-making factors for choosing a collegiate flight program.

3. Methodology

The purpose of this study was to determine which of the decision-making factors in choosing an undergraduate collegiate flight program had the greatest significance on individuals. This study was guided by the following research question: What are the potential factors in the decision-making process of selecting a university with flight training for an undergraduate degree?

3.1. Context

The current study was a survey and interview conducted over a five-month period. The study analyzed the data provided by 31 participants, 27 male, and 4 females, and collected through three separate purposive samples denoted as P1-P31.The participants currently or previously attended eight universities in the United States as an undergraduate where their university offered a flight program or partnered with a local flight school as a flight training affiliate (FTA). e. Participant information was confidential.

3.2. Research Design and Data Collection Methods

The current study used two methodologies to gather data concerning participants' decision-making factors, quantitative and qualitative methodologies. For the quantitative study, participants supplied information about gender, age, military veteran status, attended university's name, university category, university size, and tuition rate. The basic qualitative/interpretive research was consistent with Ary et al., in that it helps to "understand the meaning people make of their experiences, assuming that people create their meaning as they interact with the world around them" (2010, p. 454). Additionally, this basic qualitative/interpretive research approach is appropriate due to the primary purpose of the study was to "describe and attempt to interpret…" (Ary et al., 2010, p. 453) the experiences of the participants as they navigated through the decision-making process for choosing a university. In conjunction with describing the factors associated with the decision-making process of the participants in choosing a university, the participants' comments and answers helped to establish conjectures that were inductively deduced from their responses. Furthermore, a domain analysis for each question was created to aid in the organization and initial coding of factors and responses identified by the participants.

The study was conducted by first administering a structured questionnaire that was provided to the participants through personal email. This structured questionnaire asked quantitative based questions aimed at gathering the above demographic information. After the participants returned the questionnaire, the researchers conducted the second portion of the study, basic qualitative/interpretive research conducted through individual interviews with the participants.

The basic requirement for an individual to become a participant within the current study was that they must be currently attending or have attended a university and participated in the said university's flight program or an affiliate flight training program that is partnered with the university they are now

attending or did attend as an undergraduate. The university size classification or degree offering was not a factor in who could be a participant within the current study.

4. Results

The survey questions were analyzed using Spradley's (1979) Domain Analysis and are discussed in this section.

4.1. Domain 1: University Chosen Based on Reputation Factors

Domain 1	Cover Term	Included Term	Conjectures With Respect to reputation: People will choose university…
University Reputation	Factors	Finance	1.1 Financial costs. 1.2 Family members working in the commercial aviation industry recommended the university.
		Flight training	1.3 Flight staff training. 1.4 Flight staff experience.
		Employment	1.5 Job placement for graduates. 1.6 University relationship with airlines. 1.7 Required a university that would properly train for a future career and help achieve employment. 1.8 Campus work opportunities.
		Accolades	1.9 Word of mouth 1.10 University ranking.
		Personal	1.11 University proximity to students' residence 1.12 Positive past experience with the university of family members and friends.

Table 1: Domain 1: Was the University Chosen Based on Reputation

The table containing Domain 1 corresponded to the first research interview question: Was the university chosen based on its reputation? Thirty participants selected 'yes' and one participant selected 'no.' The secondary question responses included acceptance rate, flight staff training, word of mouth, job placement opportunities, university's relationship with airlines, flight staff experience, and campus work opportunities.

The interview process for the first domain resulted in reputation of the university influencing participants' probability of attendance for universities. There were 11 participants that stated that the university was chosen based on reputation. Of the participants, 25.8%, agreed that flight staff training was one of the main reputation factors that influenced them to attend their university. Of the participants, 32.2%, selected acceptance rate as a factor in university selection. Job placement for graduates and word of mouth were selected by participants 67.7%, each. The university's relationship

with airlines were selected by 74.1%. Of the participants, 19.3% identified flight staff experience as a factor in university selection. The least important factor selected by participants at .3% were campus work opportunities.

4.1.1. Factors

Finance. Participants' comments suggest the finance had an important role in decision-making. For example, P13 said, "... has a pretty good reputation when it comes to their flight program, especially compared to the other flight schools in the area/Florida in general. What also attracted me was the amount of financial aid the school was offering towards my tuition, which would help in the flight training costs"; P28 said, "good financial aid and good goals short-term and long-term". These comments provided evidence to the value placed on financial decision.

Flight Training. Participants' comments suggest flight training had an important role in decision-making. For example, P7 stated, "They also had great mentors to help achieve your goals"; P18 said, "With flight, it's important to know that the training department has a good reputation, few errors, and good pass-rate."

Employment. The comments by the participants indicated that university's relationship with airlines' and job placement was an important decision-making factor. For example, P2 said, "I wanted to attend a school that would prepare me for flying and help me get a job when I graduated"; P4 said, "It was important that I attend a well-known university so that I would be properly trained for my future career."

Accolades. The factor 'word of mouth' was selected by 67.7% of the participants as being an important factor in their decision-making process. For example, P9 said, "I had a family friend that works at… recommended…"; P14 stated, "the individuals that gave good recommendations about… were very dear to me and their opinions mattered in correlation with the reputation… has for its flight training program."

Personal. Interviewees relied on the recommendation of a family member in selecting their chosen university when the family member worked in aviation. For example, P8 said, "my father worked at an airport at the time I was deciding on where to go to college. He said many of the pilots he talked to recommended…"; P9 said, "I had a family friend that works at… recommend…".

4.2. Domain 2: Any Family Members Attend Mentioned University

The Domain 2 question asked if family members attended the university to understand the influential factors family members can make in the decision-making process. If the participants answered yes, they were asked what type of relationship existed (i.e., father, mother, sister, aunt, etc.) and how the family members' attendance or recommendation influenced them.

Domain 2	Cover Term	Included Term	Conjectures With respect to how education was funded: People will choose university...
Family member alumni	Factor	-	2.1 Number of family member(s) alumni 2.2 Family member type (i.e., parents, siblings, grandparents, uncle, etc.).

Table 2: Domain 2: Did Family Members Attend Named University

4.2.1. Factors

The table containing Domain 2 corresponded to the second interview question: Do you have a family member that attended the named university? Sub questions for the second question included how many family members attended the named university, which type of family member, and please explain how this affected your decision and why? The comments by the participants identified one cover term factor. P6 said, “my brother said it was a good school and it helped him get a job.” P12 said, “I got a scholarship based on his attendance which influenced my decision” referring to their grandfather.

4.3. Domain 3: How Was Your Education Funded

The Domain 3 question aims to understand how participants funded their undergraduate education and to determine if the applied answers influenced their attendance. The participants were given the options to fill in all the choices that applied to their methods of funding or payment to the university. The options given were self, family, grant, loan GI Bill Education Benefits, and others. The sub question within question number three is: Please expand on the reasoning for your chosen funding for your education. The responses by the participants lead to one cover term, type. Additionally, the included terms ‘GI Bill Education Benefits’, ‘loan’, ‘scholarship’, and ‘private pay’ were listed to further identify reasoning for education funding.

Type. This cover term was divided into four separate conjectures: GI Bill Education Benefits, Loan, Scholarships, and Private pay. For example, P2 and P3 had funded their education by using their GI Bill Education Benefits.

GI Bill education benefits. Participants’ comments suggest that GI Bill had an important role in decision-making. For example, P2 said, “I didn’t have any other choice to pay for school. I didn’t want get a loan and I didn’t want to mess with trying to get some kind of grant”; P3 said, “the GI Bill was the only way I could go to school”.

Domain 3	Cover Term	Included Term	Conjectures With respect to how education was funded: People will choose university...
Funding of education	Type	GI Bill education benefits	3.1 Only available options.
		Loan	3.2 They could not afford to pay in any other way which also applied to grants and other categories that were all scholarship related.
		Scholarship	3.3This was my only choice to pay for college
		Private pay	3.4 The main reason for self-funding and family funding was that the student didn't have any loans, or the family was nice enough to cover their expenses. Parents had money. 3.5 savings account 3.6 Working a part-time job

Table 3: Domain 3: How Was Education Funded

Loan. Participants' comments suggest that loans had an important role in decision-making ; P6 said, "I didn't have any other way to pay for college except for a huge loan"; P11 said, "I knew I couldn't pay the whole bill for… and flight school out of pocket and loans were the remaining way to pay the rest of the bills."

Scholarship. Participants' comments suggest that scholarships had an important role in decision-making. For example, P1 said, "full ride scholarship for tuition"; P31 said, "I collected enough scholarships and grants to be able to study abroad and attend."

Private pay. Participants' comments suggest that private pay had an important role in decision-making . For example, P13 said, "the first semester my family helped pay for tuition after all of the grants and loans that were deducted from my tuition bill"… "my flight training costs came out of a savings account I had accumulated before attending the university"; P14 said, "my family was generous enough to help further my education so I can have a good lifestyle."

4.4. Domain 4: Was a Campus Tour Conducted of The Flight Line

The Domain 4 question was to understand the lasting impact of conducting a campus tour of the flight line on the potential students. The first question asked if the participant conducted the tour. If a tour was conducted, the participant was asked if and how the tour influenced their decision.

Domain 4	Cover Term	Included Term	Conjectures With respect to a campus tour was conducted: People will choose university...
Campus Tour	Flight Line	Flight Instructors	4.1 Interactions with the flight instructors were seamless. 4.2 Positive experience with the flight instructors. 4.3 Specific questions answered
		Training	4.3 Impressed with the flight line (i.e., well maintained aircraft, etc.).

Table 4: Domain 4: Was a Campus Tour Conducted of The Flight Line

Flight Line. The table containing Domain 4 corresponded to the fourth interview question: Did you conduct a campus tour of the flight line? In addition to question number four, there was a sub question: If yes, please explain how this affected your decision and why? The responses to this question developed one cover term, 'flight line'. Additionally, responses related to this question, participants stated, "yes"; "no"; and "I was impressed, and the school was pretty well set up…and well taken care of"'.

Flight Instructors. The participants found interaction with flight instructors influenced their decision-making. For example, P11 said, "I enjoyed seeing the facilities itself as well as hearing from staff about the flight line. I also did some poking around and the flight instructors who were currently working there gave me very sound practical advice to succeed at flying and attending... I felt like I was connecting with those in the aviation industry"; P17 said, "knowing how nice the instructors and staff were compared to other schools I visited made a huge difference."

Training. The participants found training influential in their decision-making. For example, P9 said, "the heated hangars, no planes left outside, and the whole facility was impressive. It is a… operation that looks like a small airline"; P13 said, "after already having a general knowledge of how an airport should run, it was nice seeing how efficient and clean and well managed the… flight line was. If it were bad, it would've deterred my enrollment."

4.5. Domain 5: Was Aircraft Availability a Decision-Making Factor

The Domain 5 question was introduced to establish an understanding of the participants' idea of Aircraft availability. There were not many responses but the follow-up question contained details urging participants to indicate whether aircraft availability influenced their decision-making process.

Domain 5	Cover Term	Included Term	Conjectures With respect to aircraft availability: People will choose university...
Availability of Aircraft	Availability	-	5.1 Availability of Aircraft. 5.2 Adequate number of aircraft. 5.3 Ability to finish training in an efficient manner. 5.4 Well-maintained fleet.
	Maintenance		5.5 Time it takes for maintenance to repair aircraft

Table 5: Domain 5: Was Aircraft Availability a Decision-Making Factor

The table containing Domain 5 corresponded to the fifth interview question: When seeking a flight school, was aircraft availability a decision-making factor? In addition to this question was a sub question: If yes, please explain how this affected your decision and why? In responding to this interview question, participants indicated their reasoning for why aircraft availability was a factor. Not all participants indicated that availability was a factor and from this question two cover terms developed, 'availability' and 'maintenance'.

4.5.1. Factors

Availability. Participants stated that availability influenced there decision-making. For example, P5 said, "I needed a school that had enough aircraft to train all the students who needed them"; P13 said, "as someone who had intended to get through their flight training at a fast pace, knowing that was possible because of the amount of aircraft availability available put a great ease to me and my uncle's minds. It showed us that the flight line at… was better managed than competing universities."

Maintenance. There were two participants that answered "yes" to aircraft availability being a factor, but their reasoning was due to their concern for the aircraft condition and safety. For example, P7 said, "I knew I wanted to train somewhere that had a more modern fleet with good maintenance, so I was safe…"; P10 said, "well, having insufficient aircraft or poorly maintained aircraft would mean delays in training and possible cost overruns. Both would be non- starters".

4.6. Domain 6: Was Flight Staff, Employees, and Faculty Interactions Part of Your

The Domain 6 question was asked to understand how flight staff, faculty, or instructors influenced the decision-making process. The table containing Domain 6 corresponded to the sixth interview question: When seeking a flight school, were your interactions with the flight line staff (i.e., flight instructors, head of training, faculty, staff, etc.) a decision-making factor? In addition to this question was a sub question: If yes, please explain how this affected your decision and why? The comments by the participants lead to four cover terms, flight staff, employees, faculty, flight facility.

4.6.1. Interactions

Flight Staff. For this cover term, participants indicated that the instructors were personable, caring, knowledgeable, and the university had welcoming flight staff. For example, P7 said, "the wealth of experience that the staff and instructors had instilled more confidence than some others. The instructors were more than just upperclassmen doing it to make money, they were invested in my success"; P16 said, "they seemed very interested and helpful to me and my family which is why the school attracted me to attend".

Domain 6	Cover Term	Included Term	Conjectures With respect to interactions of people at university: People will choose university...
Interactions	Flight Staff		6.1 Instructors were personable, caring, and knowledgeable. 6.2 Welcoming flight staff.
	Employees		6.3 Instructors displayed experience.
	Faculty		6.4 Specific questions could be answered.
	Flight Facility		6.5 The organization felt put together with the flight staff being so helpful to answer questions for family members and students

Table 6: *Domain 6:* Was Flight Staff, Employees, and Faculty Interactions Part of Your

Employees. This cover term provided insight into how participants perceived the instructors' experience. For example, P17 said, “meeting the instructors helped immensely. The attitude they had vs. other flight schools I visited made me feel welcome, and that they were the best school for me to advance my aviation career”; P18 said, “having had several different types of flight instructors prior to… I knew the types of CFIs I did and did not work well with, so this was a factor in my decision, finding out if they had a diverse set of instructors if one match did not work out well.”

Faculty. Participants’ responses suggest the facility had an important role in decision-making. For example, P10 said “sort of, I was planning to also work there as an A&P mechanic, so it was as much of a job interview for me as it was a school interview for them. It was a pretty unique arrangement, but the best way to make sure your planes are well maintained is to have your mechanic also be a student”; P11 said, “I explained in question 4 a part of it. I really enjoyed my interactions at the flight line tour.”

Flight Facility. Participants’ responses suggest the flight facility had an important role in decision-making. For example, P16 said, “they seemed very interested and helpful to me and my family which is why the school attracted me to attend”; P21 said, “professionalism, organization, and enthusiasm all contributed to my decision in joining…”.

5. Conclusion

During the study, the most significant factor in choosing a college or university was based on finances. A reoccurring theme found within the financial factors provided by participants was location of the school; in-state, out-of-state, or international students. This was due to the high cost of tuition and living expenses. The second most important factor was the reputation of the university whether it was in education, job opportunities, word of mouth, or airline connections. Students seek a good education and aviation quality flight training coupled with the potential of obtaining lucrative jobs. Availability was the lowest contributing factor, varying between aircraft availability or maintenance availability. Lastly, participants stated that the campus tour interactions provided valuable information not found on campus websites or other sources. The findings within this study closely matched those found within the literature review regarding factors such as cost, and reputation influenced the selection of institutions more than any others.

6. References

Allen, R. T. & Barnhart, K. (2006). Influencing factors in degree selection for aviation majors at Indiana State University. Journal of Aviation/Aerospace Education & Research, 15(3), 8.

Ary, D., Jacobs, L. C., & Sorensen, C. (2010). Introduction to research in education (8th ed.). Belmont, CA; Wadsworth, Cengage Learning.

Daku, S. A. (2021). Career Aspirations of Collegiate Aviation Students (Doctoral dissertation, The University of North Dakota).

Edmonds, J. (2012). Factors influencing choice of college major: what really makes a difference? Rowan University: Rowan Digital Works https://rdw.rowan.edu/cgi/viewcontent.cgi?article=1146&context=etd

Mustafa, S. A. A., Sellami, A. L., Elmaghraby, E. A. A., & Al-Qassass, H. B. (2018). Determinants of college and university choice for high-school students in Qatar.

NCES. (2021). The National Center for Education Statistics (NCES) Fast Facts Tool provides quick answers to many education questions. National Center for Education Statistics (NCES), U.S. Department of Education. https://nces.ed.gov/fastfacts/display.asp?id=51.

Spradley, J. (1979) The Ethnographic Interview. Holt Rinehart & Winston, New York.

Steckel, R., Lercel, D., & Matsuo, H. (2010). Factors that influence an undergraduate student to choose a career in aviation and enroll in the Aviation Science Program at Parks College of Engineering, Aviation and Technology. The Collegiate Aviation Review International, 28(2).

On-Machine Coordinate Measuring for In-Situ Quality Control

William D. Goheen, Jr.[1]
Ridge D. Towner[1,2]
Wilfredo Moscoso-Kingsley[2]
Deborah S. Carstens, Ph.D., PMP[1]

[1]*Spirit AeroSystems, Wichita, Kansas, USA*
[2]*Industrial, Systems and Manufacturing Engineering, Wichita State University, Wichita, Kansas, USA*

wilfredo.moscoso@wichita.edu; william.d.goheen-jr@spiritaero.com; ridge.d.towner@spiritaero.com

Abstract

The capability of a computer numerical control (CNC) machine tool equipped with direct computer control coordinate measuring software and high accuracy contact probing is validated for in-situ machine health monitoring and in-situ part quality control. The validation conforms to international standards for performance evaluation of commercially available coordinate measuring machines (CMMs). The capability of the CNC system to perform CMM-type measurements is demonstrated via a case study. The equivalency between part dimensional measurements obtained directly from the use of the CNC machine tool as a CMM and from part dimensional measurements performed using commercially available CMMs is established via a correlation study.

Keywords: machining, CNC, coordinate measuring, CMM, first article inspection, in-situ quality control.

1. Introduction

This work was aimed at the development of a procedure to combine production, machine monitoring and part dimensional measurement using computer numerical control (CNC) machine tools equipped with in-situ, self-validated probing systems, to be utilized in the aerospace manufacturing sector, specifically at Spirit AeroSystems. A methodology in which the machine tool completes the required part operations, and then functions as a coordinate measuring machine (CMM) is laid out, to eliminate the need to perform long and expensive ex-situ CMM measurements. The novel, in-situ probing procedure is especially attractive for the completion of automated, daily machine health checks and first article inspections that are regulated by international standards (SAE AS9102B: Aerospace First Article Inspection Requirement 2014). The advantages are reduced operating cost due to reduced inspection labor/time and part rework requirements, and increased conformance to part quality specifications. The procedure aids in the certification by aerospace quality audit criteria (NADCAP Audit Criteria for Measurement and Inspection 2013).

A qualification method is applied to verify that the machine tool can be used as a CMM with sufficient accuracy and repeatability, and to ensure that the daily machine performance and first article

Submitted: April 30, 2023
Revised: August 16, 2023

inspections conducted with the in-situ CMM probing system are accurate. The qualification method is based on the standards that apply to commercial CMMs. That is, standards ANSI/ASME B89.4-1997 (Hook 2001), including addenda ANSI/ASME B89.4a-1998 and ANSI/ASME B89.4b-2001, and ISO 10360-2:2009 (ISO/TC 2009). These standards are henceforth referred to as ASME B89.4 and ISO 10360-2.

To operate the machine tool as a CMM, a high precision spherical probe (Renishaw Rengage, model RMP600 (RMP600 radio machine probe 2008) is mounted directly on the machine head, to trigger the reading of machine X, Y and Z coordinates, which are taken as the coordinates of the point of interest. The methodology is validated following a case study involving the drilling of holes on a family of aircraft floor beams using a computer numerical control (CNC) machine tool – a Bavius 5-axis machining center. The holes are located at various locations on the long faces of the floor beams. A picture illustrating the Bavius CNC machining center and the definition of its axes is shown in Figure 1.

Figure 1. A picture of the Bavius CNC machining center.
The machine coordinate system is superimposed on the picture.
When the machine rotary axis A = 0°, the spindle is vertical as shown.

2. Goals of the research study

The research study presented herein was aimed at establishing a comparison a via round robin-type study between measurements reported by the in-situ CMM probing system and conventional, commercially available, probing systems including laser trackers, laser scanners and point probing (Zhao, Xu and Xie 2009).

After a brief background of the literature in the field of CMM probing, the machine tool qualification method, including daily machine performance check and first article inspection procedures are described. Then, details of the round robin experimental setups are presented, and the results are analyzed via correlation. Finally, concluding remarks are given.

3. Background

Qualification of the use of the CNC machining center as a CMM is performed following two procedures. Thes are: 1) volumetric testing and 2) interim performance evaluation (daily checks).

Volumetric testing involves measuring the displacement of the CNC machine drives using a calibrated instrument of sufficient range, accuracy and repeatability, twice a year. In general, the machine is to be commanded to move its head along several paths, over a volume that matches the regular operating volume of the CMM. The selected paths include space diagonals requiring 3-axis interpolation (p.32 of ASME B89.4 and p. 8 of ISO 10360-2). Presumably, 3-axis interpolation motion is the most inaccurate kind of machine motion (Suh, et al. 2008). The diagonals illustrated in Figure 2 represent the paths to be implemented during the volumetric testing described herein. The machine head is stopped at predetermined distance intervals, to permit several measurements of actual head position along the length of each diagonal. As per the ASME B89.4, for large CMMs of the size and axis aspect ratio of the Bavius CNC machining center, at least ten (10) measurements should be performed on each diagonal (p. 37 of ASME B89.4). As per the ISO 10360-2, at least five (5) measurements should be performed on each diagonal, distributed evenly over the length of the diagonal (p. 6-7 of ISO 10360-2).

An interim performance evaluation is used to determine the likelihood that a CMM is working within its accuracy and repeatability, between full volumetric tests. As per the ASME B89.4 and ISO 10360-2 standards, the goal of the interim test is to identify and stop CMMs that are out of accuracy and repeatability, before a significant number of bad parts are accepted or good parts rejected. The interim test should be applied frequently to increase confidence in the CMM's performance. It may be based on measurements made on a test workpiece of the same family that the machine is to test regularly or on measurements made on an artifact specifically designed for CMM testing. After a full volumetric test, ten (10) consecutive interim tests should be conducted, and the mean deviations from the artifact's nominals used to establish a baseline value for the artifact, with the range of deviations taken as an indication of the expected, typical variation from nominals. Deviations from the artifact's nominals should also be within the accuracy and repeatability tolerances of the CMM. Historical data from regular interim tests should be within the range of deviations established by the ten (10) initial interim tests.

4. Volumetric Testing of the Bavius CNC Machining Center

Volumetric testing is adapted from standard procedures described in the background and involves measuring the displacement of the CNC machine drives using laser tracker (API R-50 Radian, serial number 60166) traceable to NIST, twice a year. In general, the machine is to be commanded to move its head along several paths, over a volume illustrated in Figure 2. This matches the regular operating volume of the CNC machine. To qualify the Bavius CNC machining center for the parts to be produced with it, the volumetric testing involved taking diagonal motion measurements every 14.5 in of machine head travel. This produces a total of 10 measurement positions along each diagonal. The Bavius CNC machining center is compensated for ambient temperature, using a built-in sensor and compensation algorithm (Wu, et al. 2012). Therefore, displacement commands represent part lengths at the standard temperature of 68 °F. The drives are set at feed rate equal to the feed rate to be used during the regular operation of the CNC machine as a CMM.

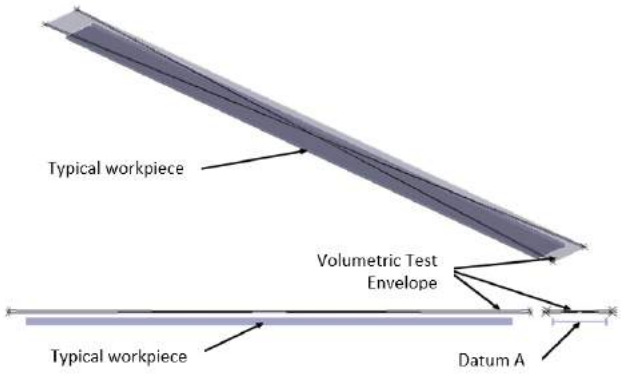

Figure 1. Illustration of a typical workpiece processed by the Bavius CNC Machining Center and the volume over which the volumetric test is to be applied.

The laser tracker's reflector is mounted on the tip of a tool holder inserted in the machine head, while the laser source/receiver unit is held stationary at a convenient location on the machine frame. The laser tracker is compensated for ambient temperature, atmospheric water pressure (air humidity), and atmospheric pressure, using built-in sensors and a compensation algorithm. Therefore, measurement values are true values at 68 °F. The start of each diagonal is taken as the zero-length reference. The difference between corresponding commanded and measured lengths are calculated. The measured length is the cumulated length along a diagonal. That is, the laser tracker is only zeroed at the start of a diagonal. The diagonal motions, and the measurements, are performed four (4) times. The start of each diagonal is taken as the zero-length reference. The difference between the four (4) measured lengths corresponding to the same location along a diagonal are calculated. For each measurement location, the range of the four measured lengths is calculated. The maximum range is taken as the machine repeatability index. This repeatability index can be used to assess machine performance over time. The difference between the most positive error and the most negative error, regardless of measured length, is taken as the machine accuracy index. Commonly applied industrial practice dictates that this accuracy index shall be at least four (4) times smaller than the smallest tolerance of the dimensions to be measured with the machine.

Figure 3 shows a plot of the deviation of the measured length with respect to the nominal length vs. the nominal length given as commanded motion to the Bavius CNC machining center, all along the four diagonals defined in Figure 2, including all repeat measurements. From Figure 3, the repeatability and accuracy indices of the Bavius CNC machining center are 0.0006 in and 0.0012 in, respectively.

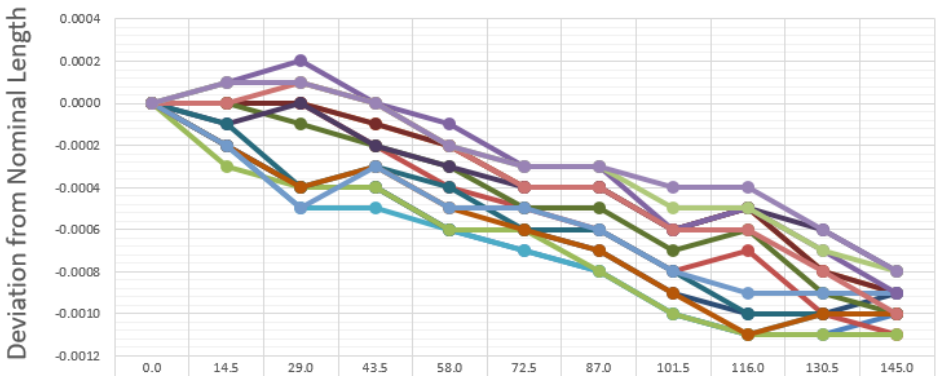

	0.0	14.5	29.0	43.5	58.0	72.5	87.0	101.5	116.0	130.5	145.0
Error - Diagonal 1, Measurement 1	0.0000	-0.0002	-0.0004	-0.0004	-0.0006	-0.0007	-0.0008	-0.0010	-0.0011	-0.0011	-0.0010
Error - Diagonal 1, Measurement 2	0.0000	-0.0002	-0.0005	-0.0005	-0.0006	-0.0007	-0.0008	-0.0010	-0.0011	-0.0010	-0.0010
Error - Diagonal 1, Measurement 3	0.0000	0.0000	0.0000	-0.0001	-0.0002	-0.0004	-0.0004	-0.0006	-0.0005	-0.0008	-0.0009
Error - Diagonal 1, Measurement 4	0.0000	-0.0002	-0.0004	-0.0004	-0.0006	-0.0006	-0.0007	-0.0009	-0.0010	-0.0010	-0.0009
Error - Diagonal 2, Measurement 1	0.0000	0.0000	0.0000	-0.0002	-0.0004	-0.0005	-0.0006	-0.0008	-0.0007	-0.0010	-0.0011
Error - Diagonal 2, Measurement 2	0.0000	0.0000	0.0000	-0.0001	-0.0002	-0.0004	-0.0004	-0.0006	-0.0005	-0.0008	-0.0009
Error - Diagonal 2, Measurement 3	0.0000	0.0000	-0.0001	-0.0002	-0.0003	-0.0005	-0.0005	-0.0007	-0.0006	-0.0009	-0.0010
Error - Diagonal 2, Measurement 4	0.0000	-0.0001	0.0000	-0.0002	-0.0003	-0.0004	-0.0004	-0.0006	-0.0005	-0.0006	-0.0008
Error - Diagonal 3, Measurement 1	0.0000	-0.0003	-0.0004	-0.0004	-0.0006	-0.0006	-0.0008	-0.0010	-0.0011	-0.0011	-0.0011
Error - Diagonal 3, Measurement 2	0.0000	-0.0001	-0.0004	-0.0003	-0.0004	-0.0006	-0.0006	-0.0008	-0.0010	-0.0010	-0.0010
Error - Diagonal 3, Measurement 3	0.0000	-0.0002	-0.0004	-0.0003	-0.0005	-0.0006	-0.0007	-0.0009	-0.0011	-0.0010	-0.0010
Error - Diagonal 3, Measurement 4	0.0000	-0.0002	-0.0005	-0.0003	-0.0005	-0.0005	-0.0006	-0.0008	-0.0009	-0.0009	-0.0009
Error - Diagonal 4, Measurement 1	0.0000	0.0001	0.0002	0.0000	-0.0001	-0.0003	-0.0003	-0.0006	-0.0005	-0.0007	-0.0009
Error - Diagonal 4, Measurement 2	0.0000	0.0000	0.0001	0.0000	-0.0002	-0.0004	-0.0004	-0.0006	-0.0006	-0.0008	-0.0010
Error - Diagonal 4, Measurement 3	0.0000	0.0001	0.0001	0.0000	-0.0002	-0.0003	-0.0003	-0.0005	-0.0005	-0.0007	-0.0008
Error - Diagonal 4, Measurement 4	0.0000	0.0001	0.0001	0.0000	-0.0002	-0.0003	-0.0003	-0.0004	-0.0004	-0.0006	-0.0008

Figure 3. Results from a volumetric test performed on the Bavius CNC machining center. The plot shows the deviation of the measured length with respect to the nominal length vs. the nominal length given as commanded motion to the Bavius CNC machining center. All dimensions are inches.

4.1. Interim performance evaluation (daily checks)

Daily checks are adapted from standard interim performance evaluations described in the background, and involve the use of the high precision contact probe (Renishaw Rengage probe RMP600 (RMP600 radio machine probe 2008)) and a program written in a CNC/CMM software (CAPPS-NC), to command machine motions to the various probing points. The software complies with international standards traceable to the National Institute of Standards and Technology (NIST).

The interim performance evaluation described herein is designed to check the accuracy and repeatability of the X, Y, Z and A drives of the Bavius CNC machining center, which are involved in part processing and measurement. The machine tool and the definitions of its X, Y, Z and A drives are illustrated in Figure 1. The interim performance evaluation is to be conducted against two specially designed artifacts: A five (5)-sphere calibrated artifact (Figure 4) and two (2) calibrated bushings embedded on the hard tool (Figure 5).

These “checks” mimic measurement of location and diameter of holes made by the Bavius CNC machining center on XY and XZ planes of a specific family of parts. The Bavius CNC machining center is utilized to make holes on the XY and two XZ planes of parts of this family. Then, the Bavius CNC machining center is utilized to measure the location and diameter of these holes. The measurements are below the operating envelop of the Bavius CNC machining center. Thus, the interim testing

complements the volumetric test measurements described in the previous section, which involved measurement along diagonals located above the operating envelope of the machine.

The five (5)-sphere calibrated artifact (Figure 4) is qualified using a standard CMM (Hexagon 152210-Chrome) traceable to NIST. During the qualification, the artifact is free from loads resulting from clamping against the metrology table. The artifact is glued to the table of the Bavius CNC machining center to keep it free from loads throughout the interim testing. The qualification is conducted in a controlled atmosphere at 68 °F. The artifact is made of the same material (same aluminum alloy) as the parts being processed on the Bavius CNC machining center. This enables thermal compensation, during the interim testing, using the standard procedure deployed by the Bavius CNC machining center for regular part processing. The artifact's nominals are taken from these qualifications. The nominals are average values of the X,Y, Z coordinates of the five (5) spheres, with local coordinate system as defined in Figure 4.

The two (2) bushings embedded on the hard fixture (Figure 5) are qualified using a laser tracker scaled against a linear laser (API XD1LSP) traceable to NIST. The qualification is conducted directly on the Bavius CNC machining center, but the temperature of the machine bed is measured, and the dimensions obtained from the qualification corrected for thermal growth due to temperature deviations with respect to 68 °F. The hard fixture holding the bushings are also made of the same material (same aluminum alloy) as the parts being processed on the Bavius CNC machining center. This enables using the standard procedure deployed by the Bavius CNC machining center for the thermal compensation. The artifact's nominals are taken from these qualifications. The nominal is the center-to-center distance from bushing 1 to bushing 2, with local coordinate system as defined in Figure 5.

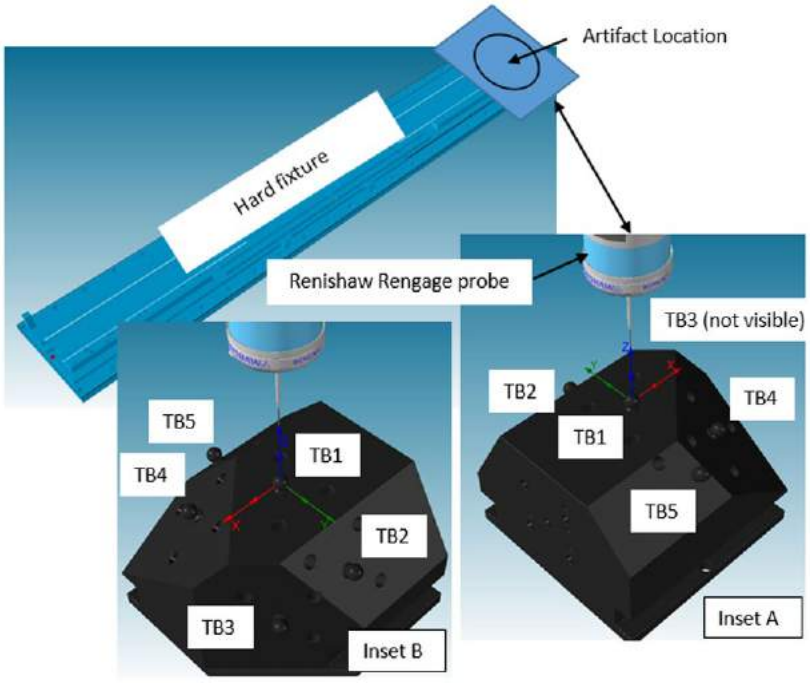

Figure 4. Schematic illustrating the arrangement of the five (5)-sphere calibrated artifact used to qualify the Bavius CNC machining center, by probing with the Renishaw Rengage probe. Inset A shows the artifact in regular

orientation. Inset B shows the artifact from "behind", to make all spheres visible. Spheres are labeled TB1 to TB5.

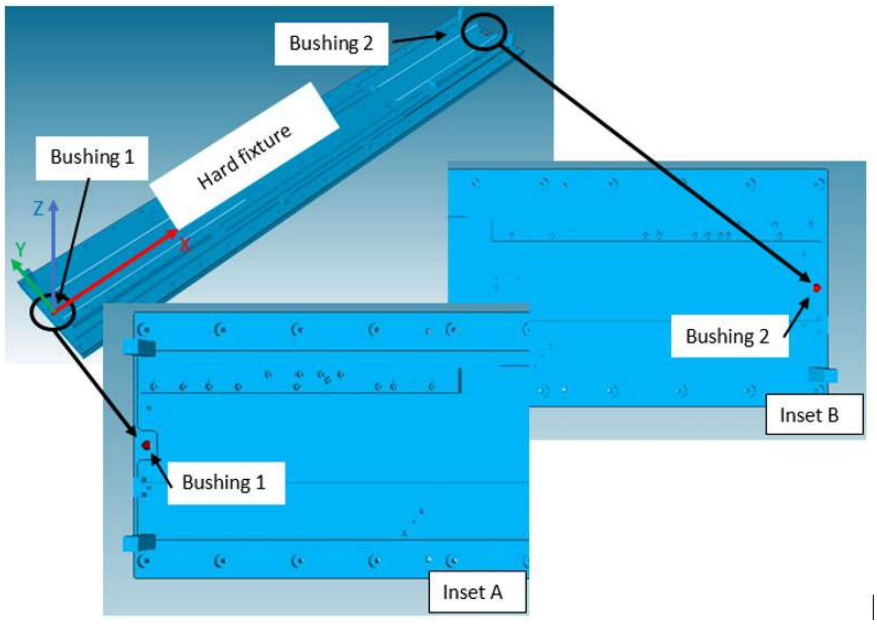

Figure 5. Schematic illustrating the arrangement of the two (2) calibrated bushings embedded on the hard tool to be used to qualify the Bavius CNC machining center, by probing with the Renishaw Rengage probe. Bushings are labeled as Bushing 1 (left) and Busing 2 (right). Insets A and B show close, top views of area surrounding the bushings.

5. Experimental Configuration

The FAIs involve the use of the high precision contact probe (Renishaw Rengage probe RMP600 (RMP600 radio machine probe 2008)) and a program written in a CNC/CMM software (CAPPS-NC), to command machine motions to the various probing points. The software complies with international standards traceable to the National Institute of Standards and Technology (NIST). The probing points are selected to define the position of the holes to be inspected. Figure 6 shows the probe performing an FAI on a generic part.

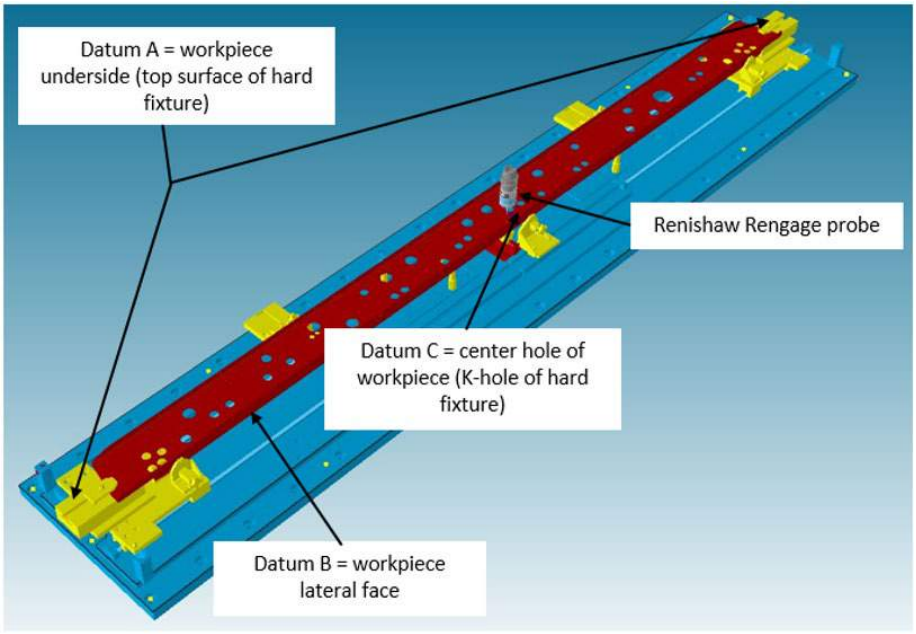

Figure 2. Schematic illustrating the arrangement of the machine bed of the Bavius CNC Machining Center. Milling floor of the hard fixture (blue), datums and clamps of the hard fixture (yellow) and a generic workpiece (red). The Renishaw Rengage probe is being used to measure the position of all the holes of interest, directly on the machine. Typical holes are on the horizontal or vertical long faces of the part.

One beam was processed by the Bavius CNC machining center by drilling holes that are required to be made at the center. The beam was run through an FAI procedure using the Bavius CNC machining center as a CMM, as described in the preceding sections. To validate the measurement procedure, the same beam was subject to measurements using several other standard CMMs and clamping methods. The results from this round robin test are shown and discussed in the following sections.

6. Experimental results

Figure 7A shows the relationship between measurements of the diametral error of position using the Bavius CNC machining center as a CMM vs. using a Creaform laser scanner in an environmentally controlled metrology room. Figure 7B shows the error relationship, but after measurement using the Bavius CNC machining center and a Leica laser tracker, without dismounting the beam between measurement runs with one device or the other. Note the equation of the linear regression line between errors reported by one measurement procedure and the other, and the coefficient of correlation (R), both given in the figure insets. When the beam is dismounted to be taken to metrology, the regression line fails to explain the relationship between errors measured by the Bavius vs. the laser scanner (R is high, but regression line constant is less than 1). However, when the beam is held on the machine tool and both the Bavius and the laser tracker are used to measure the errors of position, the regression line explains the relationship between the errors reported by these two measurement methods (R is high, and regression line constant is about 1).

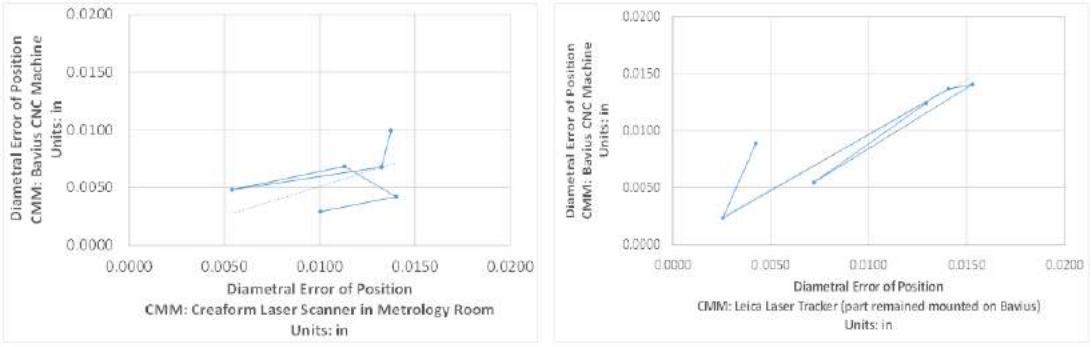

A: Regression line Y = 0.51X, R = 0.94 B: Regression line Y = 0.96X, R = 0.98

Figure 3. A) Relationship between measurements of the diametral error of position using the Bavius CNC machining center as a CMM vs. using a Creaform laser scanner in an environmentally controlled metrology room. B) The error relationship, but after measurement using the Bavius CNC machining center and a Leica laser tracker, without dismounting the beam between measurement runs. Y and X are diametral position errors measured by the two methods compared, respectively. R is coefficient of correlation.

Moreover, as evident from Table 1, the regression line is found to explain the relationship between the position error measured by the Bavius CNC machine only when the part remains mounted on the it for the measurement run following the alternative method.

Test Set	Comparison between:	Regression line	R
1	Bavius CNC Machine vs. Creaform Laser Scanner in Metrology Room	Y = 0.5X	0.94
2	Bavius CNC Machine vs. Leica Laser Tracker (part remained mounted on Bavius)	Y = 1.0X	0.98
3	Bavius CNC Machine vs. Creaform Point Probe (part remained mounted on Bavius)	Y = 0.6X	0.99
4	Bavius CNC Machine vs. FaroArm Contact Point Probe (part remained mounted on Bavius)	Y = 0.8X	0.96
5	Bavius CNC Machine vs. Bavius CNC Machine (part remounted between measurement runs)	Y = 0.5X	0.82

Table 1. Results from round robin tests. Regression line and coefficient of determination between position error measurement procedures. Y and X are diametral position errors measured by the two methods compared, respectively. R is coefficient of correlation.

7. Concluding remarks

A CNC machining center was fitted with high resolution contact probing to enable drive position readings triggered by the probing to be utilized for part measurement. Standard volumetric and interim tests that apply to performance evaluation of conventional CMMs were adapted for performance evaluation of the CNC machining center when it is used as a CMM for automated machine tool health monitoring and for FAIs. Immediate advantages from this operating procedure were obtained on the shop floor, including reduced inspection labor/time and part rework requirements, and increased conformance to part quality specifications.

It was found, by round robin testing following measurement of drilled holes position error by several methods that proper part clamping is critical. Measurements of hole position error using the CNC machine tool itself ensures that part clamping is standard, thus measurements more repeatable.

The proposed use of the CNC machine as a CMM shall be a cost-effective method for metrology inspection whenever the measurement cycle time is a small fraction of the manufacturing cycle time. The method is particularly attractive in the aerospace sector, where low production volume is associated with high machine tool idle time. For these applications, in-situ probing results in minimally disruptive part measurement.

8. Acknowledgements

The authors would like to express their sincere gratitude to Terry J. George, AMS Manager of Spirit AeroSystems and to Dr. Anthony Muscat, Dean of the College of Engineering of Wichita State University, for the financial support to complete this project. The authors would also like to acknowledge the following staff members of Spirit AeroSystems for their many contributions with computer programming and dimensional measurements: William R. Cox (Manufacturing Research and Development), Charles J. Haley (Research and Development), Daron L. Mann (Tooling), Joseph A. Nellis (Research and Development), Carl L. Peterson (Numerical Control Programing), Zahir Rachedi (Research and Development), Jeffrey S. Stewart (Manufacturing Research and Development), Long T. Tuong (Quality Engineering).

9. References

Hook, R. B., ed. 2001. *Methods for Performance Evaluation of Coordinate Measuring Machines*. The American Society of Mechanical Engineers.

ISO/TC, Technical Committee, ed. 2009. *Geometrical Product Specifications (GPS) - Acceptance and Revirification Tests for Coordinate Measuring Machines (CMM) - Part 2: CMMs Used for Measuring Linear Dimensions*. Swedish Standards Institute.

2013. *NADCAP Audit Criteria for Measurement and Inspection*. Performance Review Institute.

2008. *RMP600 radio machine probe. Technical Specifications, Renishaw*. https://www.renishaw.com/en/rmp600-high-accuracy-machine-probe--8880.

2014. *SAE AS9102B: Aerospace First Article Inspection Requirement*. SAE International.

Suh, Suk-Hwan, Seon-Kyono Kang, Dee-Hyuk Chung, and Ian Stroud. 2008. *Theory and Design of CNC Systems*. London: Springer Series in Advanced Manufacturing.

Wu, Ching-Wei, Chia-Hui Tang, Ching-Feng Chang, and Ying-Shing Shiao. 2012. "Thermal Error Compensation Method for Machine Center." *The International Journal of Advanced Manufacturing Technology* 10: 681-689.

Zhao, Fiona, Xun Xu, and S Q Xie. 2009. "Computer-Aided Inspection Planning - The State of the Art." Computers in Industry 60 (7): 453-466.

ThreshNet: a Novel Machine Learning Technique to Optimize Sensitivity and Specificity Performance

Shirley Xu[1]
[1]*The Bishop's School*
La Jolla, CA, 92037
shirleytxu@gmail.com

Abstract

In image classification applications for medical diagnosis, sensitivity and specificity are important performance metrics that are often inversely related. Both high sensitivity and high specificity are not always achievable for a given neural network; the trade-off and balance between them are not easily controllable. This paper proposes "ThreshNet", a novel method to address this dilemma. ThreshNet is composed of an ensemble of different neural networks. Many well-known networks were leveraged through transfer learning. With custom-designed dense layers, network parameters were tuned to optimize performance and enhance the diversity of members in the ThreshNet networks ensemble. To yield the ThreshNet system's decision, a threshold-based algorithm is proposed. Demonstrated with a brain tumor MRI dataset, ThreshNet systems consistently outperform individual networks. Specific sensitivity-specificity trade-offs and optimization goals can conveniently be achieved by adjusting the threshold parameter. Performance variance among ThreshNet systems is smaller than those among individual networks. To locate tumor(s) predicted by ThreshNet, a ResUNet-based image segmentation model was developed, achieving a Tversky index of 90.49% in predicting pixel-wise masks to mark tumor locations.

Keywords:.

1. Introduction

Machine learning algorithms are widely used in medical image processing and diagnosis classification applications, where a network is typically tuned to optimize particular performance metrics. Sensitivity and specificity are the statistical measures of performance in binary classification tests. (Hanga, 2015) provides an overview of the metrics and their applications in clinical research: "In clinical research, the sensitivity of a medical test is the probability of its giving a 'positive' result when the patient is indeed positive and specificity is the probability of getting a negative result when the patient is indeed negative." (Hanga, 2015). Sensitivity and specificity are also important performance metrics in image classification applications, and they are often inversely related. The weight placed on sensitivity and specificity also depends on application. In medical diagnoses, "disease prevalence should also merit consideration when providers examine their diagnostic test metrics" (Shreffler, 2023). The seriousness of the diagnosed disease also impacts the significance on sensitivity and specificity. Both high sensitivity and high specificity are not always achievable for a given neural network, and trade-offs and balance between them are not easily controllable. In this paper, a new method named "ThreshNet" is proposed

Submitted: April 30, 2022
Revised: November 8, 2022

to address this dilemma.

ThreshNet is a threshold-based algorithm that utilizes results from an ensemble of individual classification neural networks. Applying the ThreshNet technique to a brain tumor diagnosis example, this paper shows that overall classification performance outperforms individual networks in multiple metrics. Furthermore, different sensitivity and specificity trade-offs and balance scenarios can conveniently be satisfied through the implementation of a threshold parameter.

In addition, to locate tumor(s) predicted by ThreshNet's classification system, this paper developed a ResUNet-based image segmentation model, achieving a Tversky index of 90.49% in predicting pixel-wise masks to mark tumor locations. ResUNet was originally developed by Zhengxin Zhang et al. (2017).

2. Methodology

This paper uses the brain tumor MRI dataset provided by Buda et al. (2019). The dataset contains 3929 brain MRI images with human professional diagnosis results. To predict whether a tumor is present and generate pixel-wise masks to mark the location of the tumor on the image, the following three steps of classification and segmentation implementations were conducted:

- Step 1: Develop, train, tune and select individual classification neural networks
- Step 2: Build ThreshNet system with an ensemble of networks selected in Step 1
- Step 3: Develop, train, and tune ResUNet-based image segmentation neural network

Each step is further elaborated on below.

2.1. Individual classification neural networks

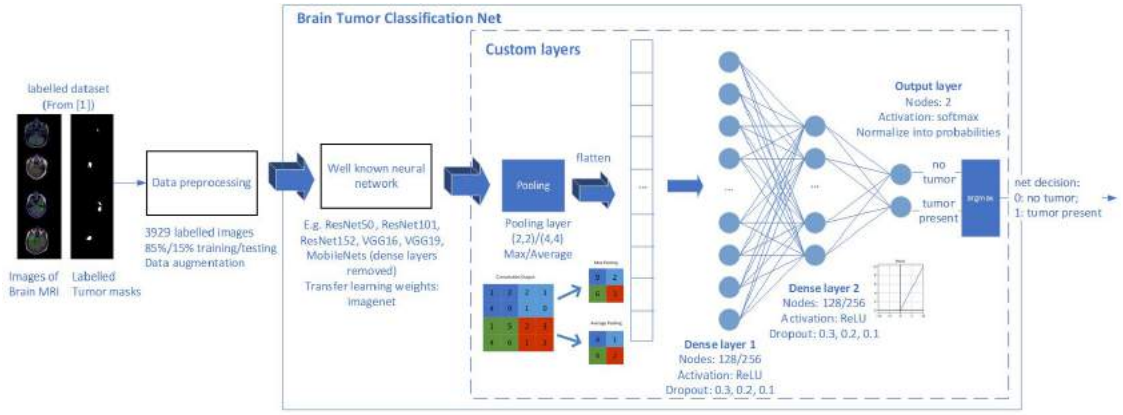

Figure 1. Individual Classification Neural Networks

As shown in Figure 1, data augmentation (rotation angle, horizontal flip, vertical flip, rescaling, brightness) was applied to enrich the dataset. Transfer learning techniques were applied on a variety of well-known networks, including ResNet50, ResNet101, ResNet152, MobileNet, MobileNetV2, VGG16, and VGG19. Custom dense layers (variations of Pooling Flatten Dense Dropout Dense Dropout Dense layer) were added and optimized for different networks, and network configurations and parameters were tuned to optimize performance and enhance diversity. Table 1 lists the network

parameters varied in different individual networks.

Operation	Parameters
Pooling	Pooling Type: {average pooling; max pooling} Pooling size: {(2,2); (4.4)}
Dense layer activation function	{ReLu, Softmax}
Loss/metric function	Loss: categorical_crossentropy Metrics: {accuracy, FalseNegatives}
Optimizer	{Adam, Adagrad}
Dropout	{0.1, 0.2, 0.3}

Table 1. Network parameter variations

Networks were trained with a maximum of 50 epochs (with early-stopping enabled). Each individual classification network outputs its decision of whether a tumor is present (0: no tumor; 1: tumor present). Out of all the neural networks trained, 33 networks that each had >91% accuracy performance were selected as candidate networks for the ThreshNet system in the next step.

2.2. The ThreshNet System

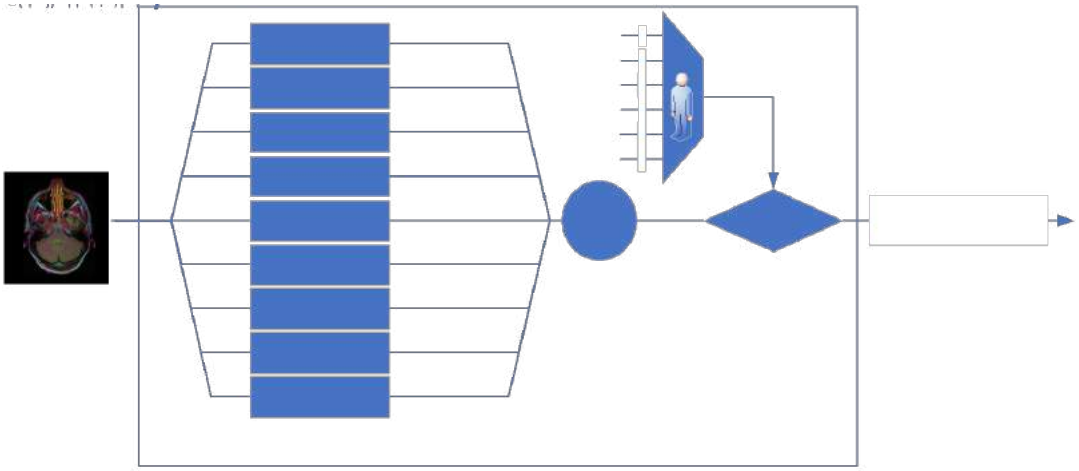

Figure 2. ThreshNet System

To construct the ThreshNet system, 9 networks were randomly selected out of the 33 networks from 2.1. The 0 (no tumor) or 1 (tumor present) decisions of all individual networks in the system are accumulated, and the sum is compared against the ThreshNet threshold parameter. This threshold parameter denotes the number of individual networks needed to "agree" with a positive diagnosis for the ThreshNet system to declare a positive diagnosis. The performance of varying ThreshNet parameters (the threshold value) between 1-6 is shown in 3.

2.3. The Segmentation Network

If the ThreshNet system generates a positive (tumor present) diagnosis, a ResUNet based network is applied to perform image semantic segmentation.

ResUNet refers to Deep Residual UNET. It's an encoder-decoder architecture proposed in (Zhang, 2018) for semantic segmentation. It was initially used in remote sensing image analysis for the road

extraction from high-resolution aerial images. ResUNet combines the strength of U-Net, a "U"-shaped fully convolutional network proposed in (Ronneberger, 2015), and residual neural network. The benefits of this combination are: *"First, residual units ease training of deep networks. Second, the rich skip connections within the network could facilitate information propagation, allowing us to design networks with fewer parameters however better performance."* (Zhang, 2018)

The ResUNet as shown in Figure 3 is developed, trained, and tuned to predict pixel-wise tumor masks to mark the locations of tumors. This ResUNet consists of three parts:

- Encoder Path (res-blocks & maxPooling) (5 stages)
- Decoder Path (res-blocks & upSampling) (5 stages)
- Bottleneck (connection between Encoder Path and Decoder

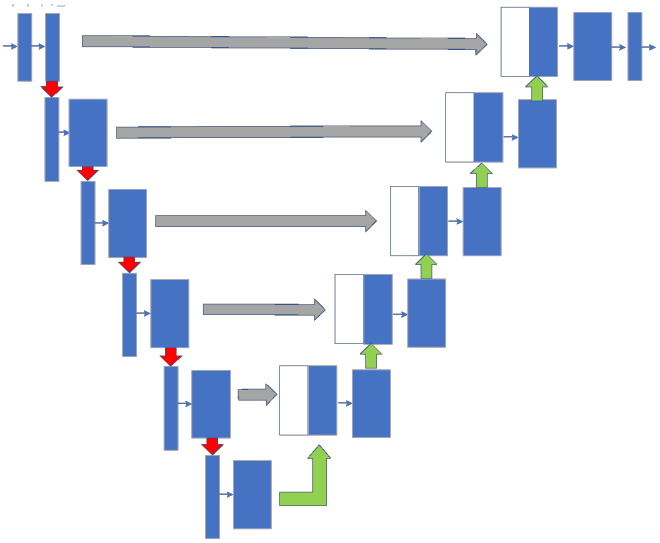

Figure 3 ResUNet Segmentation Network

3. Results

Ten ThreshNet systems were constructed, each with 9 randomly selected individual networks from the candidates in 2.1.

Figure 4 and Figure 5 are violin and box-and-whisker plots that show the sensitivity and specificity metrics, respectively, of the individual networks in each of the ten ThreshNet systems. As shown, networks with higher sensitivity performance tend to have lower specificity performance and vice versa.

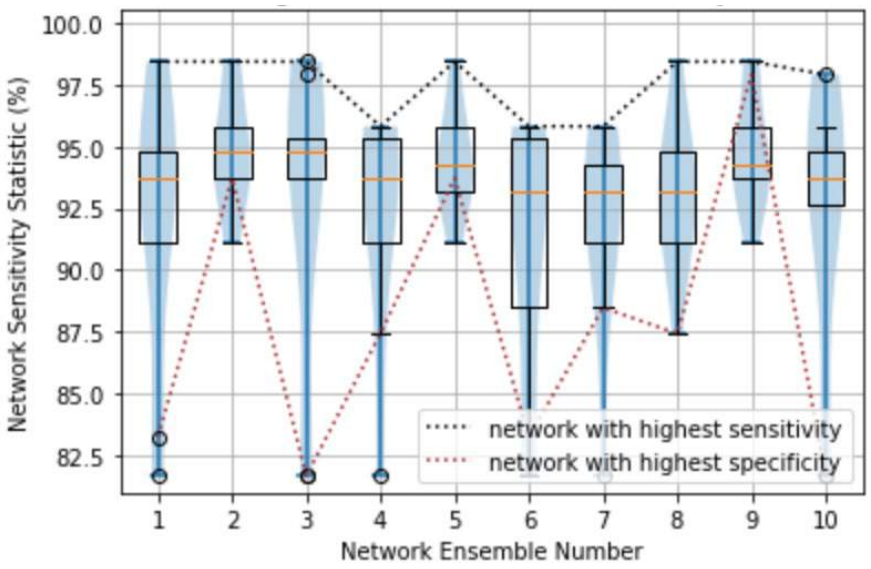

Figure 4. Individual Network Sensitivity

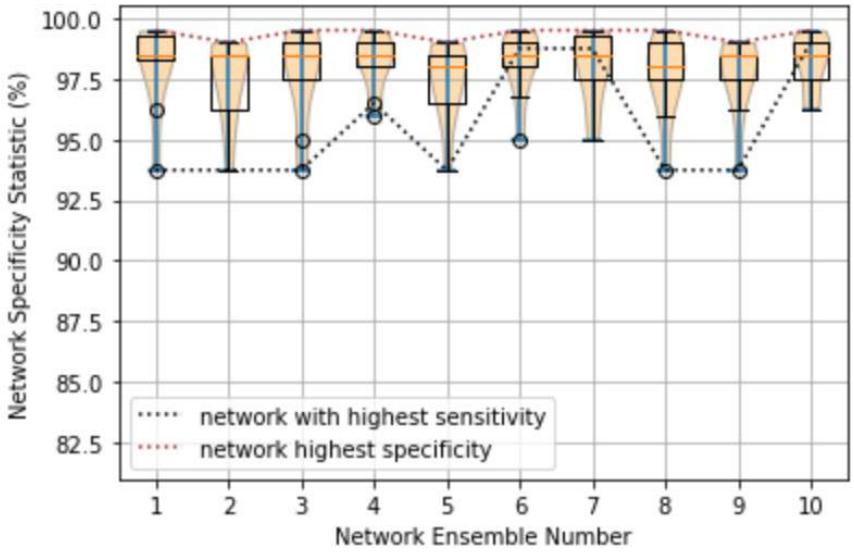

Figure 5. Individual Network Specificity

As described in 2.2, the ThreshNet system contains a configurable threshold parameter. Test results of threshold values 1-6 are shown in this paper. As shown in Figure 6, smaller ThreshNet threshold settings offer better sensitivity performance, and larger ThreshNet threshold settings offer better specificity performance. The tradeoff between sensitivity and specificity can be conveniently achieved by adjusting ThreshNet's threshold parameter. In addition, when compared to Figure 4 and Figure 5, the variance of sensitivity and specificity of the ten ThreshNet systems are smaller than those of individual networks. This indicates that ThreshNet systems offer more consistent and predictable performance than individual networks.

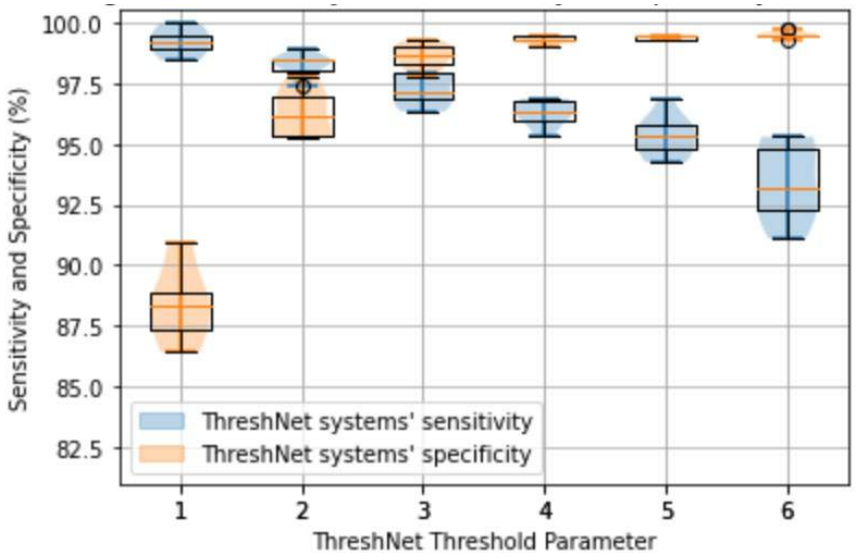

Figure 6. ThreshNet Systems' Sensitivity and Specificity Tradeoff

Figure 7 and Figure 8 compare the sensitivity and specificity of ThreshNet systems under different threshold settings (1 to 6) against those of individual networks (individual networks with the highest sensitivity and highest specificity respectively in each ThreshNet ensemble are selected for comparison).

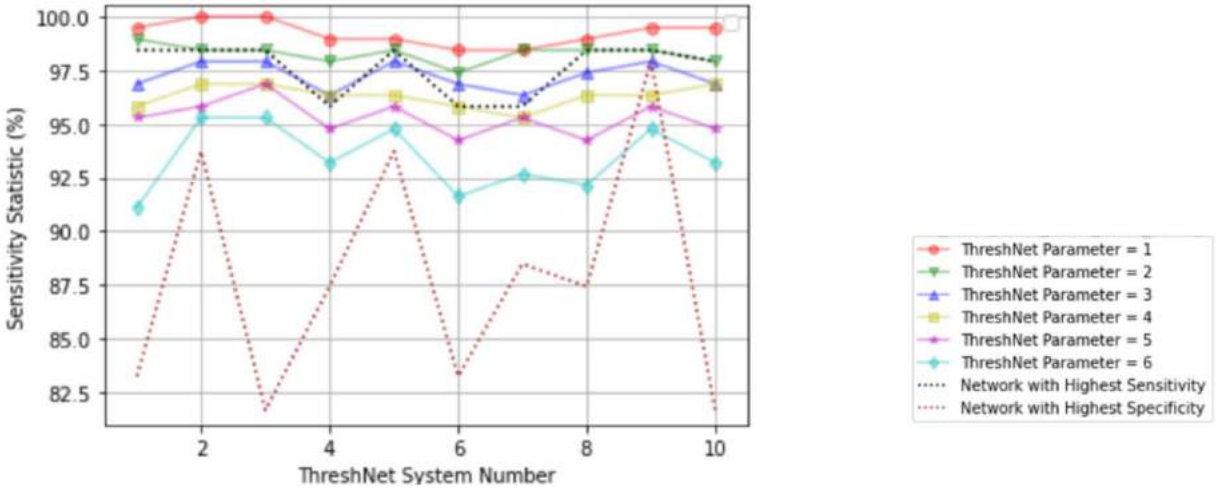

Figure 7. ThreshNet Systems vs Individual Network Sensitivity

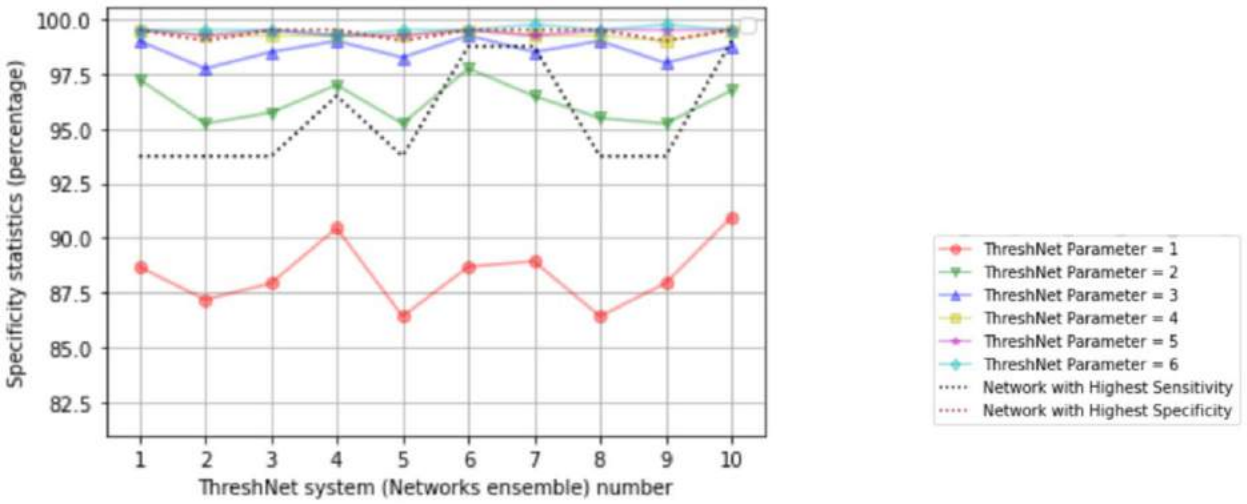

Figure 8. ThreshNet Systems vs Individual Network Specificity

The following are observed with different ThreshNet threshold parameter ranges:

- Lower ThreshNet threshold parameter values (1-2):
  - Sensitivity (range is 97.3% - 100%): always outperforms best sensitivity individual network. Some threshold=1 ThreshNet systems achieve 100% sensitivity while keeping specificity in an acceptable range.
  - Specificity (range is 86.4% - 97.9%): threshold=1 ThreshNet systems have lower specificity performance than best specificity individual networks, while threshold=2 ThreshNet systems outperform the best specificity individual networks 70% of the time.
- Higher ThreshNet threshold Parameter Values (4 - 6):
  - Specificity: Similar to best specificity individual network (difference <1%)
  - Sensitivity: Significantly improved (up to 15.2%) compared to best specificity individual network
- Medium ThreshNet threshold Parameter Values (3 - 5):
  - Well-balanced sensitivity and specificity performance metrics
  - Sensitivity and specificity metrics are all in high 90%s

An ROC curve is a graph showing the false positive (sensitivity) and the true positive (1-specificity) performance of a classification model at different classification thresholds. Figure 9 compares the ROC curves of ThreshNet systems with different threshold parameters against the ROC curves of individual networks. As shown, the ThreshNet systems' ROC curves are closer to the upper left corner of the graph, indicating better performance than the individual networks.

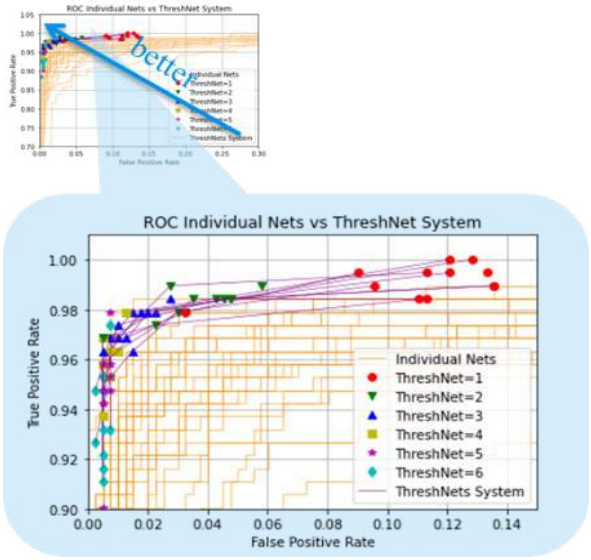

Figure 9. RoC Individual Nets vs ThreshNet Systems

To further investigate how sensitive the ThreshNet systems' performance is to the choice of individual networks in the ThreshNet ensemble, instead of randomly selecting individual networks (as in Figure 9), two specific ThreshNet systems were constructed, consisting of the nine best-sensitivity individual networks and nine best specificity networks respectively. The ROC results are shown in Figure 10. The performance of these two ThreshNet systems with the "best" individual networks performs similarly when compared to the randomly selected ones. This indicates that ThreshNet does not need the "best" members to achieve high performance.

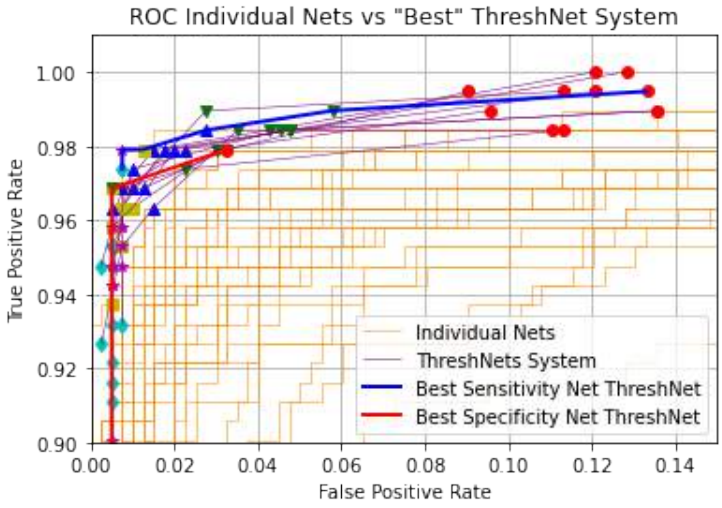

Figure 10. RoC of "best" ThreshNet Systems

The performance of the ResUNet segmentation model was measured with Tversky accuracy, which represents the similarity between the labeled mask's pixels and the predicted mask's pixels through Equation 1 (X = labeled, Y = prediction):

$$(\boldsymbol{X},\ \boldsymbol{Y}) = \frac{|\boldsymbol{X} \cap \boldsymbol{Y}|}{|\boldsymbol{X} \cap \boldsymbol{Y}| + \boldsymbol{\alpha}|\boldsymbol{X} - \boldsymbol{Y}| + \boldsymbol{\beta}|\boldsymbol{Y} - \boldsymbol{X}|}$$

Equation 1 Tversky Accuracy

α =0.7, β=0.3 was used in this paper. With this parameters configuration, pixels that ResUNet's prediction missed (false negatives) were penalized more heavily than pixels ResUNet's prediction overmarked (false positives). The ResUNet network achieved a Tversky accuracy of 90.49%.

Figure 11 shows examples of MRI test images and results in the following order (columns from left to right): brain tumor MRI image test cases; tumor masks labeled by human professionals provided in the dataset; ResUNet predicted masks; predicted masks overlayed with MRI test images. Visual inspection confirms that ResUNet's predicted tumor locations match closely with the masks from the labeled data set.

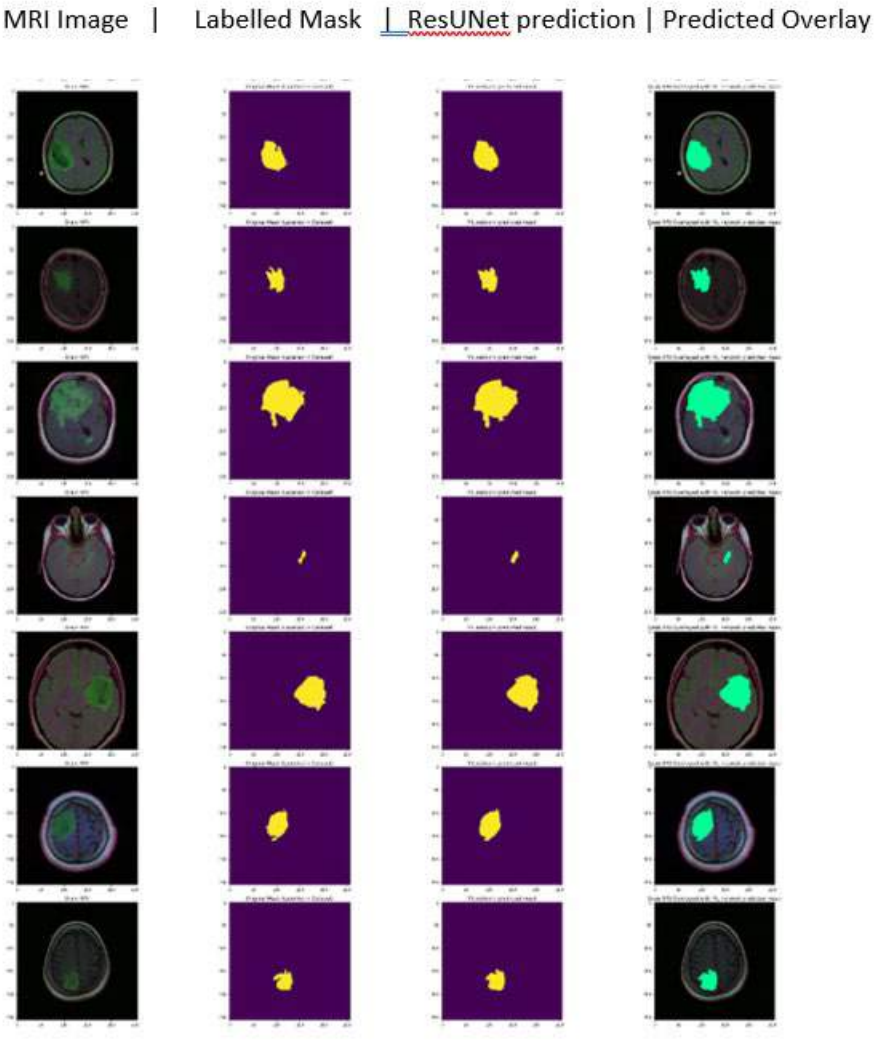

Figure 11. Visualization of ResUNet segmentation results

4. Conclusions and Applications

This paper proposed ThreshNet, a threshold-based classification algorithm utilizing an ensemble of networks. It is demonstrated that the ThreshNet system performs better than individual member networks in particular performance metrics and/or across all performance metrics.

The ThreshNet system provides convenient means to achieve specific performance and trade-off goals between sensitivity and specificity by adjusting the ThreshNet threshold parameter. The corresponding Threshold parameter configuration setting for particular optimization goals is described in Table 2.

Optimization goals	ThreshNet threshold configuration
High sensitivity	Low
High specificity	High
Balance between sensitivity and specificity	Medium

Table 2. ThreshNet threshold configurations for optimization goals

Variance among ThreshNet systems is smaller than variance among individual nets- more consistent performance, and ThreshNet system's performance is tolerant of variations in its member individual network performance.

ResUNet segmentation model's ResUNet segmentation model's predictions closely match the labeled mask in the dataset and achieved a Tversky accuracy of 90.49%.

Potential applications of the work in this paper include:

- Screening tool for brain tumor MRI scans and other medical diagnoses
- Establishing an urgency-based priority queue for medical scans through the threshold parameter
- Visualizing tumor locations through ResUNet image segmentation can assist in professional diagnosis.

5. References

Abdulla, W. (2018 – March 19). Splash of Color: Instance Segmentation with Mask R-CNN and TensorFlow. http://engineering.matterport.com/splash-of-color-instance-segmentation-with-mask-r-cnn-and-tensorflow-7c761e238b46.

Amato, F., Lopez, A., Pena-Mendez, E. M., Vanhara, P., Hampl, A., Havel, J. (2013). Artificial neural networks in medical diagnosis, 11, 47–58. Journal of Applied Biomedicine. 10.2478/v10136-012-0031-x

Brownlee, Jason. (2019, July 5). Best Practices for Preparing and Augmenting Image Data for CNNs. Machine Learning Mastery. http://machinelearningmastery.com/best-practices-for-preparing-and-augmenting-image-data-for-convolutional-neural-networks/

Buda, M., Saha, A., Mazurowski, M. A. (2019). Association of genomic subtypes of lower-grade gliomas with shape features automatically extracted by a deep learning algorithm. Computers in Biology and Medicine, 109, 218-225. 10.1016/j.compbiomed.2019.05.002

Grote, T., Berens, P. (2020). On the ethics of algorithmic decision-making in healthcare. Journal of Medical Ethics, 46, 205-211.

Hanga, A., Alalyani, M., Hussain, I., Musa, Almutheibi, M. (2015). Brief review on Sensitivity, Specificity and Predictivities. IOSR Journal of Dental and Medical Sciences. 14. 10.9790/0853-14456468

Lecun, Y., Kavukcuoglu, K., Clement, F. (2010). Convolutional Networks and Applications in Vision. ISCAS 2010 - 2010 IEEE International Symposium on Circuits and Systems: Nano-Bio Circuit Fabrics and Systems. 253-256. 10.1109/ISCAS.2010.5537907.

Li, J., Liang, X., Li, J., Xu, T., Feng, J., Yan, S. (2016, August 18). Multi-stage Object Detection with Group Recursive Learning. Arxiv. http://arxiv.org/abs/1608.05159v1. Retrieved July 24, 2020.

Mazurowski, M. A., Clark, K., Czarnek, N. M., Shamsesfandabadi, P., Peters, K. B., Saha, A. (2017). Radiogenomics of lower-grade glioma: algorithmically-assessed tumor shape is associated with tumor genomic subtypes and patient outcomes in a multi-institutional study with The Cancer Genome Atlas data. Journal of Neuro-oncology, 133(1), 27-35. 10.1007/s11060-017-2420-1

Opitz, D. & Maclin, R. (1999). Popular Ensemble Methods: An Empirical Study. Journal of Artificial Intelligence Research, 11, 169-198. 10.1613/jair.614.

Ronneberger, O., Fischer, P., Brox, T. (2016, August 18). U-Net: Convolutional Networks for Biomedical Image Segmentation. International Conference on Medical image computing and computer-assisted intervention. Springer, 234–241.

Sensitivity and Specificity. (2021, January 28). In Wikipedia. http://en.wikipedia.org/wiki/Sensitivity_and_specificity.

Sharma, P. (2019, July 22). Computer Vision Tutorial: Implementing Mask R-CNN for Image Segmentation (with Python Code). www.analyticsvidhya.com/blog/2019/07/computer-vision-implementing-mask-r-cnn-image-segmentation/.

Shreffler, J., Huecker, M. (2023). Diagnostic Testing Accuracy: Sensitivity, Specificity, Predictive Values and Likelihood Ratios. www.ncbi.nlm.nih.gov/books/NBK557491.

Zhang, Z., Liu, Q., Wang, Y. (2018). Road Extraction by Deep Residual U-Net. In IEEE Geoscience and Remote Sensing Letters, 15(5), 749-753. 10.1109/LGRS.2018.2802944

Zhao, Z., Zheng, P., Xu, S., Wu, X. (2019). Object Detection with Deep Learning: A Review. In IEEE Transactions on Neural Networks and Learning Systems, 30(11), 3212-3232. 10.1109/TNNLS.2018.2876865

Design, Fabrication, and Testing of a Dual-Axis Solar Turtle

Jengnan Juang[1]
R. Radharamanan[1]
Spencer Lowe[1]
Thong Nguyen[1]
Trenton Williams[1]
[1]Mercer University
Macon, GA, USA
Juang_jn@mercer.edu; radharaman_r@mercer.edu

Abstract

A portable, light weight, low-cost, dual-axis solar turtle prototype with dynamic self-tracking solar panel was designed and fabricated using 3D printed, machined, and purchased components to charge a battery large enough to run multiple devices. The base and body of the design housing is a locking lid rolling cooler that insures if the unit is tipped over the components inside will not be damaged. The design also makes the unit slightly weather resistant. Utilizing a fixed main post made from lightweight strong material allows for the main panel to have a height of 5 feet off the ground or 1 foot off the base of the design for the solar cell to operate. PVC was chosen due to its hollow center and strong and slightly flexible body that is lightweight. All parts needed for the prototype design were purchased along with some parts being 3D printed. Some aluminum milled pieces were used in the final design due to the large amount of load needed to handle at certain points of the build. Implementing a practical "yes/no" function will verify proper angle and exposure of the panel towards the sun, using miniature solar panels that will be eclipsed by the larger solar cell whenever directly facing the sun itself. The dual-axis solar turtle built is marketable and more efficient than static panels due to auto-tracking. When tested, it collected 19.9% more solar energy than static panels.

Keywords:.

1. Introduction

In the United States, the top three energy sources of electricity in 2022 are, natural gas at 39.8%, all coal at 19.5%, and nuclear at 18.2% and (U.S. – EIA, 2023). These forms of energy are nonrenewable meaning they will eventually be depleted. For this reason, it is important to seek renewable sources of energy for they are cleaner, easier to use, require less maintenance, and will always be available. This project focuses on solar energy, which is a renewable form of energy. On average the earth surface receives about 600 W/m2 of solar energy (Kothari, 2003). This value depends on several factors such as the time of the day and the atmospheric conditions. In 2022, only 3.4% of solar energy was used to generate electricity (U.S. - EIA, 2023). It is estimated that solar energy will become the largest source of electricity by the year 2050 (Kothari, 2003). For this reason, there should be a larger investment in harnessing solar energy. People who live in secluded areas have limited access to efficient power

Submitted: June 30, 2023
Revised: November 26, 2023

because it is unavailable or too expensive. Also, with the rising cost of fossil fuel most people who live in standard-sized homes are interested in finding alternative energy sources to reduce domestic electricity costs. Solar energy is an abundant source of renewable energy which makes it a good solution for people living under these circumstances. In a single day, the amount of sunlight hitting the United States is more than 2,500 times the entire country's daily energy usage (Chandler, 2013). The most efficient solar panels of today's technology harness less than 20% of available solar energy (Solar Technologies, 2013). Although this is a small percentage, it is a helpful amount of energy that may one day allow for independence from nonrenewable forms of energy. This paper provides the description of a senior design student project including the goal of the project and the design specifications. The overall objective is to design and build a dual-axis solar turtle using a portable, light weight, low cost, and dynamic solar panel capable of charging a battery large enough to run multiple devices. Previous attempts to achieve an effective dynamic solar panel adjusting unit relied on logic or GPS coordinates to track the location of the main solar panel. The system typically did not work properly if the code was incorrect which might have caused the system to lock up. Further, GPS costs a large sum of money to buy and install.

2. Background

Installing a dual-axis solar tracker on rooftop to meet the soaring demand of energy in developing countries have been studied and discussed (Farhana et al., (2013). Deepthi et al (2013) made a comparative study on the efficiencies of single-axis and dual-axis tracking systems with fixed mounts. A solar tracking system for renewable energy is designed and built to collect free energy from the sun, store it in the battery, and convert this energy to alternating current (AC). This makes the energy usable in standard-sized homes as a supplemental source of power or as an independent power source (Juang & Radharamanan, 2014). Twisha et al. (2014) introduced dual-axis solar tracker with reflector to increase optimal electricity generation in Bangladesh. A comprehensive study on dual-axis solar tracking system was made by Chhoton & Chakraborty (2017). A discussion on how solar panels work was made by Dhar (2017). A step-by-step guide explaining how solar panels work has been presented and discussed (SVTAdmin, 2018). A solar powered phone charger was designed, built, and tested (Juang & Radharamanan, 2019). Aggarwal (2020) discussed solar panels available in the market and indicated the most efficient solar panels for purchase and installation. In this paper, the authors designed, fabricated, and tested a portable dual-axis solar turtle that is more efficient due to auto-tracking and collects about 20% more solar energy compared to static panels

3. Methodology

The visual concept design of a dual-axis solar turtle is shown in Figure 1. Building of prototype started with the proof of concept regarding eclipsing the rear control panels with the main solar panel during the beginning stages of the preliminary construction. Sizes were initially based on a 50W panel. This was not efficient for recharging the solar battery within 8 hours. Therefore, the decision was made to increase the size to an 80W panel. The preliminary proof of concept is shown in Figure 2.

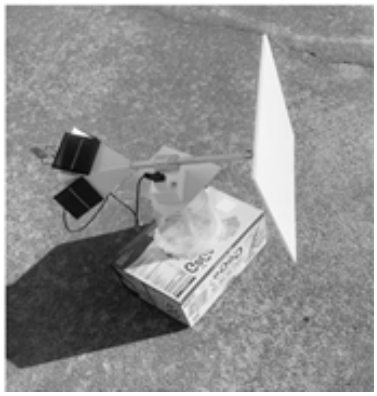

Figure 1: Visual Concept Design

Figure 2: Preliminary Proof of Concept

3.1. Beginning Building Stage Problems

The focus was engineering a top unit that would incorporate all components needed for X and Y axis movement, while still maintaining proper structural integrity (10 pounds). The operating mechanism of the upper unit was tested/troubleshooted while simultaneously milling custom parts. Various configurations of sensor control panels were tested, with the best results coming from having 212V solar panels set in parallel to achieve a maximum current of 500mA powering multiple DC motors. Efforts were made to reduce friction by adding an axial bearing to the top of the aluminum cap, helping the motors have the least amount of friction to start the rotations. Then the bottom of the box was extended to fully enclose around the aluminum cap to better displace the weight on the bearing, all while eliminating the amount of wiggle during windy days.

3.2. Final Building Stages Problems

Still having problems with binding and motor shafts getting stuck, the other areas were looked that could throw the level off. The main pole being loose, and swaying was assessed to be a problem, one solid piece of 5-foot PVC eliminated movement and the unit was rebalanced and leveled. Weights were added to the body box as a balance for keeping the weight over the axial bearing, ensuring enough downward force is on the bearing to allow the motor to effortlessly rotate the shaft, even in the event of small winds. Finally, the solar module components were secured to the outside/inside of the rolling container and were shielded by 3D printed structures to help with slight weatherproofing. Unit housed the battery and power inverter which were secured with straps and screws to keep them stable during transportation of the unit.

3.3. Final Design and Construction: Base and Frame

The base of the unit is made from a rolling cooler with an attached handle and wheels for better portability. While also serving as the storage compartment of the unit and protecting the components from the elements. A 3D printed carbon fiber base coupling is installed using screws, holding the bottom of the main 2” PVC pipe center for added stability. Between the wheel wells, the battery is held in place with reinforced straps and screws to prevent it from sliding into the main support post. The charge controller is attached to the front side of the base cooler housing using screws and was slightly protected from weather by a flexible 3D printed awning installed with screws above the controller.

3.4. Final Design and Construction: Base and Frame 2

Next to the charge controller, still under the same awning, is the kilowatt monitor. This is used for measuring the electrical power usage of appliances the customer decides to use in the field, allowing it to be read kilowatts per hour. The DC power inverter connects the battery to the monitor and was installed with straps on the underside of the lid to allow for easy access for potential maintenance. The power outlet was connected to the monitor using a short extension cord tucked inside the cooler. The battery is connected to the inverter through securing jumper cables from the back of the inverter to the positive and negative terminals of the deep cycle battery. Figure 3 shows the final solar turtle bottom unit assembly.

Figure 3: Final Solar Turtle Bottom Unit Assembly

3.5. Final Design and Construction: Tracking Mechanism

A round aluminum cap has a cutout 3⁄4 the thickness of the axial bearing on top of it, allowing for the bearing to be secured in place, but still give enough space for the main upper unit box to float. This is placed on top of the main support pole. A set screw is bored into the aluminum cap to allow the motor stem shaft to be secured, and this is what allows our rotation of the upper unit in relation to the bearing and aluminum support cap.

Two 12V 500 mA DC motors are responsible for causing the rotation once a control panel was exposed to sunlight generating power. These motors are installed in their own 3D printed mounts located on the main body box. The first DC motor is inside the bottom of the head unit; a stem shaft extension was fixed to the motor shaft, which is then secured to the aluminum cap with the set screw. The stem shaft was fit into the hole found in the center of the axial bearing.

The second DC motor is inserted into a shaft that rotates a spool turning a wire that moves the y-axis up and down, holding the unit in place as well as keeping constant tension. The opposite end of the spool is held in place with a rod running through the entire frame. A guide pulley is mounted on a rear rod to keep tension on the wire where the main horizontal support pole was fed through a vertical pivot mount and secured with a steel rod through the body.

3.6. Final Design and Construction: Tracking Mechanism 2

The attached main 80W solar panel was placed on the tip of the horizontal 1" PVC pipe support pole. Using a simple set pin and a predrilled hole that holds the main panel in place during operation. Toward the mid-section of the horizontal support pole, a vertical predrilled hole serves as the anchor point for the wire and spool y-axis unit. The wire was fed through the vertical hole and the excess was wrapped around the pole to ensure a tight no slip hold on the wire.

From the rear of the support pole, a 3-way collar was slid into place just behind the wire anchor, this 3-way collar is what holds the 3 control panels. The control collar is fixed into place with a predrilled hole and set pin as well. Three equal length 1" diameter poles slide into the slots in the 3-way collar and are faceted with set pins. The control panel housings were installed. Within each housing unit is a 12V 500mA solar panel set up.

The left and right panels are connected to the same control circuit to allow for proper clockwise and counterclockwise movement. The bottom horizontal movement motor is connected to the same breadboard where the top panel is directly connected to the vertical movement motor attached to the wire spool.

3.7. Final Design and Construction: Tracking Mechanism 3

Using the steel rods ran through the main body box of the motor housing assembly allows for attaching the small weights using a tension cable. This provides enough downward force to keep the unit from tipping in windy conditions and ensures the center of mass is full on the axial bearing. Light emitting diodes built into the control circuit will both become illuminated indicating the left and right panel are providing power as a check for the customer. If the left panel is covered, the left LED should turn off. This test ensures the connections were made correctly. In the event the opposite LED or the covered panel shuts off, then the connections are backwards. This is simply fixed by swapping opposite solar panel positive and negative terminal wires.

3.8. Final Design and Construction: Monitoring System

Kilowatt monitor will display the current power consumption of any electrical appliances connected to it when the customer needs electricity. The main power capacity can then be divided by the number indicated on the monitor to calculate the amount of energy available in hours remaining on the battery.

$$\frac{Indicated\ Battery\ Capacity * Percentage\ of\ Charge}{Kilowatt\ Monitor\ Indicated} = Power\ Available\ in\ Hours$$

3.9. Final Design and Construction: Monitoring System 2

With an upgraded 80W solar panel the power supply is capable of recharging within 8 hours of direct sunlight. If the electrical load is less than 80W per hour, then the appliance used will run directly off the solar panel and will not draw power from the battery power bank. Both the battery and main solar panel could be increased in capacities if desired in future models. Figure 4 shows the final prototype of solar turtle solar charge unit.

3.10. Future Recommendations: 1

3D printed parts made it possible to implement quick design changes ready to test daily. This helped to find the proper performance needed in tandem with the already machined mechanical parts. If possible, machining these final 3D parts out of a metal would ensure a tighter fit of components and increased stability.

Figure 4: Final Prototype of Solar Turtle Solar Charge Unit

3.11. Future Recommendations: 2

Some of the parts that were 3D printed were prone to breaking under any non-ideal movement. The DC motors had a small amount of free space in the mounting frame that would cause a shift in angle of them operating, causing the motor to have an unacceptable amount of strain coming from the spinning shaft. This could be fixed by using larger and more structurally enforced motors, which is highly recommended for the next iteration of the solar turtle.

The size of panel to motor ratio is linear, so with stronger parts everything can be upsized. Meaning if a bigger panel or larger power supply needs to be added, the size of the sensor panels will increase along with the size of the motors that run the unit itself.

3.12. Future Recommendations: 3

For better performance and large scaling of components, a microcontroller might be more suitable. If an Arduino were running directly off the main solar panel, it could be used as a digital switch. Using a digital switch would allow the current to build to max in the solar panel before passing through the DC motors. A larger current is needed to torque a larger motor. Regulating when and how much current passes would make the system operate with the same components but be able to facilitate moving a larger panel and increase the structural integrity of the top tracking unit. No photoresistors or sensors will be needed because the control solar panels will still do the sensing of the sun and power the motors directly. The Arduino would be nothing more than a simple programmed switch if larger motors were required.

Additionally, DC to DC converters could be used to alter the voltage and currents being produced by the control panels. This would allow the user to match the specifications of the DC motor exactly and then control the flow of current through the digital switch.

These simple changes would cost no more than $30, making these upgrades relatively feasible. However, this method would use code to operate and if the sun were not optimal, then the Arduino may never get enough power to run.

3.13. Future Recommendations: 4

It is important to remember to keep the power sources separate when making this change, to keep the main power source unaffected by the new code used in the tracking mechanism. A small battery could be used in this system in conjunction with the sensor panels to maintain a regulated input voltage and current to the Arduino, which would help fix this problem. If in the event the sensor panels are too weak to run a larger motor, then the use of a DC-to-DC converter off the main panel can be used to temporarily route power from the main solar panel through the DC motor.

The Arduino would still act as a digital switch, but the larger solar panel DC supply connects to an H-Bridge (Figure 5). An H-Bridge is made of 4 BJT transistor current controlled devices. The Arduino would only send a base signal to the current controlled device to allow flow of larger power to the motor without messing up the Arduino. Figure 6 shows H-bridge addition movement.

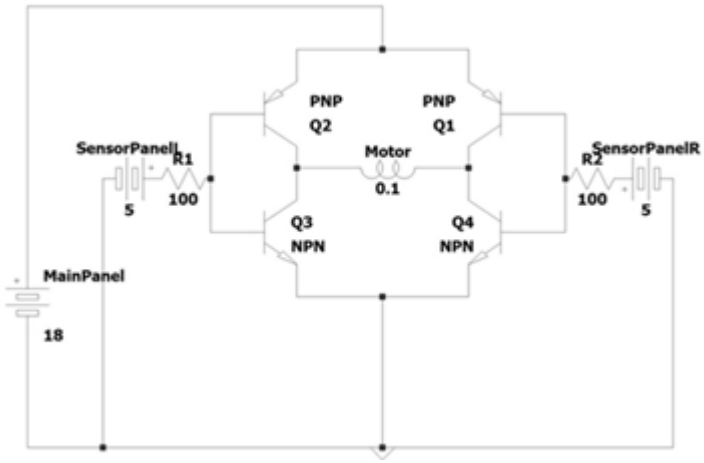

Figure 5: Circuit Diagram of an H-bridge

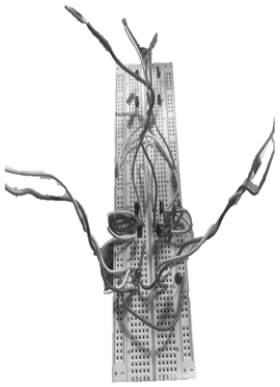

Figure 6. H-bridge Addition Movement

4. Results and Discussions

4.1. Checking the Battery Charge State

For checking the battery, one can use the solar charge controller or a multimeter. Initially checking the battery with a multimeter showed 11.2V. A trickle charger for battery was used. Table 1 shows the charge state of gel battery and AGM battery.

Safety Precautions

Use proper protective equipment such as gloves and protective eyewear when connecting the inverter to the battery. Use a two-pin switch instead of a three-pin switch. Solar inverter is strapped to prevent sliding or falling. Battery is strapped to the inside right-hand side of the cooler.

Charge State	Gel Battery Voltage	AGM Battery Voltage
100%	12.85+	12.8+
75%	12.65	12.60
50%	12.35	12.30
25%	12.00	12.00
0%	11.80	11.80

Table 1: Charge State of Gel Battery vs AGM Battery

4.2. Human Acceptance Test

The process was modeled on how to set up the system. 14 students agreed setting up the system was easy while another 5 disagreed. 73.68% agreed that the set-up process was easy.

Figure 7: Human Acceptance Test Data

4.3. Performance Tests: 1

The advantage of the tracking system is that the solar panel maintains its most effective tracking angle throughout the day. Table 2 shows voltage, current and power values for fixed panel for different times whereas Table 3 shows these values for tracked panel. Figure 8 shows the relation between time and power for fixed and tracked panels.

Time	Voltage (V)	Current (A)	Power (W)
8	12.7	2	25.4
9	12.9	2.5	32.25
10	14.1	3	42.3
11	14.2	4.2	59.64
12	14.2	5.3	75.26
13	14.2	5.2	73.84
14	14.2	5	71
15	13	4.8	62.2
Total			441.89
Mean			55.23

Table 2: Fixed Panel vs Time

Time	Voltage (V)	Current (A)	Power (W)
8	13	3.4	44.2
9	13.1	3.5	45.85
10	14.2	4.8	68.16
11	14.2	5.2	73.84
12	14.2	5.4	76.68
13	14.2	5.3	75.26
14	14.3	5.3	75.26
15	14.1	5	70.5
Total			529.75
Mean			66.22

Table 3: Tracked Panel vs Time

The formula used to track the improvement of the collected solar energies is shown below:

$$\% \textbf{ Improvement in Power } = \frac{\textbf{Power of Tracking Panel } - \textbf{ Power of Fixed Panel}}{\textbf{Power of Fixed Panel}} \textbf{ x 100}\%$$

$$\% \textbf{ Improvement in Power } = \frac{\textbf{66.22 } - \textbf{ 55.23}}{\textbf{55.23}} \textbf{ x 100}\% \textbf{ = 19.9}\%$$

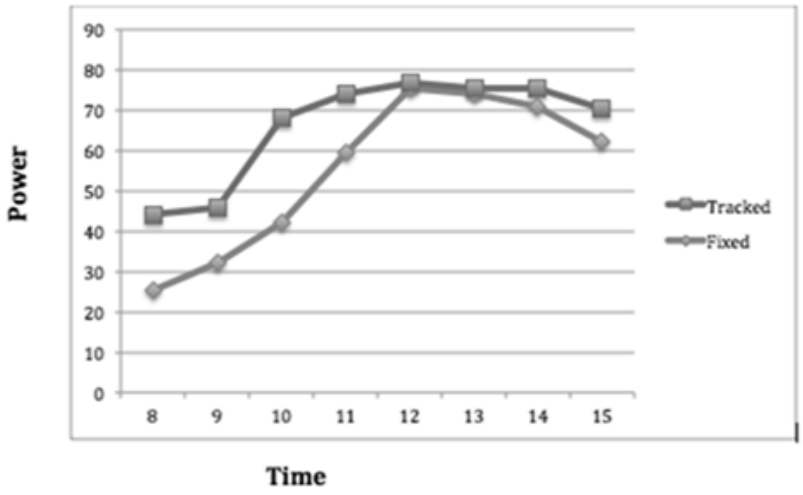

Figure 8: Time vs power

5. Conclusions and Recommendations

The final prototype build came in slightly over the initial budget of $300. The total amount spent building the prototype was $406.89. There would be more possibilities with cutting costs when it comes to functionality and overall build quality with having parts milled and manufactured wholesale, purchasing complete solar modules is more cost effective compared to getting the components individually. It is recommended that a microcontroller of some sort is powered through its own independent solar panel. This microcontroller would detect voltages at the smaller control panels and appropriately route power through a larger DC motor. This recommendation comes from size ability in mind. A system that could be used on a larger tracking system could reduce production cost because the control panels will not need to be increased in size to facilitate a larger DC motor and increased generator capacity. If the scale of the module was increased, then it could be used as a more permanent solar power generator capable of auto-tracking the sun. This could potentially increase the effectiveness of all solar panel powered systems including the industrial sized arrays.

In conclusion, the dual-axis solar tracking system contains significant components in comparison to the fixed system. The mini control panels were used to provide current to rotate the DC motors. The mini panel wires are connected inversely to turn the motor clockwise or counterclockwise to help the panel to maximize the absorption of energy. This resulted in generating a higher wattage than the fixed panel. Overall, the dual-axis solar tracking system is more effective in providing the best electrical performance.

6. References

Aggarwal, V. (2020). Solar Panel Efficiency: What Panels Are Most Efficient? EnergySage. Retrieved February 18, 2020, https://news.energysage.com/what-are-the-most-efficient-solar-panels-on-the-market/

Chandler, Nathan. "How Does Solar Power Help the Environment?" 29 August 2012. HowStuffWorks.com. 29 August 2013.

Chhoton, A. C., & Chakraborty, N. R. (2017). Dual Axis Solar Tracking System-A Comprehensive Study: Bangladesh Context, *Proc. 4th International Conference on Advances in Electrical Engineering (ICAEE), 28-30 September, Dhaka, Bangladesh, PP. 421-426*.

Deepthi, S., et al. (2013). Comparison of efficiencies of single-axis tracking system and dual-axis tracking system with fixed mount, *International Journal of Engineering Science and Innovative Technology 2, no. 2, pp. 425-430*.

Dhar, M. (2017, December 6). How Do Solar Panels Work? Retrieved from: https://www.livescience.com/41995-how-do-solar-panels-work.html

Farhana, A., et al. (2013). Installing dual axis solar tracker on rooftop to meet the soaring demand of energy for developing countries. *Proc. IEEE Annual Conference in India (INDICON),* pp. 1-5.

Juang, J . N., & Radharamanan, R. (2014). Design of a Solar Tracking System for Renewable Energy, *Proc. 2014 ASEE Zone 1 Conference, Bridgeport, CT, April 3-5, pp. 1-8*. https://www.asee.org/documents/zones/zone1/2014/Professional/PDFs/48.pdf.

Juang, J. N., & Radharamanan, R. (2019). Design, Build, and Test a Solar Powered Phone Charger, *Proc. 2019 IEEE SoutheastCon, Paper ID 177*.

Kothari, D. P., & Nagrath, I. J. (2003). *Modern Power System Analysis*. 3rd ed., Tata McGraw-Hill Pub. Co., New Delhi.

Solar Technologies | Photovoltaic Solar Panels | Thin Film Solar Panels | Solar Thermal. (n.d.). Solar Panels, Photovoltaic Systems, Solar Solutions for Home, Business & Utility-Scale — SunPower. (2013). Retrieved August 29, 2013, http://us.sunpowercorp.com/solar-resources/howsolar-works/solar-technologies/

SVTAdmin. (2018). A Step-by-Step Guide to How Solar Panels Work. Retrieved May 4, 2018: http://www.solarvtech.com/2018/05/03/a-step-by-step-guide-to-how-solar-panels-work/

Twisha, T., et al. (2014). Introducing dual axis solar tracker with reflector to increase optimal electricity generation in Bangladesh, In Developments in Renewable Energy Technology (ICDRET), Proc. *IEEE 3rd International Conference*, pp. 1-6.

What is U.S. Electricity Generation by Energy Source? - FAQ - U.S. Energy Information Administration (EIA). (n.d.). (2023). U.S. Energy Information Administration (EIA). Retrieved February 20, 2023.

The Relationship Between Pilot Experience and Aviation Safety Attitudes

Isabella Piasecki[1]
Steven Le Gall[1]
Brooke Wheeler[1]
[1]*Florida Institute of Technology*
Melbourne, FL. 32901
bellapiasecki@att.net; bwheeler@fit.edu; slegall2017@my.fit.edu

Abstract

Although the influence of safety attitudes on pilot performance has been documented and research has been conducted on how training can increase safety attitudes, little research has been conducted to understand the relationship between experience and a pilot's safety attitudes. The purpose of this study was to determine whether there is a relationship between pilot experience and pilot attitudes toward safety issues. Pilot attitudes towards safety issues were measured using Hunter's Aviation Safety Attitudes Scale (ASAS). A survey was distributed that included both ASAS and demographic questions. The relationship between flight hours (pilot experience) and the ASAS score was examined.

Keywords: Pilot experience, safety attitude, flight training, safety attitudes.

1. Introduction

Currently, Part 61 of the Federal Aviation Regulations (FAR) requires a student pilot to acquire a minimum of 40 hours of in-flight experience before becoming a private pilot. Shortly after a certificate is awarded, a zone varying from 50 to 350 hours proves to be more dangerous for pilots at risk (Craig, 2013). Similar findings were obtained for military airmen (Joseph & Reddy, 2013). Examining the relationship between pilots' experiences and their safety attitudes allowed for a deeper, more thorough understanding of the factors that could contribute to unsafe behaviors inside and outside the cockpit.

The purpose of this study was to determine whether there is a relationship between pilot experience and pilot attitudes toward safety issues. Pilot experience was measured by the number of hours a pilot has in an aircraft, the ratings they hold, and the ground training course they were currently enrolled in. Pilot attitudes toward safety issues were measured using the aviation safety attitude scale developed by Hunter (1995). The research question was "What is the relationship between pilot experience and pilot attitudes towards safety issues?" We expected that there would be a relationship between pilot experience and pilot attitudes towards safety issues.

This study provided information about pilots' attitudes towards safety issues; findings from this research may find a correlation between a pilot's level of experience and their attitudes towards safety issues. These correlations may help flight schools and/or companies understand where more safety training is needed to decrease incident and accident rates among pilots at these levels of experience.

Submitted: June 30, 2023
Revised: November 12, 2023

Providing pilots with the knowledge they need to feel comfortable and confident in every safety-related situation is crucial to increasing the safety of the aviation industry. Identifying when to administer recurrent safety training can allow for a more efficient and well-tailored approach to safety education.

The results of this study are generalizable to pilots currently training at a southeastern university with a Part 141 flight program because of the characteristics of the groups to which the survey was distributed. Collected data were checked to determine whether the sample was representative of the wider population before drawing conclusions about the greater populations listed above.

2. Literature Review

The following section reviews the literature on safety attitudes toward aviation. To understand the importance of studying safety attitudes as they relate to aviation, the basic requirements for becoming a pilot must be examined, in addition to the influence of human factors, risk, and decision-making. General aviation represents most air operations and has the highest rate of accident and incident events. Although the rate of annual events has decreased over time, it appears that student pilots have been involved in 14.6% of fatal cases in the last two decades (Knecht, 2013). Herein, A more in-depth examination of risk, decision-making, and safety attitudes might help to better understand better the role of human factors in lessening events, implying general aviation flying students.

An overwhelming majority of aircraft operations in the United States are related to general aviation, with approximately 90% of registered aircrafts and 80% of certified pilots devoted to general aviation (K. Davis, 2019). While accident rates for commercial aircraft have been hailed as lower, and therefore safer than travel by car, general aviation cannot say the same, with the accident rate per 100,000 flight hours being 36 times higher for general aviation than commercial aviation (Goldman et al., 2002). Two primary approaches have been used to reduce the number of accidents and fatalities in general aviation. The reactive approach determines the possible causes of an accident or incident and makes recommendations to prevent further accidents due to similar causes (Official Guide to Government Information and Services, n.d.). A proactive approach works to prevent accidents through training and dissemination of information.

Most of the preventative training is completed during the initial training for the private pilot license, which is the minimum of the first 40 hours of a pilot's training. After this initial certificate is received, the only other mandatory training for a private pilot is a bi-annual flight review designed to refresh a pilot's memory of their initial training. Therefore, it is important to pay attention to the indicators affecting the likelihood of a dangerous situation during this initial training to reduce the accident rate.

2.1. Human Factors Contribution to Accidents

Human factors are a critical variable for aviation safety; they are variable and include the factors of the pilot, air traffic controllers, and other people when considering the aviation system. Human factors are cited as the cause of approximately 75% of accidents or incidents (Kharoufah et al., 2018). Due to the high volume of situations in which human factors are a cause, pilots are made aware of these factors during training. It is hoped that if pilots can identify these factors, they can mitigate their effects. For example, fatigue has been shown to significantly decrease pilot performance (O'Hagan et al., 2016). Pilots are informed of this and recommended not to fly when fatigued and to plan when they know they

are scheduled to fly to ensure they get enough rest.

These human factors can extend further than physical traits, with factors such as psychology and personality being considered in current research. Temperamental traits have been associated with poor performance under stress and low endurance on long flights (Makarowski et al., 2016); which is an aspect of personality that should be considered when pilots are selected for military missions or other aspects of aviation, where pilots may encounter high stress on long flights. Lower levels of self-confidence and a poor attitude towards safety have been correlated with higher risk-taking tendencies among military pilots (Joseph & Reddy, 2013). The effects of personality traits and personal psychological differences on pilots and air traffic controllers have been extensively studied (D. Davis et al., 2002; Hedayati et al., 2021; Slazyk-Sobol et al., 2021); however, there has not been much research on how this knowledge should be applied to the industry other than increasing awareness.

2.2. Risk and Decision Making

The minimum training required for obtaining a commercial pilot license under Part 61 is 250 flight hours. This minimum might place student pilots in the "killing zone," defined by Craig (2013) as a time window between 50 and 350 total flight hours where most accidents and incidents occur for private or student pilots (p. 2). Knecht's (2013) models support Craig's findings by indicating the existence of a "killing zone": accident rates for general aviation pilots rise early in their post-certification careers, peak, and then fall with more flying experience to a baseline, non-zero value. However, Craig's "killing zone" may be far more significant than anticipated. A significant risk remains well beyond 2,000 flying hours before leveling down to a baseline rate (Knecht, 2013). This may be due to a mismatch between the risk that a pilot is willing to accept and their abilities and experiences. If a pilot believes that they can handle a situation, they may make poor decisions that result in an accident.

In addition, contributing to the level of risk a pilot is willing to accept are the hazardous attitudes that they exhibit. Hazardous attitudes have been identified in aviation as characteristics that may make pilots more likely to exhibit poor decision-making skills. Jensen (1989) published a report on crew resource management and included the five major hazardous attitudes: anti-authority, impulsivity, invulnerability, machoism, and resignation. While these attitudes and their anecdotes are taught in initial flight training, Scharf and Cross (2019) found in an international survey that this training does not fully mitigate the effects of hazardous attitudes and identified weak points including safety orientation, or individual safety attitudes, of pilots. By understanding safety attitudes and how they affect flight training students, better decision-making skills can be developed among pilots.

2.3. Safety Attitudes

Safety attitudes pertain to an individual person's feelings regarding safety issues. Although safety attitudes affect safety culture, and safety culture can affect safety attitudes, they are not equivalent (Homan et al., 1998). Poor safety attitudes can lead to increased risk-taking, which increases the likelihood of an accident occurring. However, not all hope is lost; if lower attitudes towards safety are prevalent, training can be implemented to improve safety attitudes (Cromie, 1997). Detecting these safety attitudes in advance and treating them accordingly through a review of current training programs could potentially reduce accident rates among student pilots.

Unfortunately, safety attitudes have been found to decrease as pilots get further away from training (Börjesson et al., 2011). This can be especially dangerous when a pilot's perceptions of risk, experience, and abilities cannot compensate for poor safety attitudes. Little research has been conducted to examine safety attitudes during training, with the hope of cultivating an individual's safety attitude that lasts longer after the initial training has been completed. This heightened safety attitude would allow not just for a safer aviation environment, but also better performance among pilots due to the link between safety attitudes and pilot performance (Sexton & Klinect, 2017).

Hunter's Aviation Safety Attitudes Scale (ASAS) (1995) was used in this study. While it was initially developed as a measure of engagement in potentially risky behaviors in aviation that do not result in accidents, the ASAS has been used as a proxy for actual accident involvement in studies of risk-taking and hazardous attitudes and was recently reviewed for use in armed forces (D. Hunter & Stewart, 2011). The outcomes may help gain a better understanding of the factors that influence student pilot experience decision-making, as well as their potential relationship with proper safety attitudes. These findings may also aid in demonstrating the adequacy of a revised training program for attitude identification and management.

This study determined whether there was a relationship between pilot experience and pilot attitudes toward safety issues. Although the influence of safety attitudes on performance and safety has been well documented, and research has been conducted on how training can increase safety attitudes, little research has been conducted to understand which segments of the flight training population should be targeted to increase safety attitudes. Due to the lack of research, a better understanding of the relationship between pilot experience and pilot attitudes towards safety issues, especially among both pilots in training and those with higher levels of experience, is needed. In addition, current safety training does not provide ample feedback regarding pilots' safety attitudes of pilots (Scharf & Cross, 2019). Therefore, research is needed to identify deficient safety attitudes, so that steps can be taken to develop a more comprehensive training program.

3. Methods

This was a quantitative correlational study to determine whether there was a relationship between pilot experience and pilot attitudes towards safety issues. Since data was collected via a survey, IRB approval was required and an exemption was granted (#22-100). There was no greater risk to the participants than for normal activities. The survey was anonymous, which further minimized the risk by providing researchers with de-identified data. No video or audio recordings were collected.

A survey was distributed that included both questions from Hunter's Aviation Safety Attitudes Scale (1995) and demographic questions. Pilot experience was measured by asking respondents to report their number of hours of experience in an aircraft and their current ratings and certificates. Students in a collegiate Part 141 program in the Southeastern US were also asked to report the ground training course they were enrolled in. Pilot attitudes toward safety issues were measured using the aviation safety attitude scale developed by Hunter in 1995. In 2005, Hunter measured the internal reliability of each subscale: self-confidence had an internal consistency of α=.76, risk-orientation had an internal consistency of α=.59, and safety-orientation had an internal consistency of α=.40. It also showed validity by comparing the aviation safety attitude survey to the aviation safety locus of control, the new

hazardous attitude scale, and the thrill and adventure-seeking scale, among others (Hunter, 2005). The demographic information included age, biological sex at birth, and typical flight operations.

The first target population was flight students at a southeastern university with a Part 141 flight-training program. Stratified sampling was used to ensure that the representation was given to each experience level. Approximately 500 Part 141 flight training students who are currently registered for core ground courses comprise the student population, with most of the population between the ages of 18 and 25. A minority of students may be over the age of 25 because of the spread of age among students. Individuals younger than 18 years were not eligible to participate in the survey. Sex was not a factor in data recruitment; however, due to the low female-to-male ratio in the aviation industry, counting more male than female students was expected. The accessible population included current flight training students and their personal and professional contacts using social media, email, and a snowball convenience sampling strategy. Participants were recruited by researchers visiting core aeronautics courses (e.g., Aeronautics 1, 2, 3, 4, and instructional techniques), emails distributed to collegiate Part 141 flight school employees, and emails distributed to college faculty and alumni.

This study utilized a survey methodology and correlational design. Ground-training instructors were emailed to ask for consent to visit each class to distribute the survey. A survey was distributed to Part 141 collegiate school students, employees, and alumni, and their professional contacts to collect the data. All participants were asked to distribute the survey to any contacts that fit the selection criteria.

All data was downloaded from Qualtrics into an Excel file. Cronbach's alpha was calculated to determine the internal reliability. The safety attitude scores were calculated following Hunter (1995) by converting the worded Likert scale to numerical values, with strongly disagree (1) to strongly agree (5). After converting to numerical values, the aviation safety attitude scale item responses were totaled to determine the total score on Hunter's (1995) ASAS. Descriptive statistics were calculated using Microsoft Excel. These statistics include the mean, median, mode, range, and standard deviation of the responses. Inferential statistical analyses were performed using the R Studio version 4.2.0. Cronbach's alpha was calculated to determine the internal validity. Pearson's r product moment was used to determine the correlation between pilot experience and safety attitudes.

4. Results

A total of 175 responses were collected, with a response rate of 52.3% compared to the total population. Twenty-one responses were excluded, due to incomplete surveys (18) and age < 18 years (1) or > 100 years (2). There were eight participants whose data were excluded from the analysis because of outliers in the number of flight hours. After these exclusions, 140 responses were analyzed.

The average age of the participants was 20.11 years old, with a minimum of 18 years and a maximum of 31 years. Males (78%) were more represented than females (20%), which is consistent with the aviation industry and accessible population. Three participants did not report sex. Geographic data was also collected by region; regions are detailed in Figure 1. Participants from the southeastern region of the United States were over-represented when compared to population data from the U.S. Census Bureau (2020 Census); however, it is worth noting that participants from the northeastern region of the United States were also well represented (see Figure 2).

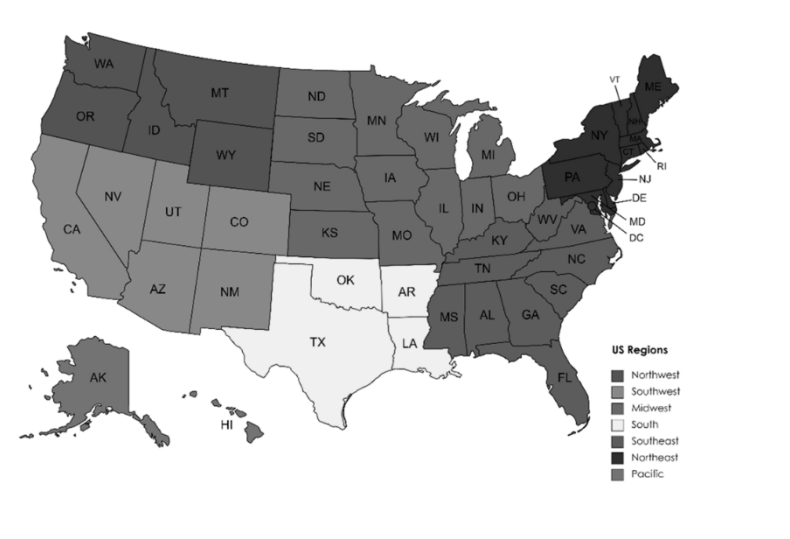

Figure 1. Detailed Region Information for Geographic Data

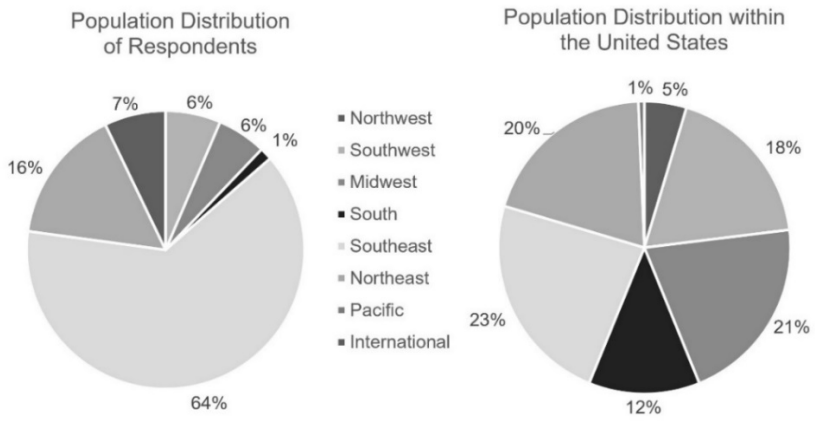

Figure 2. Comparison Between Study Sample and United States Population

Note. Reponses by international residents were also included. There were also no respondents from the Northwest or Pacific region. Data for population distribution within the United States are from the 2020 U.S. Census.

Descriptive statistics were computed for the total ASAS score and the number of flight hours reported. The experience level was bimodal at 15 and 90 hours and ranged from 0 to 500 hours (M = 109 hours, SD = 99). The total ASAS score was 87, ranging from 58 to 113 (M = 90.8, SD = 9.3). When the total ASAS score was compared to the experience level in hours, the relationship was weakly linear, as shown in Figure 3.

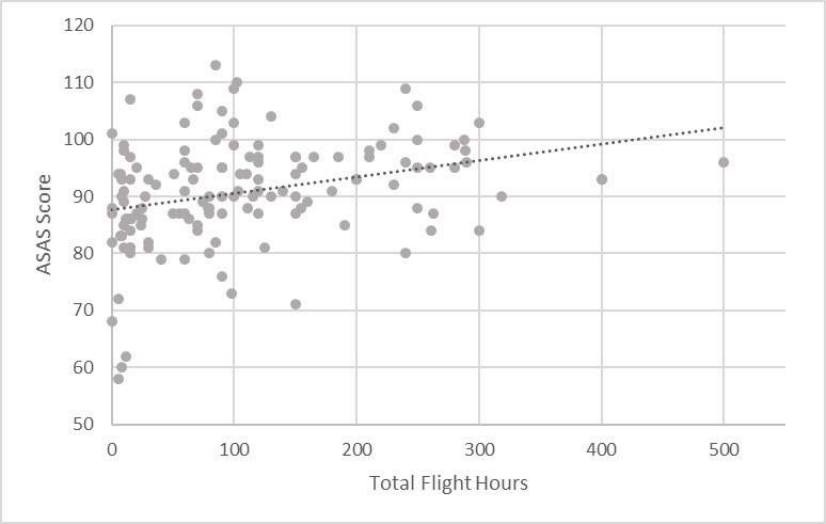

Figure 3. Flight Hours vs. Aviation Safety Attitude Score

Respondents also noted the ground training course in which they were enrolled, from private pilot to flight instructor. Although new knowledge is taught in each class, no significant difference was noted between the classes, as shown in Figure 4.

Cronbach's alpha showed an internal consistency of .71, which was acceptable. Pearson's product moment correlation was statistically significant and positive, but weak, r = .31 (p =.0002).

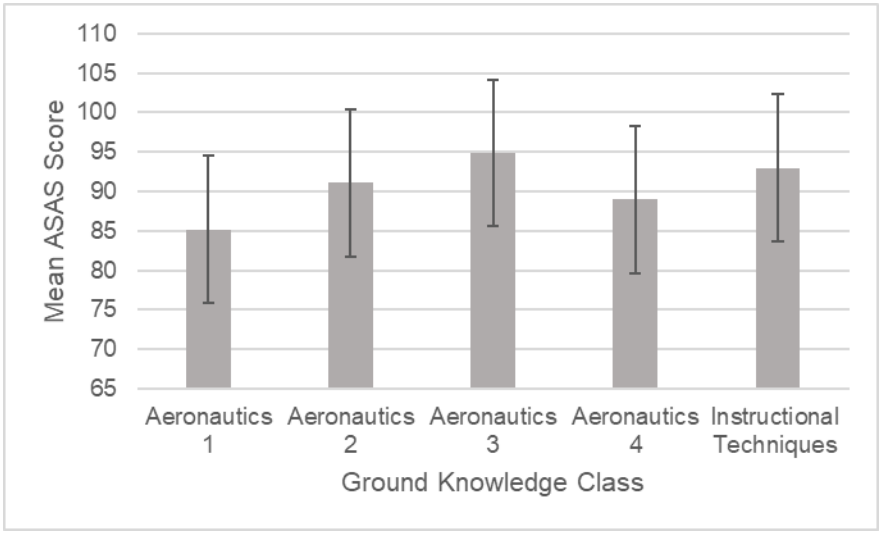

Figure 4. Ground Knowledge Class vs. Mean ASAS Score

5. Discussion

The null hypothesis, that there is no relationship between pilot experience and safety attitude was rejected (p = .0002). The flight hours reported by participants showed an average flight experience of slightly above 100, which placed them in the "killing zone, " as defined by Craig (2013). The relationship between these flight hours and the ASAS scores suggests a possible correlation between lower pilot

flight experience and a riskier approach to safety. However, the relationship was weak (r =.31), allowing only a cautious interpretation of the data. It is interesting to note that the lowest ASAS scores within the sample were provided by participants with a small number of flight hours at the start of training and participants with more than 300 flight hours who had completed most of their training. However, lower ASAS scores were not widely present among students currently in the training.

As multiple participants completed the survey during the in-class sessions, it is possible that the results were influenced by time restrictions, for example, when nearing the end of the time allocated to them. Previous research (Joseph & Reddy, 2013) has shown the ASAS to be a reliable test; however, it may not be sensitive enough to detect a large difference in attitude among pilots with a similar number of flight hours. The study was limited by online recruitment, which is influenced by the limited distribution time and accessible populations. Other limitations to data collection included missing data and dropout rates from the study by participants who did not complete all the online questions. In addition, this study was only geographically representative of the southeastern and northeastern United States, and the sample only included students from a collegiate Part 141 population.

Future research should determine whether there is a more accurate predictor of safety attitudes among the pilots. Research should determine the difference in the relationship between the given sample and a wider population, including more experienced pilots, Part 61 pilots, and a larger geographical region. Future research at the same college may also help to monitor the safety attitudes of pilots at this institution over time and allow the safety curriculum to change as the environment changes.

Overall, this study has added aviation knowledge and may be beneficial both in its own right and as a catalyst for subsequent research. The relationship discovered through this study is just the beginning of understanding the potential causes for pilots' safety attitudes and has the potential to improve safety for all pilots.

6. References

Börjesson, M., Österberg, J., & Enander, A. (2011). Risk and Safety Attitudes Among Conscripts During Compulsory Military Training. Military Psychology, 23(6), 659–684. https://doi.org/10.1080/08995605.2011.616815

Craig, P. (2013). The Killing Zone: How and Why Pilots Die (2nd ed.). McGraw-Hill Education.

Cromie, S. (1997). The impact of safety training on safety climate and attitudes. 649–660.

Davis, D., Mihalecz, M. C., & Schutte, P. C. (2002). Personality as it Relates to Decision Making, Information Processing and Error Management in Commercial Aviation. https://ntrs.nasa.gov/citations/20020067405

Davis, K. (2019). State of General Aviation (p. 18). Airplane Owners and Pilots Association.

Goldman, S. M., Fiedler, E. R., & King, R. E. (2002). General Aviation Maintenance- Related Accidents: A Review of Ten Years of NTSB Data (DOT/FAA/AM-02/23; p. 14).

Hedayati, S., Sadeghi-Firoozabadi, V., Bagheri, M., Heidari, M., & Sze, N. N. (2021). Evaluating differences in cognitive functions and personality traits among air traffic controllers with and without error history. Safety Science, 139, 105208. https://doi.org/10.1016/j.ssci.2021.105208

Homan, W. J., Rantz, W. G., & Balden, B. R. (1998). Establishing a Total Safety Culture within a Flight Department. Journal of Aviation/Aerospace Education & Research, 8(2). http://www.proquest.com/ataindex/docview/1689580834/abstract/98FFB5F8E1B54FC6PQ/9

Hunter, D. R. (1995). Airman Research Questionnaire: Methodology and Overall Results (DOT/FAA/AM-95/27; p. 69).

https://www.faa.gov/data_research/research/med_humanfacs/oamtechreports/1990s/media/am95-27.pdf

Hunter, D., & Stewart, J. (2011). Hazardous Events and Accident Involvement by Military and Civilian Pilots. The International Journal of Aviation Psychology, 21, 123–134. https://doi.org/10.1080/10508414.2011.556451

Jensen, R. S. (1989). Aeronautical Decision Making—Cockpit Resource Management. Systems Control Technology. https://apps.dtic.mil/sti/citations/ADA205115

Joseph, C., & Reddy, S. (2013). Risk Perception and Safety Attitudes in Indian Army Aviators. International Journal of Aviation Psychology, 23(1), 49–62. https://doi.org/10.1080/10508414.2013.746531

Kharoufah, H., Murray, J., Baxter, G., & Wild, G. (2018). A review of human factors causations in commercial air transport accidents and incidents: From to 2000–2016. Progress in Aerospace Sciences, 99, 1–13. https://doi.org/10.1016/j.paerosci.2018.03.002

Knecht, W. R. (2013). The "killing zone" revisited: Serial nonlinearities predict general aviation accident rates from pilot total flight hours. Accident Analysis & Prevention, 60, 50–56. https://doi.org/10.1016/j.aap.2013.08.012

Makarowski, R., Makarowski, P., Smolicz, T., & Plopa, M. (2016). Risk profiling of airline pilots: Experience, temperamental traits and aggression. Journal of Air Transport Management, 57, 298–305. https://doi.org/10.1016/j.jairtraman.2016.08.013

Official Guide to Government Information and Services. (n.d.). National Transportation Safety Board. Retrieved October 2, 2022, from https://www.usa.gov/federal-agencies/national-transportation-safety-board

O'Hagan, A. D., Issartel, J., Fletcher, R., & Warrington, G. (2016). Duty hours and incidents in flight among commercial airline pilots. International Journal of Occupational Safety and Ergonomics, 22(2), 165–172. https://doi.org/10.1080/10803548.2016.1146441

Scharf, M. T., & Cross, J. D. (2019). Analysis of Low-Time Pilot Attitudes in University Aviation Association Member Flight Schools. The Collegiate Aviation Review International, 37(2), Article 2. https://doi.org/10.22488/okstate.19.100216

Sexton, J. B., & Klinect, J. (2017). The link between safety attitudes and observed performance in flight operations. Human Error in Aviation.

Slazyk-Sobol, M., Dobrowolska, M., & Flakus, M. (2021). Predictors of the Feeling of Stress in the Aviation Sector. Medycyna Pracy, 72(5), 467–478. https://doi.org/10.13075/mp.5893.01084

U.S. Census Bureau. (2020). Census Bureau Data. https://data.census.gov/cedsci/

Willingness to Fly in an Electric Aircraft

Brooke E. Wheeler[1]
Saud Binhalil
Mohammed Mallah
Luis Tobar
[1]*Florida Institute of Technology*
Melbourne, FL. 32901
bwheeler@fit.edu

Abstract

This study examined US consumers' willingness to fly in an electric aircraft and an aircraft with an internal combustion engine for either one hour or 30-minute flight durations. The participants were provided with four different scenarios: electric engine 30-minute flight, electric aircraft one hour, combustion engine 30 minute, and combustion engine one hour. The scenarios were delivered in a random order to avoid order effects, and each flight scenario explained that the weather was clear and calm and had a knowledgeable pilot. The U.S. Amazon Mechanical Turk (MTurk) consumers' willingness to fly showed no significant differences between type of engine or duration of flight. On average, the participants were willing to fly in electric aircraft, which is promising for the aviation industry.

Keywords: Electric aircraft, willingness to fly, aviation consumers.

1. Introduction

With the current push towards sustainability and interest in developing Urban Air Mobility, aviation is focused on developing new aircraft. Currently, there are several functional electric aircraft, including both electric vertical take-off and landing (eVTOL) aircraft and fixed-wing electric aircraft. Companies such as Beta, Eve, Joby, Pipistrel, and others are actively pursuing electric aircraft, and the Pipistrel Velis Electro is already certified in Europe, and operating in the US under experimental research and development certificates. Additionally, research has demonstrated that the power output of batteries in electric aircraft is not always as expected and decline in state of charge is not linear especially at lower battery levels (Cunha et al., 2023), which means pilots will need to adjust their fuel planning and be trained to make decisions based on the new propulsion type. The aviation industry is at a point where consumer perceptions need to be monitored, as these aircraft become more common and are integrated into our airspaces.

The purpose of this study was to determine whether there was a difference in willingness to fly (Rice et al., 2020) in an electric aircraft as opposed to an aircraft with a combustion engine for either 30 minutes or one-hour flight. Participants were recruited from among US users of Amazon MTurk. The study used a questionnaire that included four hypothetical scenarios involving an electric aircraft and an aircraft with an internal combustion engine; the length of the flight was either 30 minutes or one-

Submitted: June 30, 2023
Revised: November 12, 2023

hour.

This study captured aviation consumers' willingness to fly at this moment in time, as electric aircraft become more available; the data can help the aviation industry learn consumer opinion towards electric aircraft. This is a starting point for consumer perceptions that can and should be followed over time because no electric aircraft is currently certified in the US. The results of this study were generalizable to American aviation consumers aged 18 years or older.

2. Literature Review

This section reviews previous research related to variables that may influence participants' decision-making when assessing their willingness to fly. Topics include internal combustion engine aircraft, environmental concerns with aviation, electric aircraft, and willingness to fly.

2.1. Internal Combustion Engine Aircraft

Internal combustion engine aircrafts have been the most common aircraft among the public for a long time. This aircraft is mainly used in the general aviation sector because jet aircraft use the same concept of supercharge or turbocharge. Aircraft combustion begins inside the engine and exits the plane through the exhaust pipe. Research on internal combustion explains the safety and efficiency of combustion aircraft certified by the FAA (Masiol & Harrison, 2014). However, Masiol and Harrison found that aircraft combustion engines are causing a critical issue with greenhouse gasses due to exhaust emissions. They reported that the strongest gas emission caused by this engine is CO2, which will increase global warming annually and cause climate change. Masiol and Harrison (2014) mentioned that aviation consumed 5.8% of the total oil in the world based on OPEC data from 2006. This massive fuel use reflects the global gas cost in the future.

Another study discussed the issue of combustion engine aircraft and their impact on the environment due to gas emissions from fuel combustion (Colvile et al., 1970). Air pollution comes from airports and aircraft, which makes this study focus more on the air transport sector. The results of the case study showed that the most influential gases emitted from aircraft are nitrous oxides, which cause global warming, in addition to the development of ozone.

2.2. Aviation and Environmental Impact in Decision Making

The aviation industry plays a vital role in increasing environmental impacts, such as global warming. Carbon dioxide is the most widely discussed greenhouse gas for global warming. In addition, nitrogen dioxide, which airplanes release into the atmosphere, there are many other emissions of concern. These gases are harmful to the environment and cause climate change (Rosanka et al., 2020). On the other hand, Automobiles use gasoline, which evaporates into the atmosphere, making up a significant proportion of emissions. In fact, 33% of carbon emissions are from automobiles (Nwona, 2013).

Given that the effects of aircraft emissions continue to accumulate over time, it is essential to study how this can influence people's decisions to choose an environmentally friendly alternative. People's decisions differ because of their different backgrounds and beliefs. Decisions are impacted by the number of alternatives the consumer receives (Bettman et al., 1991). In addition, decisions can be biased based on the options and deals they receive. Berger et al. (2022) measured one of the European airlines'

passengers' willingness to pay more to offset their flight emissions. There were 63,520 passengers in this study; however, only 4.46% decided to offset their flights (Berger et al., 2022). This illustrates that people are not willing to pay more to offset their flight emissions.

2.3. Electric Aircraft

Although multiple avenues are being pursued in aviation to decarbonize the industry and reduce the environmental impact of aviation. Electric aircraft already exist and are being promoted as a next step for aircraft development, particularly in urban air mobility settings. Kozakiewicz and Grzegorczyk (2021) described and explained the concept of electric aircraft growth. They state that electric aircraft would help reduce air pollution and minimize noise pollution. In addition, they split electric aircraft into three types: hybrid electric, turbo electric, and all-electric. The first two types combine traditional turbo engines and electric energy engines. All electric aircraft have electric energy as the primary source for the engine (Kozakiewicz & Grzegorczyk, 2021). However, they found that electric aircraft are expanding, especially in general aviation. Still, the only aircraft certified by the European Aviation Safety Agency (EASA) is the Pipistrel Velis Electro; this aircraft received the approval and certificate in 2020. Kozakiewicz and Grzegorczyk claimed a Pipistrel aircraft could provide a 50-minute flight time and still have the required 10-minute reserve under EASA regulations. The cruising speed of the aircraft was 160 km/hr. However, at this stage, few commercial aviation companies are developing applications and plans to transfer their aircraft to an all-electric engine.

On the other hand, Sarlioglu and Morris (2015) addressed the difficulties that could be faced by More Electric Aircraft (MEA) for commercial transport. They discussed how conversion to an electric engine would have challenges, for example, the engine's efficacy and size. To generate a powerful generator for the engine during flight, the primary onboard generator size should be increased. Another challenge is that the new electric system requires a function or a control system to maintain a safe temperature when climbing to higher altitudes to ensure the separation module (Sarlioglu & Morris 2015). Additionally, there are challenges in retraining pilots in decision making, to ensure that they understand remaining power availability when battery state of discharge is not linear and full power may not be available at low charge when a safety-critical go-around may be required (Cunha et al., 2023). Electric aviation is already feasible with many benefits, but still has challenges remaining in its development.

2.4. Fear of Flying

In addition to environmental impact, another factor that can and does impact the decision to fly is fear of flying. Half of the world's population shows some level of fear of flying (Fleischer et al., 2012), making this a common and widespread influence. Different factors have been evaluated that trigger the level of fear of flying, including terrorist events such as 9/11, which resulted in a sharp decrease in the demand for flights. Passengers who show symptoms of fear of flying tend to have different features that alleviate their level of fear, such as non-stop flights and home carriers. According to Fleischer et al. (2012), these attributes are considered when booking flights, in addition to pricing, and carrier preferences. Fleischer and colleagues also found that people are more willing to pay an additional cost for risk reduction when traveling by air compared to other means of travel, such as taxis. Another factor contributing to the fear of flying is that some people fear dying while traveling (Oakes & Bor, 2010). However, the aviation industry has demonstrated that air travel is safer than cars.

2.5. Willingness to Fly and Risk Acceptance

Rice et al. (2020) developed two measures: a passenger willingness to fly scale and a willingness to pilot scale. They highlighted that consumer willingness to fly could be difficult to measure but useful in aviation. Therefore, they used a multi-stage process to develop the instruments: generation of a broad list of potential items, testing with a large sample of participants to narrow down the items, factor analysis, and sensitivity testing. This resulted in a seven-item willingness to fly scale that has been validated. The scale had a high internal reliability with a value of .96 for Guttmann's split-half test (Rice et al., 2020). The researchers also posited that MTurk has been widely used and has since been developed to assist in conducting electronic surveys (Rice & Winter, 2020).

Winter et al. (2020) examined the impact of propulsion systems on willingness to fly using a hypothetical scenario. They determined that people are familiar with sustainable alternatives and willing to pay to reduce environmental impacts, such as traveling by electric or solar aircrafts. This study also indicated that consumers preferred traditional fuel, biofuel, and then electric options. Mayer et al. (2012) examined passenger perception towards different airlines and determined that although passengers may be able to differentiate airlines based on environmental friendliness, their perceptions vary depending on their flying history and whether they have flown with a particular airline before. Thus, air travel history can impact decision-making regarding preferences for environmentally friendly aircraft.

The willingness to fly scale (Rice et al., 2020) has been used to measure Amazon MTurk participants' willingness to fly, making it ideal for the current investigation. Some factors may contribute to willingness to fly, such as the fear of flying, environmental considerations, and overall risk acceptance. The aviation industry's contributions to greenhouse gases and to global warming has led to consumer concern over environmental impact and some research indicating that passenger would even pay more for an environmentally friendly option. A sustainable alternative for combustion aircraft would help decrease the emissions that evaporate into the atmosphere. Electric aircraft are an alternative to combustion aircraft, which can help to minimize noise and emissions impacts (if renewable energy is used to charge them). In the United States, no electric aircraft have been certified to date. Therefore, the willingness of consumers to fly in electric aircraft is unknown and needs to be quantified and monitored as more electric aircraft are developed, certified, and put into use.

3. Methods

This within-subjects design used a questionnaire and standard survey methodology. The dependent variable was willingness to fly, which was measured using the seven-item scale developed by Rice et al. (2020). The independent variables were the flight duration, either 30 min or 1 hr, and the type of aircraft, electric, or internal combustion. The specific aircraft were selected as equivalent versions with the mode of propulsion being the main difference: a) Pipistrel Velis Electro– Electric motor – Powered by two batteries - Two seats, light sport aircraft, and b) Pipistrel Velis Club– Internal Combustion Engine – Powered by AVGAS - Two seats, light sport aircraft. Participants were presented with four flight scenarios (both aircraft in the 30 min and 1 hr flights) in a random order to avoid any order effects.

The target audience was American air travelers, and the accessible audience was American users of MTurk. The study recruited users of MTurk, who were in the United States, 18 years or older, and had a

minimum positive rating of 75 % on prior MTurk jobs. The a priori power analysis indicated that at least 108 participants were required to have sufficient power. An IRB exemption was received (22-102) prior to commencing the project. Participation was voluntary and anonymous, and upon completion, participants were compensated through MTurk.

Data were collected via an electronic questionnaire using Qualtrics, and researchers downloaded the raw data into an Excel spreadsheet. Likert-style responses were converted to numerical values as follows: Strongly Disagree -2, Disagree -1, Neutral 0, Agree 1, and Strongly Agree +2. Descriptive statistics, including the mean, median, mode, range, and standard deviation, were calculated using Microsoft Excel. Cronbach's alpha and a 2-way repeated measures ANOVA were analyzed in R Studio version 2022.07.2.

4. Results

The *a priori* power analysis indicated a minimum sample size of 108 participants; 209 participants (70 females, 139 males) completed the questionnaire on MTurk. All participants were 18 years old or older; however, the 22-29 years old category had the most participants (Table 1). Participants (N = 196) reported the number of flights they typically take per year on commercial airlines (Figure 1). Participants predominantly reported that environmental impact is a concern in their travel-making decisions: 75% yes, 23% no, and 2% prefer not to say.

Age Range	Participants
18-21 years	5
22-29 years	88
30-39 years	66
40-49 years	26
50+ years	24

Table 1. Participants by Age Category

Cronbach's alpha for scenarios 1, 2, 3, and 4 was .90, .91, .90, and .90, respectively. All scenarios demonstrated high internal reliability for the willingness to fly scale; therefore, the average of all seven items was calculated as the willingness to fly for each scenario and was used for all calculations.

The descriptive statistics are shown in Table 2 and Figure 2. They illustrate that there is little difference in the willingness to fly in electric versus combustion aircraft or in different flight durations (30 min or 1 hr). Figure 2 shows that the willingness to fly was positive (1 = agree) in all scenarios.

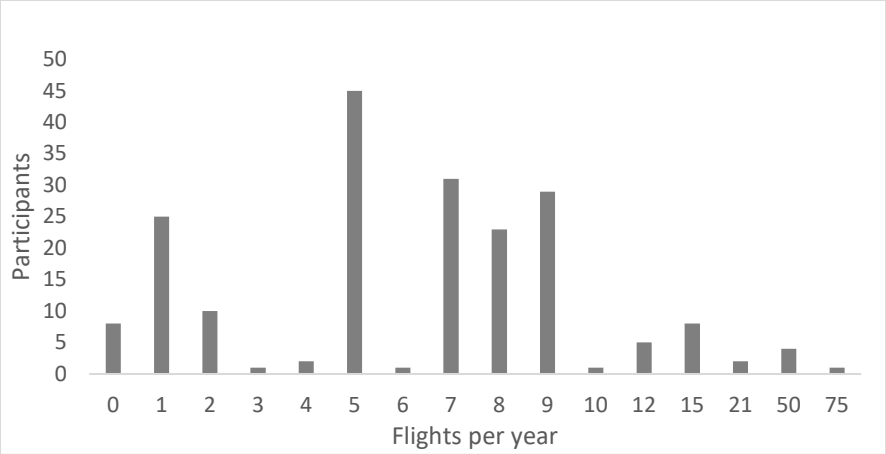

Figure 1. Number of participants by annual flights.

Note: Participants reported the number of flights they took on commercial airliners in a typical year.

Scenario	Mean	Mode	Median	Standard deviation	Minimum	Maximum
1. PV Club 1hr	0.90	1	1	0.76	-2	2
2. PV Electro 1hr	0.90	1	1	0.78	-2	2
3. PV Electro 30min	0.90	1	1	0.76	-2	2
4. PV Club 30min	0.90	1	1	0.72	-2	2

Table 2. Descriptive statistics for willingness to fly by scenario.

Note: Scenarios 1 and 4 (grey highlight) were in the Pipistrel Velis Club, a light sport aircraft with a combustion engine and two seats. Scenarios 2 and 3 were in the Pipistrel Velis Electro, a light sport aircraft that has an electric motor powered by two batteries and two seats.

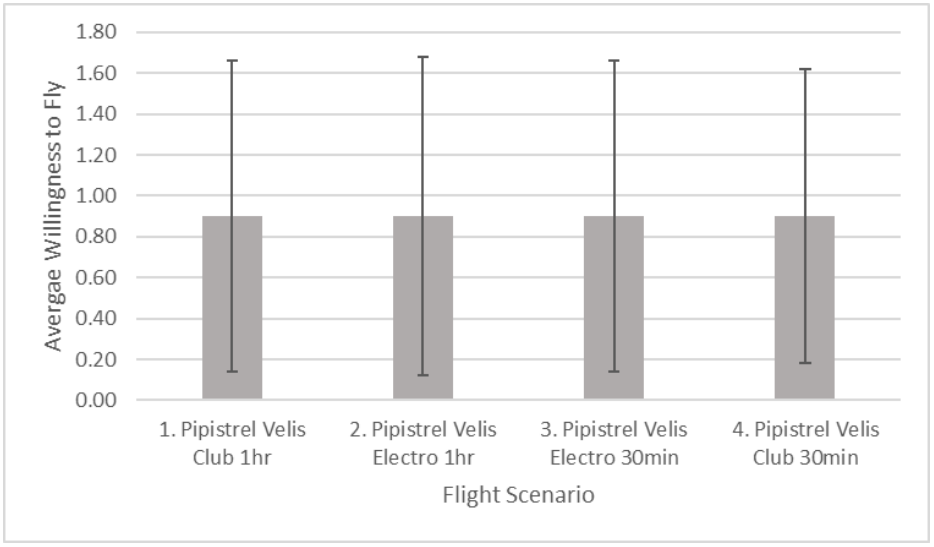

Figure 2. Average willingness to fly by flight scenario.

Note: Error bars represent one standard deviation above and below the mean. Willingness to fly ranges from -2, Strongly Disagree, to 2, Strongly Agree. Scenarios 1 and 4 were in the Pipistrel Velis Club, a light-sport aircraft with a combustion engine and two seats. Scenarios 2 and 3 were in the Pipistrel Velis Electro, a light sport aircraft that has an electric motor powered by two batteries and two seats.

The repeated measures 2-way ANOVA indicated no significant difference in the willingness to fly between the two aircraft types, $F(1, 828) = 0.12$, $p = .72$. There was no significant main effect of flight length on the willingness to fly, $F(1, 828) = 0.37$, $p = .54$. Moreover, the interaction between type of aircraft and duration of flight was not significant, $F(1, 828) = 0.005$, $p = .95$. The partial eta squared was less than 0.005, indicating a small effect size.

5. Discussion

The sample contained responses from 209 participants (66.5% male) from the US, and only eight of these reported flying zero flights in a typical year (Figure 1), which is noteworthy given that travel on airlines decreased during the COVID-19 pandemic. The frequency distribution in Figure 1 indicates a cross-section of the annual frequency of travel from zero to 75 flights per year. This points to a sample that likely represents the range of the American flying public regarding frequency of travel but captured more responses from men than would be representative. Additionally, 75% of the sample were concerned with the environmental impacts of their travel decisions.

The willingness to fly scale (Rice et al., 2020) was highly consistent across all four scenarios, illustrating internal consistency. The results were somewhat unexpected because the participants were approximately equally willing to fly in all scenarios (Figure 2 and Table 2). Willingness to fly was 0.90 (~agree) in all scenarios, suggesting that the American public is moderately willing to fly in a light sport aircraft with either type of engine: electric or combustion. The 2-way repeated measures ANOVA indicated that neither independent variable (engine/time) significantly affected the participants' willingness to fly, meaning that participants were equally willing to fly in an aircraft with an electric motor and combustion engine, and both durations of flights (Figure 2). There was also no significant interaction between independent variables. This means that the data support the null hypothesis that there is no difference in willingness to fly in electric versus combustion aircraft, nor between 30 min and 1hr long flights.

There are several plausible explanations for these results. First, because there are no certified electric aircraft in the US at this point in time, the lack of familiarity with either electric propulsion or light sports aircraft may have influenced the responses. Second, because major manufacturers (e.g., Tesla, Nissan, Rivian, General Motors, and Ford) are producing electric vehicles, and they are now fairly common in the US, participants may already be comfortable with the idea of electric motors and battery-powered vehicles. Third, for the duration of flight, we expected to see an effect such that there was lower willingness to fly with the longer flight time, given that 1 hr would be approximately the maximum flight time for a Pipistrel Velis Electro (depending on weather, weight, mission, etc.). The lack of knowledge of battery limitations is the most likely explanation for the lack of difference in willingness to fly between these conditions; essentially, the American public is currently unaware of risks with other modes of propulsion in aircraft. Fourth, most of the sample (75%) expressed concern for environmental impact with their travel decisions, which may have led to a more positive perception of electric aircraft. Berger

et al. (2022) examined whether travelers were willing to pay more to offset their flight emissions, acting to support their expressed environmental concerns, and found that less than 5% agreed to pay more to offset their flight emissions. The Berger et al. study showed that people care about the environment but are not willing to pay more to offset their flight emissions. Unlike the willingness to pay research, our study did not detect any difference in willingness to fly between an aircraft with a combustion engine and an electric motor, despite consumer reported environmental concern.

This study examined consumers' willingness to fly in an electric aircraft as opposed to a combustion aircraft for both 30 min and 1 hr long flights. We determined that US adult air travelers are, on average, willing to fly in both aircraft types and flight durations. Overall, these results are extremely positive for the aviation industry. In all scenarios, the electric motor and combustion engine, and both 30 min and 1 hr duration flights, US consumers demonstrated a positive willingness to fly. This indicates an openness to travel as a passenger on aircraft with new forms of propulsion and fuel, specifically electric motors powered by batteries. In addition, it supports the trend of manufacturing and certifying electric aircraft.

As electric aircraft become certified in the US and aviation also pursues hybrids and aircraft with other forms of propulsion to improve sustainability, it is increasingly important to gauge consumer perception and track willingness to fly over time. The results of this research can form both a baseline and a stepping-off point for future examinations of aviation consumer perceptions, specifically willingness to fly in particular aircraft as they enter our fleet. Future research could examine willingness to pay more to travel with an electric aircraft and other options to promote aviation sustainability.

6. References

Berger, S., Kilchenmann, A., Lenz, O., & Schlöder, F. (2022). Willingness-to-pay for carbon dioxide offsets: Field evidence on revealed preferences in the aviation industry. *Global Environmental Change*, *73*, 102470. https://doi.org/10.1016/j.gloenvcha.2022.102470

Bettman James R., Johnson Eric J., and Payne John W. (1991), "Consumer Decision Making," in Handbook in Consumer Behavior, Robertson Thomas S., and Kassarjian Harold H., (eds.), Englewood Cliffs, NJ: Prentice-Hall, Inc., 50–84.

Colvile, R. N., Hutchinson, E. J., Mindell, J. S., & Warren, R. F. (1970, January 1). The transport sector as a source of Air Pollution. UCL Discovery. Retrieved October 14, 2022, from https://discovery.ucl.ac.uk/id/eprint/894/

Cuhna, D., Wheeler, B., Silver, I., & Andre, G. (2023). Electric aircraft battery performance: examining full discharge under two conditions. *International Journal of Aviation Science and Technology (IJAST)*. *4*(1): 5-13. DOI: 10.23890/IJAST.vm04is01.0101

Fleischer, A., Tchetchik, A., & Toledo, T. (2012). The Impact of Fear of Flying on Travelers' Flight Choice: Choice Model with Latent Variables. *Journal of Travel Research*, *51*(5), 653–663. https://doi.org/10.1177/0047287512437856

Kozakiewicz, A., & Grzegorczyk, T. (2021). Electric Aircraft Propulsion. *Journal of KONBiN*, *51*(4), 49–66. https://doi.org/10.2478/jok-2021-0044

Masiol, M., & Harrison, R. M. (2014). Aircraft engine exhaust emissions and other airport-related contributions to ambient air pollution: A review. *Atmospheric Environme*nt, *95*, 409-455.

Mayer, R., Ryley, T., & Gillingwater, D. (2012). Passenger perceptions of the green image associated with airlines. *Journal of Transport Geography*, *22*, 179–186.

Nwona, H. A. (2013). Climate change: causes, effects and the need for science education for sustainable development. *Mediterranean Journal of Social Sciences*, *4*(8), 35.

Oakes, M., & Bor, R. (2010). The psychology of fear of flying (part I): A critical evaluation of current perspectives on the nature, prevalence and etiology of fear of flying. *Travel Medicine and Infectious Disease*, *8*(6), 327-338. https://doi.org/10.1016/j.tmaid.2010.10.001

Rice S., & Winter S.R. (2020) A practical guide for using electronic surveys in aviation research: best practices explained. *The International Journal of Aviation, Aeronautics, and Aerospace*. *7*(2):1–21.

Rice, S., Winter, S. R., Capps, J., Trombley, J., Robbins, J., Milner, M., & Lamb, T. L. (2020). Creation of Two Valid Scales: Willingness to Fly in an Aircraft and Willingness to Pilot an Aircraft. *International Journal of Aviation, Aeronautics, and Aerospace*, *7*(1). https://doi.org/10.15394/ijaaa.2020.1440

Rosanka, S., Frömming, C., & Grewe, V. (2020). The impact of weather patterns and related transport processes on aviation's contribution to ozone and methane concentrations from NOx emissions. *Atmospheric Chemistry and Physics*, *20*(20), 12347-12361. https://doi.org/10.5194/acp-20-12347-2020

Sarlioglu, B., & Morris, C. T. (2015). More electric aircraft: Review, Challenges, and opportunities for commercial transport aircraft. *IEEE Transactions on Transportation Electrification*, *1*(1), 54–64. https://doi.org/10.1109/tte.2015.2426499

Winter, S. R., Lamb, T. L., & Baugh, B. S. (2020). Passenger perceptions on sustainable propulsion systems: which factors mediate or moderate the relationship? *International Journal of Sustainable Aviation*, *6*(3), 195-219. https://doi.org/10.1504/IJSA.2020.112111

Mismanagement of Technology

Gordon W. Arbogast[1]
Arpita Jadav[1]
[1]*Jacksonville University*
Jacksonville, FL, USA
garboga@ju.edu; ajadav@ju.edu

Abstract

This is a paper that investigates how major problems in corporations can occur if the Management of Technology is not properly administered. The purpose of this paper is to review large firms and people that relied on technology and who had serious failures caused by mismanagement. Such mismanagement had a variety of causes such as incompetence, poor ethics, abuse, and outright corruption. Over the years there have been individuals and firms who have been seriously sanctioned based on crimes such as fraud. This paper focuses on some of the most egregious cases that have occurred during the past four decades.

This manuscript documents a considerable number of major corporations that experienced such problems and suffered subsequent profound consequences. Two that are examined in detail are Volkswagen and Theranos. These two firms provide significant illustrations of how mismanagement of technology was a prime factor that caused catastrophic failure in their operations. Enough other big firms that are cited lead to the inference that mismanagement of technology was involved on a major scale.

Keywords: Mismanagement, A Ponzi scheme, The digital revolution, Corruption.

1. Background

Technology has been expanding exponentially over the past forty years. Even if a firm is not a technology firm per se, it has not been immune to the effect that the Digital Revolution, rapid growth of computers, software systems, the Internet, Web Sites and apps, cell phones, social media and other forms of newer technologies has had on all firms. Use of these technologies has been integrated into virtually all strategic actions that firms use daily to achieve success in their respective businesses. Mismanagement of technology in corporations needs to be examined, as it may well have played a key role in the failure of some of these firms. This paper looks at a number of failed major firms and individual entrepreneurs to determine if the mismanagement of technology may have been a factor in their demise.

A variety of companies that potentially failed due to their mismanagement of technologies cover a wide spectrum. A number will be mentioned in this study. The Literature Review primarily covers major firms that failed in the latter part of the 20th century. Then moving into the early part of the 20th Century, there are several major firms that will be discussed that appear to have failed partly due to

Submitted: July 7, 2023
Revised: November 17, 2023

the mismanagement of technology. The major portion of the study will cover a new major factor that needs to be examined i.e., the increasing mismanagement of ethics and its interaction with technology in major corporations. Several firms that will be discussed include several of the major banks in the 2008-2011financial crisis e.g., Moody's, Fannie Mae, Bear Stearns, Goldman Sachs, and AIG. The rest of the paper will deal in more detail with a variety of firms and individuals that also had mismanaged technology i.e., Volkswagen and Theranos. These will be looked at in some detail. The recent Bitcoin scandals using Blockchain technology are also of some note. One individual that is singled out for his mismanagement of technology is Bernie Madoff. His $20 Billion Ponzi scheme was a particularly egregious example of how one individual defrauded thousands of investors of their hard-earned money.

2. Literature Review

In the years leading up to 2000, there were a respectable number of company failures due to the poor management of technology. These failures involved a variety of reasons that seem to come under the heading of mismanagement of technology. Some of these reasons were management's inability: (a) to recognize that the mismanagement of technology resulted in poorly designed products; (b) to determine that the technology was not mature enough "for prime time"; (c) to properly estimate the large costs that would be involved in the development, production and operations of products using the newer technology; and lastly (d) to recognize that in the firm's industry that there had been a paradigm shift to newer technology that was replacing a firm's older, established technology.

First, poorly designed products will be addressed. Personal computers (PCs) and cell phones began to appear on the market in the early 1980s. PCs immediately experienced a good deal of competition, as firms were anxious to take the lead in this new market. The market quickly became flooded with devices such as the Altair, Commodore 64, Kaypro II, the Apple II, the Tandy TRS-80, the Texas Instrument TI 99/4, the Atari 400, and the IBM PC Jr. With IBM mainframe dominance achieved in the 1960s, the computer industry was known as "IBM and the seven dwarfs"- the dwarfs being Burroughs, UNIVAC, NCR, Control Data, Honeywell, General Electric and RCA. However, in 1982 IBM was not really committed to their first PC- the PC Jr. Announced in November 1983, it sold only 270,000 units by 1985 and was discontinued in 1985 (Cringely, 2014). There were several factors cited for its failure. The biggest was that it was poorly engineered and designed. IBM also failed to market it properly and provided inadequate developer support. The weak backing of the PC Jr. by IBM management illustrates its mismanagement of the technology. The PC Jr. was a device that IBM produced without lofty expectations. To them the computer world was defined by massive mainframes. They considered the IBM PC Jr. to be just a toy. The lack of commitment to the PC Jr. was on full display in 1983 (Cortada, 2019). In contrast, the most popular home computers in the USA up to 1985 were: the TRS-80, various models of the Apple II, the Atari 400/800 (1979) and its follow-up models, the VIC-20, and the Commodore 64. Other poorly designed PCs that also did not do as well due to poor management of technology were the Altair and TI- 99 (Abbate, 1999).

The second factor manifested in the 1980s was that immature technology was sometimes rushed into production. Some firms became so obsessed with the potential of an unproven technology that they were willing to forge ahead with major strategic investments. A good example of this was virtual reality. Research into the viability of virtual reality (VR) systems goes back five decades. (Lum, Elliott,

and Aqlan, 2020). Several small firms jumped readily into virtual reality in the 1980s and 1990s and incorporated it into their business models. These included companies such as VPL Research. The idea of putting on special goggles and gloves and immersing oneself fully in a 3-D game or training session appealed to many who thought the technology was ready. However, the consumer public was far from being interested in engaging in VR. VR never took off commercially, even though some useful niche applications, such as providing surgeons with a way to practice difficult medical procedures were developed (Haskin, 2007).

A third factor was the inability to estimate the large costs associated with adopting the newer technologies. Iridium's idea to launch sixty-six satellites that could be linked in a network to route calls all around the world seemed to be the future of world-wide instant communications. Working with Motorola, Iridium strove to be the pioneer of instant worldwide telephone service. However, Iridium's managers grossly miscalculated the cost of the technology needed to bring such a complex satellite system into fruition (Collins, 2018). Most potential users did not wish to pay Iridium's estimated dollars per minute of call time. Another factor was that the users were unwilling to carry around a phone larger than a brick. Less than a year later, after losing nearly US $1 billion in two disastrous quarters, the engineering marvel Iridium is in danger of becoming the "Ford Edsel of the sky" (Ibid).

The Apple Newton was another product that used the most modern technology. However, it was overpriced when it debuted in 1993. Pushing the state-of-the-art, the Newton promised many features that were too advanced for its time e.g. personal information management. However, the device was huge and expensive. It cost approximately $700 for its first model and $1,000 for a later, more advanced model (Muniz, 2005). Released in 1995 the smaller, cheaper PalmPilot became the device that the market much preferred. When Steve Jobs returned to Apple in 1997, he killed the Apple Newton (Isaacson, 2011).

A last factor affecting the management of technology was the industry paradigm shifts that occurred in technology. The Digital Revolution that occurred in the 1980s and 1990s is noteworthy. A major firm that completely missed the decline of analog technology and the rise of digital technology was Kodak (Lucas and Groh, 2009). A technology company that had dominated the photographic film market during most of the 20th century, Kodak used analog photographic chemicals and film. Kodak's management was so focused on the success of photography film that they missed the future major paradigm shift in technology. When the Digital Revolution occurred, Kodak decided that its future was with their venerable, analog processes (Kotter, 2012). Even though they had developed the world's first digital camera, Kodak's management was so focused on the success of photography film that they missed the onslaught of the digital revolution. They failed to keep innovating and filed for bankruptcy in 2012 (Ho and Chen, 2018).

Fujifilm, a competitor of Kodak, pursued a completely different strategy in the management of their technology (Shibata, Baba, Kodama, and Suzuki, 2018). While Kodak continued using their traditional analog "silver halide" technology, Fujifilm and other competitors took different paths. Fujifilm moved into the digital mainstream (Ibid). In this way Fujifilm, the closest challenger of Kodak learned to be bold and innovative to close the gap. They opened digital factories in the USA, daring to challenge the Kodak marketing empire in its backyard. In a major coup, it won the rights to sponsor the 1984 Los Angeles

Olympics (Kmia, 2022). Hewlett-Packard, Canon, and Sony also outmaneuvered Kodak. They launched digital products based on home storage with home printing capabilities. They also uncovered new demand for convenience, storage, and selectivity. Facebook was born, and prints became outdated. Most consumers stopped printing pictures; instead, they began to share them online (Ibid).

Another leader in its field that failed to adapt to the Digital Revolution was Motorola. In 1995 they were the best cell phone maker in America (Richtel, 2009). AT&T requested Motorola to furnish them with one million digital cell phones. Motorola responded that they would be happy to honor AT&T's request but insisted that they be analog cell phones (Nair, Ramalu, and Kumar, 2014). AT&T thanked Motorola but advised them that they needed the phones to be manufactured using the new digital technology. Instead, AT&T turned to a little telephone manufacturer in Finland and asked if they could provide the requisite number of digital cell phones. Nokia advised that they had to scale up their operations to provide such a large quantity of phones, but that they would do so at the right price. AT&T complied, and the order put Nokia on the map as a major digital cell phone provider (Vecchio, 2017).

3. Post 2000 Mismanagement of Technology

The Literature Review covered primarily Pre-2000 Mismanagement of Technology. The focus on this section will be on the trends that have occurred in the most recent twenty years. It will be noted that there were new major factors that now became evident and added significantly to the reasons previously mentioned in the mismanagement of technology. One new factor was the inability to maintain good ethics in firms as it pertained to the burgeoning changes in modern technology. With the advent of major deregulation in the 1980s, corruption in firms started to occur at an increased rate as the 21st Century approached. This was due in large measure to more cases involving bribery, commodities fraud, price fixing, tax evasion, and insider trading of stock (Ferguson, 2012). Ivan Boesky, Michael Milken, Charles Keating, and celebrities such as Martha Stewart went to jail for violations involving these practices.

A second major trend that arose in the early part of the 21st century was the sudden increase in the scale of corruption. Corruption began to reach new heights where it now was resulting in the demise of entire corporations. The most famous case that occurred in 2003 was the ENRON Corporation. Enron was an oil and gas company that engaged in huge fraud transactions. Chief Financial Officer Andrew Fastow used new accounting software to create a network of shell companies designed solely to do business with Enron, for the ostensible dual purposes of shielding Enron money and hiding its increasing debts. He also used broadband technology illegally to trade commodities. Enron was able to record non-existent profits from these ventures (McLean and Ekland, 2013). Both initiatives eventually failed. Other such fraud initiatives were employed by also manipulating ENRON's accounting software. This resulted in the firm's Chapter 11 bankruptcy in 2001 (Ibid). Due to this massive fraud, many of its employees lost their pensions and life savings, while investors lost over $11 billion in shareholder value. CEO Ken Lay was sentenced to prison but died before entering jail. Both Andrew Fastow and his complicit wife also served prison sentences. Around the same time Bernie Ebbers, the CEO of WorldCom, engaged in similar unlawful activities. WorldCom collapsed in 2002 amid revelations of major accounting irregularities. This was one of the largest accounting scandals in the United States (Jeter, 2003). Ebbers was convicted of fraud and conspiracy and served 13 years of a 25-year sentence. Due to these and several other huge

fraud cases (i.e., Tyco International and Adelphia), Congress enacted the Sarbanes-Oxley Act in 2002. This act targeted the mismanagement of public companies, as well as their Board of Directors. It added criminal penalties for management misconduct, and required the Securities and Exchange Commission to create regulations to define how public corporations were to comply with the law (Arbetter etc., 2009).

The Financial Crisis of 2007- 2009 brought a new wave of major, unethical behavior, primarily in the banking and other financial sectors of the economy. The crisis was a systemic failure brought about by a variety of contributing factors such as: (a) the virtually unregulated growth in subprime mortgages; (b) the creation by the banks of new, damaging, high risk financial instruments such as Collateralized Mortgage Obligations (CMOs), Collateralized Debt Obligations (CDOs), and Credit Default Swaps (CDSs); (c) the failure of the Rating Agencies (Moodys, Standard and Poors, and Fitch) to properly rate bank high risk securities; (d) the lack of oversight by financial governmental agencies (e.g. SEC and the FED); (e) the growth a new financial entities that engaged in high risk securities i.e. Hedge Funds and Private Equity firms; and (f) a collapse in the housing market. (Foster and Magdoff, 2009).

Embedded in virtually all of these major factors were the unprecedented greed and ethical lapses demonstrated by poor management in: (a) the major US banks i.e. Goldman Sachs, Bear Stearns, Lehman Brothers, AIG, and Merrill Lynch; (b) the quasi- governmental banks such as Fannie Mae and Freddy Mac; and (c) large mortgage firms that had grown rich with sub-prime mortgages such as Country-Wide and Ameriquest. Information Technology (IT) was employed by the management of all these firms to fashion and market the financial instruments which were the neutron bombs of the crisis i.e., CMOs, CDOs, CDSs etc. (Ibid). The results were catastrophic for many major financial institutions: (a) Bear Stearns and Lehman Brothers went bankrupt; (b) Merrill Lynch had to be rescued by Bank of America; (c) Fannie Mae and Freddy Mac went into conservatorship and remained there through 2022; (d) Country-wide and Ameriquest went bankrupt; and (e) AIG had to be bailed by the government with a huge loan (Arbogast, 2022). Without major government interaction and capital infusions (TARP funds and Quantitative Easing), the fallout might have been catastrophic and brought on a major depression in the United States. Many of these new financial instruments had been sold to banks and investors all over the world. Thus, the global effect of the US fiscal crisis was also toxic to many countries, who also were beset by major setbacks (Ibid).

Beside the fiscal crisis, ethics violations also began to appear in many other business areas. The first of these was the largest Ponzi scheme in history by Bernie Madoff (Henriques, 2012). Madoff had gained prominence In the 1960s, when he founded Bernard L. Madoff Investment Securities LLC as a broker-dealer for penny stocks. His firm used innovative computer information technology to disseminate its quotes. Madoff continued to use this and other information technologies which then evolved in the 1970s into the National Association of Securities Dealers Automated Quotations Stock Market (NASQAQ). Later, Madoff would become its chair. With this platform and by engaging in several humanitarian initiatives, Madoff became a highly acclaimed financier. He then launched his now famous Ponzi scheme in the 1990s. Madoff told his investors that he was investing their funds in lucrative investments. In fact, he failed to do so (Ibid). Finally, in 2009 it all came to a head when Madoff pled guilty to a variety of criminal charges including perjury, money laundering, mail fraud and false SEC

filings. Earlier criminal complaints had revealed that Madoff had defrauded his clients of almost $65 billion. Madoff was found guilty and subsequently received a maximum sentence of 150 years in federal prison Madoff later died while incarcerated. Over 24,000 investors of Ponzi were seriously injured by his scheme. These investors only recovered less than a quarter of their total investments (Jordanoska, (2017). However, the consequences of Madoff's actions went well beyond his immediate transgressions. In the past few years there has been a surge in imitation Ponzi schemes. Fifty-seven Ponzi schemes were discovered in 2022 affecting a loss of $5.3 billion in investor funds. This represented a seventy percent increase over the prior year when thirty-four schemes were discovered. The average size of a scheme in 2022 was $94 million (Ponzitracker, 2023).

The last ten years also saw mismanagement of technology in a variety of other industries: construction, extraction (oil, gas, and mining), transportation and storage, and investments and finance (Beattie, 2022). In addition, the news media has uncovered a variety of serious problems in such industries as sports (e.g., FIFA), crypto currency (e.g., Bankman-Fried at Alameda Research/FTX Crypto), health technology and automotive. This paper now addresses these latter areas with two recent egregious cases.

The Volkswagen (VW) Case- The first is the VW Emissions Scandal Case. VW is a German Engineering automobile company. In 2007 they were struggling with diesel emissions standards. Their new diesel was producing emissions that exceeded US Environmental Protection Agency (EPA) standards. VW engineers were under pressure to solve this problem. Unable to find a fix, all they could suggest to management was a "Defeat Device" that could be installed in diesel cars. This device had a binary switch so that: (a) When the diesel was tested inside, the car would operate in the dyno mode- with less power, but complying with low EPA Nitrous Oxide emissions; and (b) on the road software would switch the car into a normal operating mode with up to thirty five times the emissions of the dyno mode, well over EPA standards. This device was approved by management and installed with the full knowledge of the new CEO (Martin Winterkorn). The vehicle was produced and sold in the US between 2008 and 2015 (Arbogast, 2022).

In 2015 Hemanth Kappanna was a junior engineer working in a small team for General Motors (GM) in West Virginia. His job was automobile emissions testing. Kappanna did not do his testing in the normal laboratories, but outside. He concluded that the outside emissions from the Volkswagen diesel were dirtier than those being cited by VW. When asked to testify by GM at an emissions forum in California, the EPA was present. The EPA reacted rapidly upon realizing that they had been duped. When VW was confronted with these revelations, the 'blame game' ensued. CEO Winterkorn said it was a misunderstanding between the C-level suite and middle management. Middle management blamed the engineers. As VW had been previously caught manipulating emissions testing in the early 1970s, the EPA moved decisively. VW was forced to recall eleven million cars and pledged $6.7 billion dollars for repairs. However, that was not enough to satisfy this gross mismanagement of VW's technology. In January 2017 VW pled guilty to criminal charges of defrauding the U.S. government and obstructing a federal investigation. In addition to a $15.3 billion settlement with U.S. regulators, VW agreed to pay $2.8 billion in criminal fines and also $1.5 billion in civil penalties. This was the largest settlement in the history of an automobile-related consumer class action case in the United States. The other fall-out that

ensued was that: CEO Winterkorn was fired along with a number of key other executives; (b) the company lost 46% of its shareholder value, about 42.5 billion dollars; (c) investors suffered major losses as the VW stock price declined significantly; and perhaps worst of all; (d) the pollution in the US from 2008-2015 had put people's health at risk (Ibid).

The Theranos Case- Elizabeth Holmes was a student at Stanford University in the early 2000s. For a summer internship, she worked abroad in blood laboratories. There she was appalled at the amount of blood being drawn from patients for disease testing. Drawn to nanotechnology labs at Stanford, she set out to find a simpler way to do the tests. Dropping out of Stanford, she directed her energies to organizing Theranos, a private Health Technology company in the mid-2000s. She did this with the assistance of a chemical-engineering professor at Stanford, who was her science and technical advisor.

Holmes maintained that Theranos could use a single finger-prick of blood to accurately predict diseases. A device developed in-house to do this was named 'Edison.' Holmes was also good at raising capital. Those who invested in Theranos included several technology CEOs, two Secretaries of Defense (General James Mattis and former Sec Def William Perry); and two former Secretaries of State (Sec State) Henry Kissinger and George Shultz. Theranos raised more than $700 million from venture capitalists and private investors. This resulted in a $10 billion firm valuation by 2014. (Arbogast, 2022). Also investing heavily in Theranos was Walgreens. Theranos Wellness Centers in Walgreen's stores started to appear around the country in 2014 (Ibid). Unfortunately, Holmes had duped everyone by claiming that her Edison machine was predicting the results being furnished to Walgreen's and other customers. In fact, Edison was incapable of providing accurate results. The Edison test results were "erratic and different" compared to Siemens. Some results were used to erroneously advise patients that they had HIV and Hepatitis (Ibid).

This was known by Holmes and her executives (e.g., COO Sunny Balwani). Instead of being transparent, Theranos lied to everyone including users and investors. In fact, they were secretly diluting the finger-prick blood samples and using German Siemens machines to provide their results (Carreyrou, 2018). Also aware of this deception was Theranos' Lab Director Adam Rosendorff and several others in the lab (Assistants Adam Schulz and Erica Cheung). Rosendorff was appalled and went to Holmes on this breach of ethics. He was met with hostility and rejection. Unable to convince Holmes and Balwani to stop this charade, Rosendorff retreated, but knew something had to be done. Getting past Theranos' strict policies and guidelines was a huge challenge. Theranos' tactics were: (a) all employees were required to sign non-disclosure agreements (NDAs); (b) security cameras had been mounted everywhere and security personnel (ex-military) roamed the halls; (c) personnel could not go between labs; (d) the windows were tinted "to prevent spying"; (e) employee emails were closely monitored; and (f) any employee who indicated any dissatisfaction was intimidated and threatened with huge lawsuits. Totally stifled by these restrictions, Rosendorff decided to resign and quietly disappeared in 2014. However, soon after he felt obliged to do something. He wrote to John Carreyrou at the Wall Street Journal about the situation at Theranos (Ibid). Carreyrou would later testify that this was the first inkling of knowledge that he had about the potential fraud going on at Theranos and it put him on a trail of discovery (Carreyrou, 2020).

Two Lab workers also tried to alert higher-ups of the issues. Tyler Schulz was the grandson of former

Sec State George Schulz. He went to his grandfather to advise him of his concerns. When the elder Schulz called Holmes, he was assured that Tyler was ignorant of the big picture and that everything was ethically sound. Schulz believed Holmes. Tyler was threatened with lawsuits and elected to resign. A second concerned lab worker was Erika Chung. When she received harsh treatment (e.g., potential major lawsuits), she was so frightened that she prepared to leave the country and travel to Hong Kong. However, before leaving, Erika contacted Carreyrou with more details of Theranos' nefarious operations and emailed Theranos' accrediting agency, the Center for Medicare and Medicaid Service (CMS). On Oct 16th, 2015, Carreyrou published an article with circumstantial evidence that Theranos had defrauded their investors and the CMS. The CMS reacted quickly and investigated the Theranos operation. They found that Theranos had unreliable devices, sloppy lab practices, had cheated on proficiency testing and misled inspectors during prior visits. A subsequent CMS lab investigation found forty-five deficiencies which Theranos was unable to correct. Thereafter, the CMS permanently shut down the Theranos labs in 2016 (Arbogast, 2022).

On June 14, 2018, Elizabeth Holmes, and "Sunny" Balwani (Theranos COO) were accused on sixteen combined charges of fraud. This included: (a) Holmes had incorrectly maintained that Theranos could use a single finger-prick of blood to predict diseases; (b) Holmes had engaged in unethical actions against her employees; (c) Theranos had lied to investors and users by providing results from Siemens and representing that they were from the Edison machine; and (d) they had interfered with potential inspections and audits by government agencies. Subsequently, Walgreens, Walmart and other prominent political figures filed a class-action lawsuit (March 2020). Despite Covid delays in the trials, both were finally found guilty on all counts of fraud. Balwani received a prison term of 12 years and 9 months while Holmes received 11 years. Pregnancy delayed her incarceration, but she was finally sent to jail in May 2023.

Lessons learned from these two cases included: (a) Don't fake it, until you make it; other Silicon Valley firms have also used this strategy to acquire capital for technology based initiatives, often failing to produce the promised outcome (Ibid); (b) A failure is not a loss, but rather a lesson that you can grow from; if Holmes and Winterkorn had been willing to accept failure early, they could have potentially prevented the downfall of their companies; (c) one should accept responsibility and avoid blaming others; taking responsibility enables both the leadership and employees to own their actions and the consequences.

4. Conclusions

This paper has documented many high-profile mis-managed companies over the past forty years. It documented that a great many of the failures were caused by the firm's inability to manage technology properly. In the period before 2000, there were issues in: (a) applying incorrect technologies that resulted in poorly designed products; (b) recognizing that the technology they were trying to push the envelope on was not mature enough "for prime time"; (c) estimating the large costs involved in the development, production and operations of products using the newer technologies; and lastly (d) recognizing that in a specific industry, there had been a paradigm shift in technology.

In the 2000s another major factor that added to the failure of major firms was the lure of misusing newer technologies that crossed the traditional ethical boundaries. ENRON's new accounting software

created “paper entities” designed to hide fraud. In the Great Banking Crisis in 2008-2010, there were new financial assets created using software systems. These assets were sold in great quantities in the United States and around the world. The “neutron bombs” were known as Collateralized Mortgage Obligations (CMOs), Collateralized Debt Obligations (CDOs), and Credit Default Swaps (CDSs). While many bankers escaped being responsible for these bad assets, the country paid a high price in having to bail out many of the banks and other major firms (e.g., GM) with TARP money and Quantitative Easing infusions. Software was also used by Bernie Madoff’s in his massive Ponzi scheme and by other Ponzi imitators that followed suit. The on-going investigations into crypto currency using newer technologies such as Blockchain are further evidence that many recent scandals are intertwined with technology. The VW and Theranos cases gave two stark examples of how the technologies in health care and the automotive business were at the root of gross mismanagement of technology.

5. Recommendations

Future research should focus on educating business leaders on the risks in managing technology. Changes in technology are accelerating today, as witnessed by the new challenges being posed by major advances in Artificial Intelligence, Blockchain and the Internet-of-Things. In the past corporate leaders could rely on subordinates to monitor technology advances and advise management on its proper use in their industry. Sarbanes-Oxley and other legislation have put top management on notice that CEOs can no longer lay the blame for such failures on subordinates. Leaders will be held accountable and as such, need to be educated better on the technologies vital to their firm’s strategic future.

6. References

Arbetter, Brian, Boling, Andrew, Gomes, Matthew, Gross, Scott, (2009), Complying with Sarbanes-Oxley’s Whistleblower Provisions: Leading Lawyers on Understanding Whistleblower Provisions, Complying with Key Regulations, Brand Aspatre.

Arbogast, Stephen V., (2022), *Resisting Corporate Corruption (RCC)*, 4th Edition, John Wiley & Sons.

Beattie, Andrew, (2022), Why these Industries are prone to corruption, Investopedia, https://www.investopedia.com/articles/investing/072115/why-these-industries-are-prone-corruption.asp.

Carreyrou, John, (2020), *Bad Blood: Secrets and Lies in a Silicon Valley Startup*, Knopf, NY

Collins, Martin, (2018), *A Telephone for the World, Iridium, Motorola, and the Making of the Golden Age*, John Hopkins University Press, Baltimore, Md.

Cortada, James, (2019), IBM: *The Rise and Fall and Reinvention of a Global Icon (History of Computing),* The MIT Press.

Cringely, Robert X. (2014), *The Decline and Fall of IBM, End of an American Icon,* Published by NeRDTV, LLC.

Ferguson, Charles H., (2012), Predator Nation, Corporate Criminals, Political Corruption and the Hijacking of America, Crown Books, New York.

Foster, John B. and Magdoff, Fred, (2009), *The Great Financial Crisis: Causes and Consequences,* Monthly Review Press.

Haskin, David (2007), The 10 Biggest Technology Flops of the Past 40 Years, ComputerWorld July 9, 2007.

Henriques, Diana B., (2012), *The Wizard of Lies: Bernie Madoff and the Death of Trust*, St. Martin’s Press, McMillan.

Ho JC and Chen H, (2018), Managing the disruptive and sustaining the disrupted: The case of Kodak and Fujifilm in the face of digital disruption, Review of Policy Research, 2018 -Wiley Online Library

Isaacson, Walter, (2011),Steve Jobs, Simon & Schuster, ISBN:1451648537

Jeter, Lynne W., (2003), *Deceit and Betrayal at WorldCom*, John Wiley & Sons.

Jordanoska, Alekdandra, (2017), *Bernie Madoff and the Crisis: The Public Trial of Capitalism*, Stanford Univ Press.

Lewis, Mervyn K., (2015), *Understanding Ponzi Schemes*, Edward Elgar Publishing Limited.

Lucas, HC and Groh, JM, (2009), Disruptive technology: How Kodak missed the digital photography revolution, Journal of Strategic Information Systems, Elsevier.

Lum. HC, Elliott, LJ, Aqlan, F. (2020), Virtual Reality: History, Applications and Challenges for Human Factors Research, Proceedings of the Human Factors and Ergonomics, Society, Sage Journals.

McLean Bethany and Ekland, Peter, (2013), The Smartest Guys in the Room: The Amazing Rise and Scandalous Fall of ENRON, Penguin Books.

Muniz, Albert (2005), Religiosity in the Abandoned Apple Newton Brand Community, Journal of Consumer Research, Volume 31, Issue 4.

Ponzitracker, (2023), https://www.ponzitracker.com

Richtel, Matt, (May 1,2009). Motorola Scrambles to Restore its Lost Cell Phone Glory, New York Times.

Shibata T, Baba Y, Kodama J, and Suzuki J, (2019), Managing ambidextrous organizations for corporate transformation: a case study of Fujifilm, R&D Management, Wiley Online Library.

Vecchiato, Riccardo, (2017), Disruptive innovation, managerial cognition, and technology competition outcomes, Technological Forecasting and Social Change.

Appendix A– Ethics Cases Contained in Book "Resisting Corporate Corruption."

Carbonized PAN - Fiber Composites with Nanoscale Inclusions for Improved Thermo-Mechanical Properties

Nivedhan Ravi [1]
Md. Shafinur Murad[1]
Dinesh Gurung[1]
Mete Bakir[2]
Ramazan Asmatulu[1]
[1]Department of Mechanical Engineering
Wichita State University, 1845 Fairmount Street, Wichita, KS 67260, USA
[2]Turkish Aerospace Industries, Inc.
Fethiye Mah., Havacilik Bulvari, Kahramankazan, Ankara, 06980, Turkey
ramazan.asmatulu@wichita.edu

Abstract

Polymeric nanocomposites are generally lighter and stronger that hold key features for many industrial applications, such as aerospace, automotive, defense, packing, electrical and electronics, biomaterials, sensors, energy, and consumer products. Their exceptional mechanical, electrical, chemical, and thermal properties help bring these materials as one of the prime focus areas in the world. Extensive research studies involving thermoplastics with nanofillers (TiO2, graphene, carbon black, and carbon nanotubes) have been conducted to produce various nanocomposites. The prime objective of this study is to develop polymeric nanocomposites by incorporating nanoparticles of graphene into polyacrylonitrile (PAN) thermoplastic where fiber reinforcement bonding is used to enhance the mechanical properties leading to very high strength-to-weight ratio polymeric nanocomposites. A mixing ratio of 20:80 for PAN and dimethylformamide (DMF) solvent was used to dissolve the PAN power using magnetic stirring. Graphene nanoparticles were then added to the solution at 0-4 wt.% ratio after which the nanocomposite coupons were prepared by casting the PAN-based resin in aluminum grooves where carbon fibers and SiC fibers were placed as reinforcement materials to make them robust. After curing at room temperature, the coupons were oxidized at 200□C for 2 hours in air and then carbonized at 650□C for additional 2 hours in Ar gas. The subsequent testing and characterization studies, such as tensile, Fourier-transform infrared spectroscopy (FTIR), and water contact angle have been conducted on the prepared nanocomposites. The obtained test results indicated that the mechanical and thermal properties have been significantly enhanced after the addition of a small percentage of nanoparticles into the PAN solution. This enhancement can be attributed to the fact that the surface-to-volume ratio is high for nanoparticles, thereby making them more resilient compared to traditional composites.

Keywords: Polymeric Nanocomposites, Graphene, Carbon and SiC Fibers, Oxidation, Carbonization, Exceptional Properties.

Submitted: August 18, 2023
Revised: November 12, 2023

1. Introduction

Nanotechnology involves the fabrication, imaging, measuring, modeling, and manipulating matter at nanoscale (usually 1 – 100 nm). It aims at controlling individual atoms, molecules, or particles to notably improve the physical, chemical, physicochemical, and biological properties of novel materials and devices. It has a positive impact on a broad range of highly multidisciplinary fields such as engineering, materials science, physics, chemistry, medicine, and biology to name a few. Their applications are endless, not just limited to energy storage systems, sensors, biomedical applications, semiconductors, aerospace and defense, construction, automotive, and cosmetics [1,3-4]. Nanocomposites can be defined as the combination of two or more different compositions or structures where at least one of the materials is in the nanoscale region. The behavior of these materials is different from conventional composite materials, attributed to the fact of their microscale structure and high surface-to-volume ratio [5].

Nanocomposites are grouped according to the type of matrix material and the type of reinforcement material. The below classification is based on the type of matrix material [6-11]:

Polymer Matrix Nanocomposites: Materials having polymer as a matrix material and nano additives as reinforcement material are called polymer matrix nanocomposites. The additives can be one-dimensional (nanotubes and fibers), two-dimensional (layered materials like clay) or three-dimensional (bulk particles). A typical polymer nanocomposite is a combination of polymer (matrix) and a filler (reinforcement). Examples of this type of nanocomposites include thermoplastics, thermosets, elastomers, and natural polymers [6,12].

Ceramic Matrix Nanocomposites: Materials with at least one phase having a nano dimension are called ceramic matrix nanocomposites. They are a new generation of engineering materials, having a wide range of applications especially in the industrial sector. In general, the most common method used for preparing this type of nanocomposites are mechanical methods such as conventional powder method, polymer precursor route, spray pyrolysis, and chemical methods such as sol-gel process, colloidal and precipitation approaches and template synthesis. TiO_2 and SiC are some of the most common ceramic materials used in the fabrication of this type of nanocomposites. Some examples of ceramic matrix nanocomposites include Al_2O_3/SiO_2, SiO_2/Ni, Al_2O_3/TiO_2 and Al_2O_3/SiC [6,13].

Metal Matrix Nanocomposites: Metal matrix nanocomposites are those that are reinforced by metal-based nanoparticles such as Fe or Al-based. These composites consist of metal-based matrix filled with nanoparticles, and have physical, chemical, and mechanical properties entirely different from those of matrix material. At nano-level, the interface of particles with displacements becomes critical, and results in a significant improvement in mechanical properties. Some metal matrix nanocomposites include Fe-Cr/Al_2O_3, Ni/Al_2O_3, Fe/MgO, Al/CNT and Mg/CNT [6,14].

The main objective is to develop a multifunctional thermoplastic polymer-based carbonized (carbon-carbon and carbon-SiC) nanocomposites with enhanced mechanical, physical, chemical, electrical, and thermal properties, making them suitable for various applications, including flame retardancy, EMI shielding and lightning strike protection at a reasonable cost, ultimately replacing most of the metals and their alloys in the longer run. Another leverage that thermoplastic polymers have is that they can

be recycled and remolded into different shapes, unlike thermosetting polymers, for most of the industrial applications [15-19].

2. Experiment

2.1. Materials

Polyacrylonitrile, also known as polyvinyl cyanide, was purchased from Alibaba. It is a semi-crystalline powder having a molecular weight of 150,000 g/mol with CAS No. 25014-41-9. The organic solvent N, N Dimethylformamide (commonly known as DMF) with CAS No. 68-12-2, 99.8%, was purchased from Carolina Chemicals. Graphene dry nanopowder with CAS No. 1034343-98-0, manufactured by Graphene LTD – Redistributed by PYR-LTD was purchased through eBay with – Average thickness – 1-5 nm, 1-3 layers, and a surface area of 300 m^2/g. Carbon fiber (CF - unidirectional) (Type: T700GC) was purchased from Toray Carbon Fibers America Inc. Nicalon Silicon Carbide (SiC) unidirectional ceramic grade fiber was purchased from NGS Advanced Fibers, Ltd, Japan, and distributed by COI Ceramics Inc, USA. Figure 1 shows the carbon and silicon carbide fibers used in these studies.

(a) **(b)**

Figure 1: Images showing the a) carbon fiber and b) silicon carbide fiber used in this study.

2.2. Preparation of PAN-based Nanocomposites

PAN powder is dissolved in DMF (PAN: DMF weight ratio of 20:80) at a speed of 800 rpm and temperature of 60°C using a magnetic stirrer on a hot plate. It must be ensured that there are no agglomerated / undissolved PAN particles left. Once the viscous resin turns light yellowish color, it implies that PAN is dissolved entirely in DMF. Various concentrations of graphene powder (0, 2, and 4%) are then dispersed in the PAN resin and stirred for 10 minutes. Desiccation is performed for 10-15 minutes to remove dissolved air bubbles in the PAN solution that are trapped in the resin. Then, ultrasonication is performed for a total of 30 minutes in two intervals of 15 minutes each with optimum

amplitude to ensure that PAN and graphene are homogeneously mixed in DMF.

In the studies, the resin was poured into an aluminum groove for casting with the size of each groove of 5.65 in×0.75 in×2.6 mm (13.97 cm×1.905 cm×0.26 cm) if it is casted for an UL94 burning test coupon or a size of 10.45 in×0.9 in×1.2 mm (26.5 cm×2.3 cm×0.12 cm) for a tensile strength test coupon. Carbon fiber unidirectional strands and silicon carbide fiber yarns were uniformly placed in the casting groove for preparing carbon fiber and silicon carbide reinforced coupons separately. Then, the resin was poured on carbon fiber and silicon carbide fiber followed by placing the CF and SiC to form a sandwich type of layers. Each CF strand weighs around 0.113 g while a SiC fiber strand weighs around 0.033 g.

Proper care was taken to ensure that there are no gaps in between the fibers as it might compromise on especially the mechanical properties of the final coupon. In the case of carbon fibers, four strands of CF for each layer (a total of 2 layers of CF are used) are placed next to each other until the whole slot is covered with carbon fibers. For SiC fibers, ten strands of SiC fibers (only one layer) are placed beside each other. A wooden stick is used to level the PAN-based resin so that the final coupon has a uniform thickness. Double-sided tape is used to hold the strands of fibers to ensure that the strands do not move during the curing process, thereby maintaining the alignment of fibers to the extent possible. The room temperature greatly affects the curing time. The curing process typically takes 6-8 hours at room temperature during the summer and 12-14 hours during the winter to get a coupon with a smooth surface finish. Later, oxidation is performed at 200-250°C in the presence of air for 2 hours using a convection oven (Yamato Scientific DKN 602) while carbonization is performed at 650°C for 2 hours in the presence of Argon gas using a high-temperature furnace (MTI OTF-1200X), to get oxidized and carbonized coupons respectively. Figure 2 describes the step-by-step whole procedure graphically.

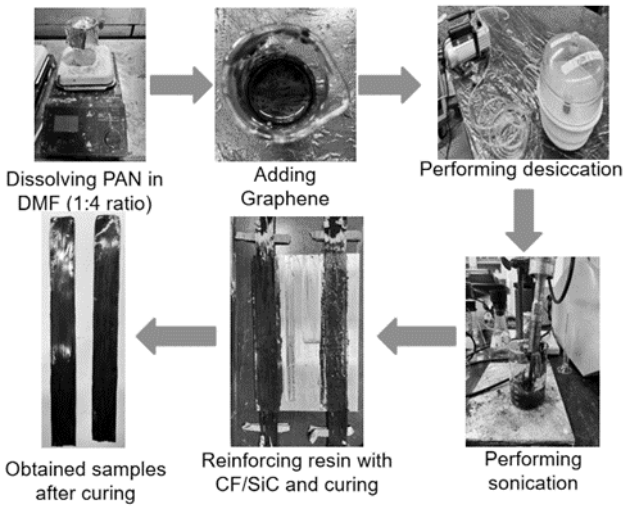

Figure 2: Preparation of graphene-based polymer nanocomposites.

2.3. Characterizations

Tensile test (MTS 810 Material Test System) was conducted to evaluate the mechanical properties of the nanocomposite coupons. To estimate the qualitative estimations of surface functional groups of composites, Fourier transform infrared spectroscopy (Thermo Scientific™ Nicolet™ iS50 FT-IR infrared

spectroscope) over a range of 500-4000 cm^{-1} was used. Thermal properties of the coupons were assessed with the help of a Q1000 TA Instrument. A contact angle goniometer was used to find out whether the coupons were hydrophilic or hydrophobic in nature.

3. Results and Discussion

3.1. Tensile Test Studies

In order to study the mechanical properties of polymer-based nanocomposites, ISO 527-5 Type-A (Test conditions for unidirectional fibre-reinforced plastic composites) specification had been picked [2]. Table 1 and Table 2 provide the the Ultimate Tensile Strength (UTS) values of carbon fiber and SiC fiber reinforced nanocomposites. Carbon fiber reinforced nanocomposites have shown great UTS values compared to the SiC fiber ones. This may be explained because only 10 single layered SiC strands were used in this research. Incorporating more strands/more layers may yield better results. Resin compatibility with fiber has a major impact on the mechanical, physical, chemical, thermal, and optical properties of the polymer nanocomposite.

Carbon Fiber Reinforcement				
Filler loading % (type of coupon)	Elastic Modulus (GPa)	Max Load or Force (N)	Peak stress (Force/Area) (Mpa or N/mm^2) (% increase/decrease with respect to 2% normal coupon)	Strain at break (mm/mm)
2% (normal)	3.55	5300.87	330.47	0.84
2% (oxidized)	3.92	7457.40	458.19 (+39%)	0.61
2% (carbonized)	3.66	682.53	45.50 (-86%)	0.03
4% (normal)	4.62	7986.36	532.42 (+61%)	0.34
4% (oxidized)	5.08	9469.88	632.81 (+91%)	0.38
4% (carbonized)	5.97	865.85	57.85 (-83%)	0.03

Table 1: Average tensile test data for carbon fiber (CF) reinforced coupons.

SiC Fiber Reinforcement				
Filler loading % (type of coupon)	Elastic Modulus (GPa)	Max Load or Force (N)	Peak stress (Force/Area) (MPa or N/mm^2) (%increase/decrease with respect to 2% normal coupon)	Strain at break (mm/mm)
2% (normal)	0.77	807.49	53.83	0.55
2% (oxidized)	1.37	1666.09	111.07 (+106%)	0.23
2% (carbonized)	1.17	831.01	55.4 (+3%)	0.15
4% (normal)	0.97	819.24	54.62 (+1%)	0.17
4% (oxidized)	1.46	1477.73	98.52 (+83%)	0.19
4% (carbonized)	1.80	627.55	41.84 (-22%)	0.1

Table 2: Average tensile test data for SiC fiber reinforced coupons.

3.2. FTIR Analysis

A strong absorption band is seen at around 2250 cm^{-1}, which corresponds to the nitrile (C≡N) stretching vibration. This peak is often used to quantify the degree of conversion of PAN to carbon fiber, which involves thermal treatment that removes the nitrile groups and converts the polymer to a more graphitic form. A weak absorption band at around 2900 cm^{-1}, corresponds to the aliphatic C-H stretching vibration. The other strong peak at around 1600 cm^{-1} corresponds to the G band. This band arises from the in-plane vibration of sp^2 bonded carbon atoms and is a signature of the graphene lattice structure. A peak at around 2700 cm^{-1} relates to the 2D band. This band arises from the two-dimensional nature of the structure of the graphene lattice.

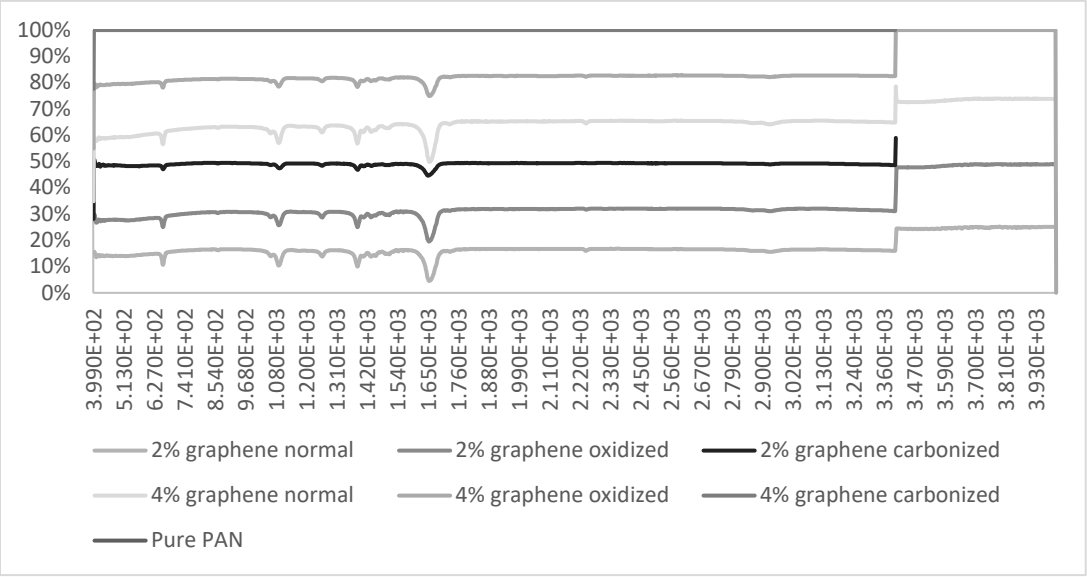

Figure 3: FTIR spectrum of CF reinforced nanocomposite coupons.

A major difference between the oxidized coupon and the normal coupon is the disappearance of the peak in the oxidized coupon graph at around 2240 cm^{-1}. This occurrence can be due to the oxidation process at 200°C causing the solvent DMF to evaporate. The absence of peaks at around 3440 cm^{-1} and 2900 cm^{-1} confirm the absence of PAN which thermally degrades during the carbonization process. Since graphene has the capability to withstand high temperatures, peaks at 2000-2500 cm^{-1} and around 1300 cm^{-1} can be seen which confirm the presence of the element.

3.3. Water Contact Angle Studies

Tables 3-6 shows the water contact angle values of the prepared carbon fiber and SiC fiber composites with nanoscale inclusions for normal, oxidized, and carbonized samples. All the coupons tested were found to be hydrophilic (water-loving) making them suitable for different industries. This can be explained because the polymer PAN is hydrophilic in nature. It was also observed that there is no significant change in water contact angle values for different percentages of graphene inclusions.

Coupon type	CA (Left)	CA (Right)	CA (Mean)	Result
Normal	60.55	63.77	62.16	Hydrophilic
Oxidized	54.51	55.36	54.93	Hydrophilic

Carbonized	48.66	50.81	49.73	Hydrophilic

Table 3: Water contact angle values for PAN+2% Graphene CF reinforced coupons

Coupon type	CA (Left)	CA (Right)	CA (Mean)	Result
Normal	45.07	50.06	47.57	Hydrophilic
Oxidized	83.5	79.82	81.66	Hydrophilic
Carbonized	50.35	51.9	51.12	Hydrophilic

Table 4: Water contact angle values for PAN+4% Graphene CF reinforced coupons

Coupon type	CA (Left)	CA (Right)	CA (Mean)	Result
Normal	46.93	46.14	46.54	Hydrophilic
Oxidized	72.79	72.08	72.43	Hydrophilic
Carbonized	48.04	52.04	50.04	Hydrophilic

Table 5: Water contact angle values for PAN+2% Graphene SiC reinforced coupons

Coupon type	CA (Left)	CA (Right)	CA (Mean)	Result
Normal	68.94	68.46	68.70	Hydrophilic
Oxidized	68.75	67.14	67.95	Hydrophilic
Carbonized	57.08	59.9	58.49	Hydrophilic

Table 6: Water contact angle values for PAN+4% Graphene SiC reinforced coupons

To determine the flame retardancy properties of the prepared nanocomposite samples, various UL-94 flame retardancy studies were conducted on the samples. The test results indicated that all the carbonized samples passed the UL-94 test standard, which can be very useful for the flame retardancy applications of these materials.

4. Conclusions

In this study, carbon fiber and SiC fiber nanocomposite materials (in carbon-carbon and carbon - SiC forms) were developed using various graphene inclusions. The prepared test coupons were characterized using different techniques. The carbon-carbon nanocomposites incorporated with carbon and SiC fibers provided promising mechanical and thermal test results for extreme materials applications. These new materials can be used in different industries, such as aerospace, helicopter, drone, automotive, ship, wind energy, energy storage, defense, packing, electrical and electronics, biomaterials, sensors, infrastructures, and consumer products. It is known that this trend will constantly increase with technological developments. More studies will be conducted in this field and test results will be shared with the scientific communities.

5. Acknowledgment

The authors gratefully acknowledge Wichita State University and Turkish Aerospace Industry (TAI) Inc. for the financial and technical support of the present study.

6. References

Asmatulu, R., and Khan, W.S. (2018). *Synthesis and Applications of Electrospun Nanofibers*, Elsevier, Cambridge, MA.

Standards, B. (2009). Plastics – Determination of tensile properties – Part 5: Test conditions for unidirectional fiber-reinforced plastic composites (ISO 527-5:2009).

Jabbarnia, A., Khan, W. S., Ghazinezami, A., and Asmatulu, R. "Investigating the Thermal, Mechanical and Electrochemical Properties of PVdF/PVP Nanofibrous Membranes for Supercapacitor Applications," *Journal of Applied Polymer Science,* Vol. 133, pp. 43707, 2016.

Murad, M.S., Asmatulu, E., Er, O., Gursoy, M., Safaker, B., Bahceci, E., Bakir, M. and Asmatulu, R. "Improving Flame Retardancy of Fiber Reinforced Composites via Modified Fire-Resistant Resins and Metallic Thin Film Coatings," CAMX Conference, Anaheim, CA, October 17-20, 2022, 8 pages.

Alarifi, I.M., and Asmatulu, R., *Advanced Hybrid Composite Materials and Their Applications, Elsevier*, Cambridge, MA, 2023.

Ravi, N. "Carbonized PAN Unidirectional Fiber Reinforced Composites with Nanoscale Inclusions for Improved Thermo-Mechanical Properties," M.S. Thesis, Wichita State University, April 27, 2023.

Alarifi, I. M., Alharbi, A., Khan, W. S., Rahman, A. K. M. S., and Asmatulu, R. "Mechanical and Thermal Properties of Carbonized PAN Nanofibers Cohesively Attached to Surface of Carbon Fiber Reinforced Composites," *Macromolecular Symposia*, Vol. 365, pp. 140-150, 2016.

Alarifi, I., Alharbi, A., Khan, W. S., and Asmatulu, R. "Carbonized Electrospun PAN Nanofibers as Highly Sensitive Sensors in SHM of Composite Structures," *Journal of Applied Polymer Sciences*, Vol. 133, pp. 43235-45, 2016.

Alarifi, I.M, Alharbi, A., Khan, W.S., and Asmatulu, R. "Thermal and Electrical Properties of Carbonized PAN Nanofibers for Improved Surface Conductivity of Carbon Fiber Composites," CAMX Conference, Dallas, TX, October 27-29, 2015, 13 pages.

Mohammad, S., Uddin, M. N., Hwang, G., and Asmatulu, R. "Superhydrophobic PAN Nanofibers for Gas Diffusion Layers of Proton Exchange Membrane Fuel Cells for Cathodic Water Management," *International Journal of Hydrogen Energy*, Vol. 43, pp. 11530-11538, 2017.

Desai, F., Seyedhassantehrani, N., Shagar, M., Gu, S., and Asmatulu, R. "Preparation and Characterization of KOH-Treated Electrospun Nanofiber Mats as Electrodes for Iron-Based Redox-Flow Batteries," *Journal of Energy Storage*, Vol. 27, pp. 101053, 2020.

Shagor, R.M.R., Abedin, F. and Asmatulu, R. "Mechanical and Thermal Properties of Carbon Fiber Reinforced Composite with Silanized Graphene as Nano-inclusions," *Journal of Composite Materials*, Vol. 55, pp. 597-608, 2021.

Kumar, S.S. A., Uddin, M. N., Rahman, M. M., and Asmatulu, R. "Introducing Graphene Thin Films into Carbon Fiber Composite Structures for Lightning Strike Protection," *Polymer Composites*, Vol. 40, pp. 517-525, 2019.

Alarifi, I. M., Khan, W. S., Rahman, A. K. M., Kostogorova-Beller, Y., and Asmatulu, R. "Synthesis, Analysis and Simulation of Carbonized Electrospun Nanofibers Infused Carbon Prepreg Composites for Improved Mechanical and Thermal Properties," *Fibers and Polymers*, Vol. 17, pp. 1449-1455, 2016.

Khan, W.S., Asmatulu, E., Uddin, M.N., and Asmatulu, R., *Recycling and Reusing of Engineering Materials: Recycling for Sustainable Developments,* Elsevier, Cambridge, MA, 2022.

Nuraje, N., Asmatulu, R., and Mul, G., *Green Photo-Active Nanomaterials: Sustainable Energy and Environmental Remediation*, RSC Publishing, Cambridge, England, November 2015.

Asmatulu, R., Khan, W.S., and Ghaddar, M.H. "Changes in Surface Energy Densities of Carbon and Glass Fiber Reinforced Composites under UV Degradations," *Journal of Research in Applied Sciences*, Vol. 2, pp. 119-130, 2015.

Alarifi, I., Alharbi, A., Khan, W.S, Swindle, A. and Asmatulu, R. “Thermal, Electrical and Surface Properties of Electrospun Polyacrylonitrile Nanofibers for Structural Health Monitoring,” *Materials*, Vol. 8, pp. 7017-7031, 2015.

Asmatulu, R., Khan, W.S., Reddy, R.J., and Ceylan, M., “Synthesis and Analysis of Injection-Molded Nanocomposites of Recycled High-Density Polyethylene Incorporated with Graphene Nanoflakes,” *Polymer Composites*, Vol. 36, pp. 1565-1573, 2015.

Sulfonated PEEK Fiber Reinforced Composites for Increased Thermal and Mechanical Properties

Dinesh Gurung[1]
Md. Shafinur Murad[1]
Nivedhan Ravi [1]
Mete Bakir[2]
Ersin Bahceci[2]
Ozlem Oncu Er[2]
Burak Safaker[2]
Mustafa Gursoy[2]
Emanual Andrade[1]
Eylem Asmatulu[1]
Ramazan Asmatulu[1]

[1]Department of Mechanical Engineering
Wichita State University, 1845 Fairmount Street, Wichita, KS 67260, USA
[2]Turkish Aerospace Industries, Inc.
Fethiye Mah., Havacilik Bulvari, Kahramankazan, Ankara, 06980, Turkey
ramazan.asmatulu@wichita.edu

Abstract

Polyetheretherketone (PEEK) is a special set of thermoplastic polymers that possess fascinating mechanical, chemical, and electrical properties for various industries, such as aircraft, biomedical, automotive, satellite, energy, and defense. Recently, sulfonated PEEK (SPEEK)-based fiber-reinforced composites have been designed and fabricated for the same purposes. However, manufacturing PEEK fiber composites is considerably difficult because of the inertness and high melting point of PEEK; thus, the sulfonation process is a necessary step to make the PEEK composites in many cases. About 5 wt% PEEK powder was initially dried for 24 hours at 100°C and then sulfonated in a 98% sulfuric acid solution for 12 hours at 65°C while continuously stirring in a closed glass beaker. The precipitation was performed afterward using the water bath technique by pouring the PEEK/acid solution into the cold water to make the SPEEK polymer particles. After washing several times in DI water (until neutralizing the pH to 6-7) and drying in an oven at 100°C for a minimum of 24 hours, the SPEEK polymer is obtained. The dry SPEEK polymers were dissolved in dimethylformamide (DMF) with a ratio of 1/2 and mixed well with Kevlar and Glass fibers in different layers by the wet layup process to produce SPEEK fiber composites under vacuum bagging at a higher temperature (200°C) till all the solvent was removed. The UL 94 standard vertical flame test results showed that the SPEEK composites had very high flame-resistant properties. The water contact angle studies indicated that the composites were highly hydrophobic. The maximum tensile strengths of glass and Kevlar fiber composites were found to be 234,99 and 376.8 MPa and flexural strengths of 51.14 and 92.95 MPa, respectively. SEM testing helped analyze the resin interaction's topology on the composite samples. The smoke density test confirmed that light visibility decreased with increased burning time.

Submitted: August 18, 2023
Revised: November 12, 2023

Keywords: Sulfonation, PEEK, Fiber Composites, Fire Resistance, Improved Properties.

1. Introduction

Polymers are divided into different categories according to their chemical structure, method of polymerization, molecular structure, application, and properties [1-4]. Based on the properties, polymers are classified into thermoplastic and thermoset polymers. The thermoplastic polymer is a polymer that once cured can be heated again and reshaped into different molds are thermoplastic polymers whereas thermoset polymers once cured cannot be reshaped again with heat or any other medium. Thermoset has an irreversible bond called a covalent bond; hence it makes the polymer hard to reshape due to the covalent bond. Polyethylene, polypropylene, polyetheretherketone, and PVC are some of the most used thermoplastics. These polymers are widely used in many applications from daily life to industries. The main disadvantage of thermoplastic fiber is the loss of properties once it is heated again as the polymer chains get broken [4].

Polymeric composites are mostly used in various industries, most notably aerospace and defense, automotive, construction and building, sporting goods, medical devices, and electrical systems [1,5-9]. Polyetheretherketone abbreviated as PEEK, is a semicrystalline thermoplastic polymer. PEEK has high-performance thermoplastic polymers with superior mechanical, thermal, and chemical properties. It belongs to the polyaryletherketone (PAEK) family, which is renowned for its remarkable mechanical strength and high-temperature and chemical stability [5,10-16].

Aerospace, automotive, electronics, medical implants, and oil and gas exploration are just a few of the industries that employ PEEK and its modified versions. In high-performance applications where sturdiness, endurance, and heat resistance are necessary, it is frequently utilized in the replacement of metals and other materials [4,5]. PEEK is desirable for medical applications like dental and spinal implants since it is also biocompatible. It is also helpful in situations where components are frequently subject to friction and wear due to their great resistance to wear and abrasion.

Because of their improved resistance to thermal gradients, thermoplastic polymers used in many applications have advanced properties, which raises their importance. Sulfonated PEEK is a thermoplastic polymer and offers excellent stability in thermal, chemical, and mechanical strength, which can become a driving force for the aerospace industry due to its non-conductive nature [6]. Hence, the focus of this study is to polymerize the SPEEK using PEEK and sulfuric acid via the sulfonation process and develop the sulfonated PEEK (SPEEK)-based fiber composites for high flame-resistant applications. In these studies, we used glass and Kevlar fibers to make SPEEK composites since carbon fiber's surface tends to have hydrophobic behavior, which requires additional surface treatments (surface plasma, laser, UV treatment, and other chemical treatments) for better bonding with reduced delamination. The composites were characterized for their mechanical thermal properties, and the test results were evaluated for aerospace, energy, defense, and other industries [16-21].

2. Experiment

2.1. Materials

Tecopeek PK40 NL T PEEK (Polyether Ether Ketone) pellets were purchased from Eurotec Turkiye.

Sulfuric acid (H2SO4) with 98% concentration was purchased from Thermofisher Scientific. The N, N-Dimethylformamide reagent ACS with 99.8% purity was purchased from Carolina Chemical. It is a colorless liquid used as a solvent. Glass fiber and Kevlar fibers (K-29 ballistic grade) are used as reinforced materials for composite making. Glass fiber is purchased from Fiberglass Supply Depot Inc., while Kevlar K-29 fiber is purchased from ArmorCo. Both fibers were woven. These materials were used in these studies without further modifications.

2.2. Preparation of SPEEK and SPEEK Composites

PEEK pellets were first dried in the oven for 24 hours at 100℃ [7,8]. The dried PEEK was mixed and stirred with sulfuric acid with a 1:19 weight-to-volumetric ratio using a cross-magnetic stirrer [9]. The sulfonation temperature was set at 65℃, and the total sulfonated time was set for a minimum of 12 hours in a closed-covered beaker [10,11]. An ice-cold water bath was used for the precipitation. Homogenous sulfonated PEEK solution was poured into ice-cold water which is stirred using a magnetic bar. Noodle-like polymer strands were obtained after final precipitation. These SPEEK polymer strands absorbed the water, swelled up, and were highly acidic. The SPEEK polymer was washed thoroughly with DI water to lower the pH value to 6-7. It was covered, sealed, and kept in the oven at 100℃ for 24 hours until it got completely dried. Finally dried SPEEK was broken into small pieces. It was weighed on the scale and then mixed with the DMF in a 1:2 weight-to-weight ratio. Dissolution of SPEEK was done at room temperature in a covered beaker [12].

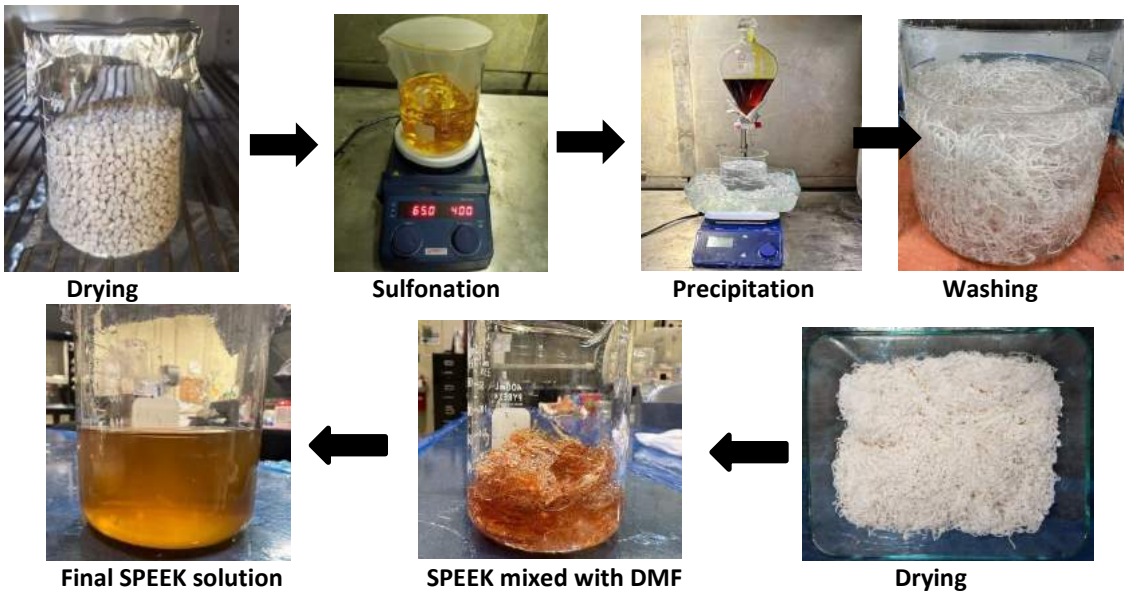

Figure 1. SPEEK-making process for fiber composite manufacturing.

Fibers were cut into the desired size as reinforced materials for the composite-making process. Eight layers of fiber were used for the composite manufacturing. Composite fibers were laminated on top of the smooth-surfaced aluminum plate. Fibers and resin matrix reinforced in a 1:2 weight-to-weight ratio. First, a mold release (Rexco PARTALL® Paste #2 Mold Release Wax) was gently applied on the smooth surface of the aluminum plate before the wet-layup process. Once the resin was ready, the fibers were impregnated layer by layer using a brush and rollers to spread the resin all over the fibers. After finishing

the wet layup, it was preheated for 15 minutes at 200℃ and then vacuum bagged and connected with a vacuum valve. The vacuum pump was connected to the valve and maintained 27 in-Hg of pressure while keeping it inside the oven. A minimum of 2 hours of oven curing was done at 200℃. After oven curing, the finally cured composite was kept for post-curing for another 2 hours. Figure 2 shows the process of wet lay-up.

Wet-layup of fibers **Vacuum Bagging** **Oven Curing** **Cured composite.**

Figure 2. Wet-layup process for SPEEK composite fabrications.

2.3. Characterizations

To determine the properties of the prepared SPEEK composites, different tests were conducted for the characterization of the samples using different tests, including UL 94V, water contact angle, SEM, tensile testing, and smoke tests.

3. Results and Discussion

3.1. UL 94 Vertical Test

Five sets of Fiberglass and Kevlar fiber SPEEK composite samples are conducted for the UL 94 test. The setup for UL 94 is the vertical one. Each test sample is burnt for 10 seconds. The initial flame time is recorded, and the sample is diminishing the flame, the sample is burnt for another 10 seconds and observed the second flame time. For both flaming no burning or dripping of samples are observed for all the test samples of both Fiberglass and Kevlar composites. The results indicate that the SPEEK composites passed the UL 94V test with V-0, V-1, and V-2 ratings.

3.2. Water Contact Angle Test

The water contact angle test is conducted using a contact angle Goniometer tester. A total of five tests are performed on different surfaces of different samples. A needle is used to drop the water on the surface of the measurement surface. Three data with intervals of 100ms are recorded and the mean contact angle is calculated accordingly. The contact angle measured for Fiberglass SPEEK composites is found to be 93.76 degrees and for Kevlar 102.24 degrees on average. The contact angle range shows the surface of the SPEEK composites to be hydrophobic in nature (Figure 3).

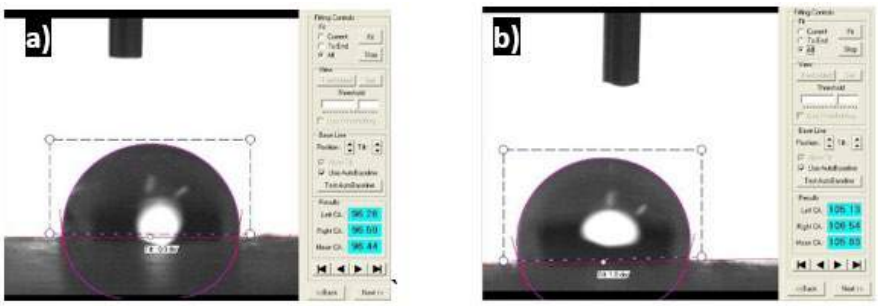

Figure 3. The water contact angle values of a) fiberglass SPEEK and b) Kevlar SPEEK composites.

3.3. FTIR Spectroscopy Analysis

For understanding the presence of different functional groups in PEEK, SPEEK polymer, and its composites, FTIR spectroscopy tests are conducted (Figure 4). All the analysis was performed using Nicolet iS50 FTIR spectroscopy and the wave spectrum is captured. The peak spectrum of PEEK polymer obtained at 1486.39cm-1 is the presence of C-C aromatic ring structure i.e., benzene rings in the polymer [13]. The peaks from 965.12 to 622.72 cm-1 corresponded to C-H out-of-the-plane vibrations. Also, sharp peaks from 1306.03 to 1009.92 cm-1 might be C-H in-plane bend vibrations. Several peaks from 1646.63 to 1411.34 cm-1 were observed and that indicated the presence of ether and ketones functional groups. The peak spectra at 3064.83 cm-1 suggested the presence of C-H stretch vibrations. The presence of a peak value of 3361.37 cm-1 of the wide band indicated the presence of alcohol group (O-H) from the (SO3-) sulfonic acid group interacting with water [13]. The peak value of 1646.20 cm-1 indicated the presence of asymmetric stretching (-C=O) band which showed the presence of ketones in the chemical structure of SPEEK. The peak value of 1216.39 cm-1 indicated the presence of the C-O functional group. The carbonyl group intensity for PEEK and SPEEK showed no changes at 1646 cm-1 bandwidth. Similarly, after the FTIR test on Kevlar SPEEK composites, the highest peak values of 3365.97 cm-1, 1647.53 cm-1, and 1216.44 cm-1 were obtained. The highest peak of 3372.95 cm-1 in the region of the wide band indicated the presence of the O-H functional representing the sulfonic group.

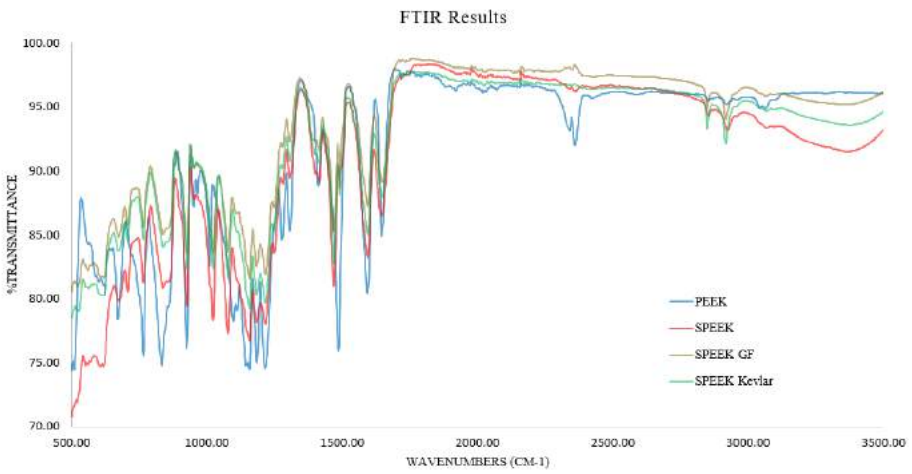

Figure 4. FTIR test results of PEEK, SPEEK, SPEEK with GF, and SPEEK with Kevlar fibers.

3.4. SEM Analysis

The surface morphology of the composites is examined using a Scanning Electron Microscope (SEM) unit. The SEM images of the SPEEK glass fiber composite are indicated as a, b, and c, and the Kevlar composite images are indicated as c, d, and e in Figure 5. The images of strands of fiber show the enrichment of the SPEEK polymer matrix on the composite surface. As the magnification of the image increases, it displays the resin embedment inside the fiber strand and confirms that the SPEEK resin is well-wetted all over the composite. The topology of the surface of the Kevlar fibers depicts the damage to the fiber which is the result of the machining of the composites. All images show the presence of less

resin in between the fibers which well-concludes the fiber delamination during sample preparation via waterjet cutting.

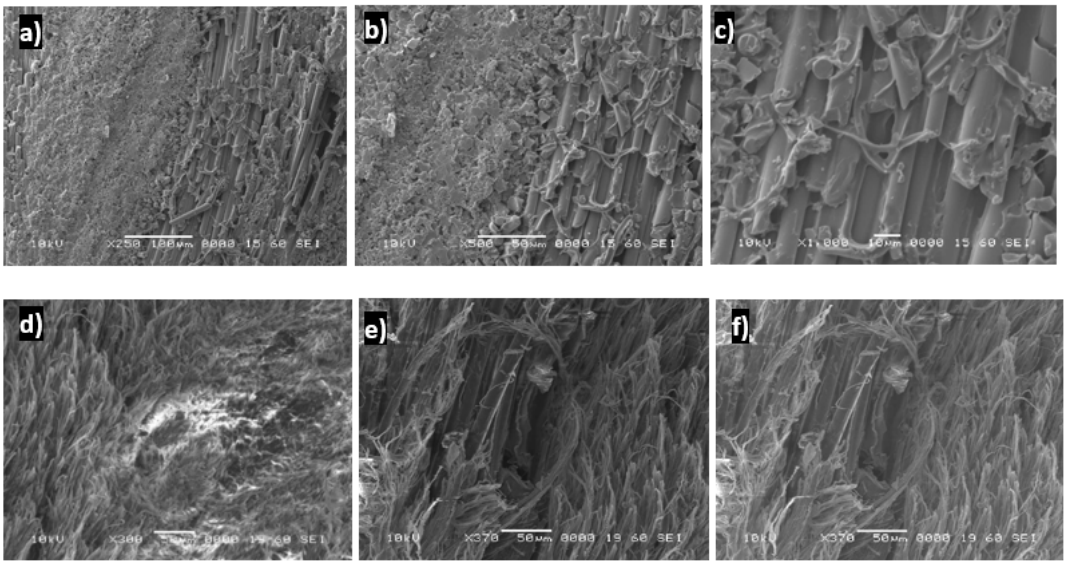

Figure 5. SEM test images of SPEEK GF composites (a, b, c) and Kevlar composites (d, e, f).

3.5. Tensile Test Analysis

Load vs extension results of GF SPEEK and Kevlar SPEEK composites are given in Tables 1 and 2. All five samples showed linear and similar results. The load is applied to the samples until they break without any stretching. Sample 2 withstood a maximum load of 17229.9 N with 0.7 mm of extension. SPEEK glass fiber composites showed a maximum extension of 10.62 mm at 14591.68 N of load by sample 1. The load vs extension data concluded that the SPEEK composites averaged a maximum load of 15879.158 N and 9.18 mm. All three samples showed linear deflection concerning load until the failure of the sample. From the load vs deflection results, sample 2 withstood 36451.37 N of load with 10.45 mm deflection however the maximum deflection exerted was by sample 3 with 10.69 mm against the load of 35728.64 N.

Sample	Load (N)	Extension (mm)
1	14591.68	10.62
2	17229.9	9.07
3	16099.18	8.38
4	15274.39	9.068
5	16200.64	8.74

Table 1. Maximum load vs extension of GF SPEEK composites

Sample	Load (N)	Extension (mm)
1	35303.88	8.51
2	36451.37	10.45
3	35728.64	10.69

Table 2. Maximum load vs extension of Kevlar SPEEK composites.

3.6. Smoke Test Analysis

Three samples of 3x3 inches glass fiber SPEEK composites are prepared only for the smoke density and toxicity test. All samples are burnt for 4 minutes inside the smoke density chamber. Before and after burning the weight of the samples is taken. The temperature, pressure, and vacuum condition inside the chamber are kept constant. Light transmittance vs time through the smoke inside the chamber is recorded and displayed in the graph shown in Figure 6a. All three tested samples show consistent results on light transmittance. Sample 2 has maximum light obscurity during the test with 75% of the light only transmitted and captured by the photosensor at its highest.

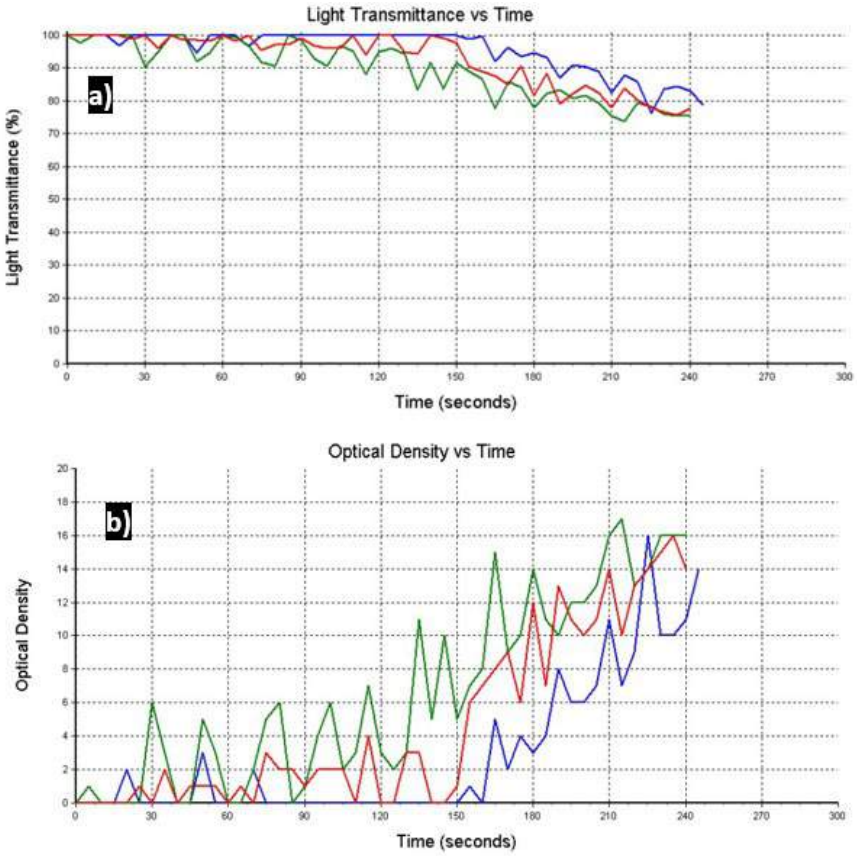

Figure 6. Smoke test results of the glass fiber SPEEK composites: a) light transmittance vs time, and b) optical density vs time.

Specific optical density is obtained for each material to evaluate the time of maximum smoke obscuration. The optical density vs time is shown in Figure 6b. Sample 2 with green color has maximum optical density as compared to the other two samples. The maximum optical density and light transmittance over 4 minutes is shown in Table 3. The total sample burnt during the test is calculated and shown in Table 3.

Sample	Optical Density Max.	Light Transmittance (%)	Weight loss after burning (gm)
1 (Blue)	16	83	2.2435
2 (Green)	17	75	1.5865

3 (Red)	16	78	2.1389

Table 3. Smoke density test results of the glass fiber SPEEK composites.

4. Conclusions

The research study indicated the use of SPEEK polymer in polymeric composite applications as a matrix has several characteristics that would be beneficial over other polymer matrices. SPEEK obtained from PEEK and sulfuric acid sulfonation was found to be soluble with DMF solvent and dissolved easily which helped make the composite materials much better. The composite panels were prepared via vacuum bagging and came out in good shape and condition. The flame-retardant UL 94 vertical test showed that the SPEEK composites are highly flame-retardant with V-0, V-1, and V-2 ratings. The water contact angle test performed on the smooth surface of the composites resulted in the hydrophobic nature of the composites. The scanning electron microscope test displayed the surface morphology of the composites in microstructural view which helped to understand the wettability of resin in between the fibers. Glass fiber composites had more resin in between the fibers than the Kevlar fiber composites. Also, fibers were dispersed and damaged because of the machining of high-strength Kevlar fibers. More tests on mechanical tensile tests indicated the samples have high properties of strength and modulus. Smoke density tests resulted in various gases and helped analyze the harmfulness to human life. This study can open new opportunities to use the SPEEK composite in various industries.

5. Acknowledgments

The authors greatly acknowledge Wichita State University and Turkish Aerospace Industries for the financial and technical support of the present study.

6. References

[1] Kesarwani, S. (2017). Polymer Composites in Aviation Sector. International Journal of Engineering Research, 6.

[2] Deo, R.B., Starnes, J.H., & Holzwarth, R.C. (2003). Low-Cost Composite Materials and Structures for Aircraft Applications.

[3] Skirbutis, G., Dzingutė, A., Masiliūnaitė, V., Šulcaitė, G., & Žilinskas, J. (2017). A review of PEEK polymer's properties and its use in prosthodontics. Stomatologija, 19(1), 19–23.

[4] Gurung, D. “Sulfonated PEEK Fiber Reinforced Composites for Increased Thermal and Mechanical Properties,” M.S. Thesis, Wichita State University, April 27, 2023.

[5] Chon, J. W., Yang, X., Lee, S. M., Kim, Y. J., Jeon, I. S., Jho, J. Y., & Chung, D. J. (2019). Novel PEEK Copolymer Synthesis and Biosafety - I: Cytotoxicity Evaluation for Clinical Application. Polymers, 11(11), 1803. https://doi.org/10.3390/polym11111803.

[6] The history of Plastics part I: 1856 through 1935. Advanced Plastiform. https://advancedplastiform.com/the-history-of-plastics-one/.

[7] Kaliaguine, S.D Mikhailenko, Wang, K.P., Xing, P., Robertson, G., Guiver, M. (203) Properties of SPEEK based PEMs for fuel cell application. Catalysis Today, Volume 82, Issues 1–4, Pages 213-222, ISSN 0920-5861. https://doi.org/10.1016/S0920-5861(03)00235-9.

[8] Othman, M. H., Ismail, A., Mustafa, A. B. (2007). Physico-chemical study of sulfonated poly(ether ether ketone) membranes for direct methanol fuel cell application. Malaysian Polym. J.. 2.

[9] Huang, R.Y.M., Shao, P., Burns, C.M. and Feng, X. (2001), Sulfonation of poly(ether ether ketone)(PEEK): Kinetic study and characterization. J. Appl. Polym. Sci., 82: 2651-2660. https://doi-org.proxy.wichita.edu/10.1002/app.2118.

[10] Yee, Rebecca & Zhang, Kaisong & Ladewig, Bradley. (2013). The Effects of Sulfonated Poly (ether ether ketone) Ion Exchange Preparation Conditions on Membrane Properties. Membranes. 3. 182-195. 10.3390/membranes3030182.

[11] Xue, S., Yin, G. (2006). Methanol permeability in sulfonated poly(etheretherketone) membranes: A comparison with Nafion membranes,European Polymer Journal, Volume 42, Issue 4, Pages 776-785, ISSN 0014-3057. https://doi.org/10.1016/j.eurpolymj.2005.10.008

[12] Lee, C., Seong, M. J., Choi, J., Baek, K., Yen, B. T., Kyratzis, I. L., & Yong-Gun Shul. (2013). SiO2/sulfonated poly ether ether ketone (SPEEK) composite nanofiber mat supported proton exchange membranes for fuel cells. Journal of Materials Science, 48(10), 3665-3671. doi:https://doi.org/10.1007/s10853-013-7162-7.

[13] Su, Y., Liu, P., Jing, D., Zhang, X., Zhang, S., J Appl Polym Sci 2021, 138(45), e51326. https://doi-org.proxy.wichita.edu/10.1002/app.51326.

[14] Gul, S., Arican, S., Cansever, M., Beylergil, B., Yildiz, M., and Okan, B.S.(2023). Design of Highly Thermally Conductive Hexagonal Boron Nitride-Reinforced PEEK Composites with Tailored Heat Conduction Through-Plane and Rheological Behaviors by a Scalable Extrusion. ACS Applied Polymer Materials, 329-341. DOI: 10.1021/acsapm.2c01534.

[15] Occupational Safety and Health Administration. https://www.osha.gov/chemicaldatabase.

[16] Mahat, K. B., Alarifi, I. M., Alharbi, A., and Asmatulu, R. “Effects of UV Light on Mechanical Properties of Carbon Fiber Reinforced PPS Thermoplastic Composites,” Macromolecular Symposia, Vol. 365, pp. 157-168, 2016.

[17] Dhanasekaran, P.S., Uddin, M.N., Wooley, P., and Asmatulu, R. “Fabrication and Biological Analysis of Highly Porous PEEK Bionanocomposites Incorporated with Carbon and Hydroxyapatite Nanoparticles for Biological Applications,” Molecules, Vol., 25, pp. 3572-3584, 2020.

[18] Brauning, K.A., Kunza, A., Alarifi, I.M., and Asmatulu, R. “Mitigations of Machine-Damaged Free-Edge Effects on Fiber-Reinforced Composites,” Journal of Composite Materials, Vol. 55, pp. 1621-1633, 2021.

[19] Shagor, R.M.R., Abedin, F. and Asmatulu, R. “Mechanical and Thermal Properties of Carbon Fiber Reinforced Composite with Silanized Graphene as Nano-inclusions,” Journal of Composite Materials, Vol. 55, pp. 597-608, 2021.

[20] Khadak, A., Subeshan, B., and Asmatulu, R. “Studies on De-Icing and Anti-Icing of Carbon Fiber-Reinforced Composites for Aircraft Surfaces using Commercial Multifunctional Permanent Superhydrophobic Coatings,” Journal of Materials Science, Vol. 56, pp. 3078-3094, 2021.

[21] Asmatulu, R., Bollavaram, P.K., Patlolla, V.R., Alarifi, I.M., and Khan, W.S. “Investigating the Effects of Metallic Submicron and Nanofilms on Fiber-Reinforced Composites for Lightning Strike Protection and EMI Shielding,” Advanced Composites and Hybrid Materials, Vol. 3, pp. 66-83, 2020.

Aircraft Interior Noise Reduction through Flame-Retardant Polymeric Porous Nanocomposite Materials

Arifa Kunza[1]
Ramazan Asmatulu[1]
[1]*Department of Mechanical Engineering*
Wichita State University, 1845 Fairmount Street, Wichita, KS 67260, USA
fxkunzaarifa@shockers.wichita.edu; ramazan.asmatulu@wichita.edu

Abstract

This study investigates the high melting temperature polymers of polyether ether ketone (PEEK) and polyaryletherketone (PAEK) incorporated with carbon and ceramic nanoparticles (graphene, multiwall carbon nanotubes, carbon black, TiO2, SiO2) for the reduction of aircraft interior noise. These materials are applicable to form porous nanocomposite structures, which are new in research with lighter weights and are suitable, especially in aircraft and other space applications. The materials' properties were characterized using scanning electron microscopy (SEM), confocal laser microscope, differential scanning calorimeter (DSC), thermogravimetric analysis (TGA), FIJI software, and noise absorption and transmission loss units. The testing parameters and variables of these porous materials could supply reliable experimental validation via special characteristics, surface morphology, and geometric microstructural analysis. The test results indicated that these porous nanocomposite materials have extraordinary physical and chemical properties and would have great potential to use in aircraft interior noise reductions and similar other sound absorption purposes.

Keywords: Nanoparticles, Porous Polymeric Composites, Sound Absorption, Mechanical Properties.

1. Introduction

Aromatic polymers, PEEK and PAEK, are specially selected because of their thermal stability, strength, durability, voltage stress, elevated temperature capability, dielectric property, and permittivity [1]. Certain compounds with particles, such as ceramic (TiO_2 and SiO_2) of various concentrations (10 wt.%, 20wt. %, and 50wt.%) [2] change the polymer chain when dispersed, thus providing stronger interaction internally, high energy density, dielectric permittivity [3] and soundproofing and absorption capability and also have the tendency to absorb visible light [4]. These inclusions enhance noise absorption [5], shielding properties, and wave-sensing abilities for electrical and electronic applications [6,7]. The high nanofiller percentages can affect sound absorption properties based on the stiffness values. Tsagaropolous et al. reported the test results of the low and high ceramic nanofillers with different sizes and shapes and stated the reduced permittivity at all frequencies, especially with TiO_2 particles in composites [3]. Figure 1 shows the conventional noise abruption materials currently used by industry [2].

Submitted: August 21, 2023
Revised: November 22, 2023

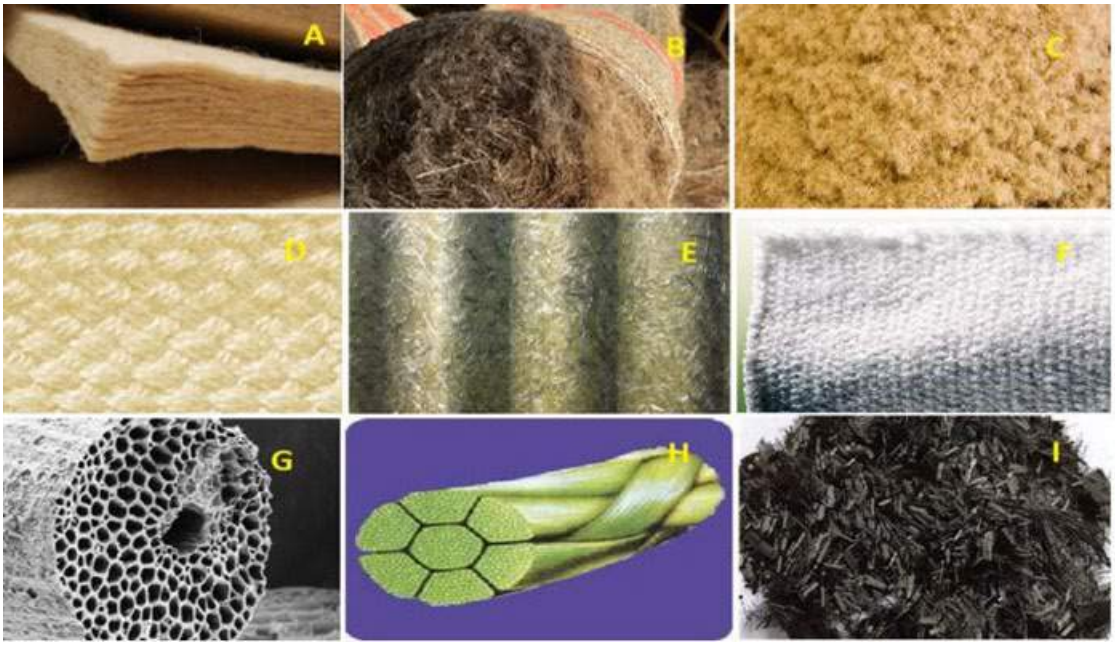

Figure 1: Images showing the various conventional noise abruption materials currently used by industry [2].

Carbon materials and other nanofillers in polymer help absorb and dissipate electromagnetic and sound waves by converting them into thermal (heat) energy. Carbon fillers also improve other properties such as thermal conductivity and stability, good electrical conductivity, energy dissipation, excellent processability, high strength, stiffness, and weights based on nanoparticle selections and concentrations in the composites. A proper quantity of nanofillers enhances surfaces and modifies functionality, reduces aspect ratio, provides alignment based on arrangement and dissipation of particles in other material compounds {multiwall carbon nanotubes (MWCNTs), graphene, carbon black} [8,9]. Recent applications of viscoelastic damping materials for noise control in automobiles and commercial airplanes greatly reduce the transmission loss [10-12].

The present study incorporated PEEK and PAEK powders with salt particles and some other inclusions and cast in cylindrical cups in a furnace. After removing the salt particles via the salt leaching process, the porous nanomaterials were received for sound absorption purposes.

2. Experiment

2.1. Materials

Aromatic high melting temperature polymer powders (PEEK, and PAEK), dimethylformamide (DMF), sulfuric and nitric acids (2:4, 3:6, 4:8, and 5:10): H_2SO_4/HNO_3, sea salt particles, epoxy resin (Epon Resin 828), ceramic nanoparticle (TiO_2 and SiO_2), allotropes of carbon such as multi-walled carbon nanotubes (MWCNTs) and graphene were purchased from Amazon and used without any modifications. Table 1 provides the selected materials and their conditions.

Polymer Nanoparticle	Solvent (liq)	Acids Ratio	Binder	NaCl Nanoparticles
PEEK	DMF	H_2SO_4/HNO_3	Epoxy & Liquid Resin	Sea Salt
4wt.%	5ml	2:4, 3:6, 4:8, 5:10	828 viscous	8wt.%
Ceramic Nanoparticles		Carbon Nanoparticles		
TiO_2	SiO_2	MWCNT	Graphene	Carbon Black
2wt.%	2wt.%	0.05wt.%,0.5wt. %,1.5wt.%	0.05wt.%,0.5wt. %,1.5wt.%	0.05wt.%,0.5wt. %, 1.5wt.%

Table 1. Contents of the composite samples with or without acids (H_2SO_4/HNO_3) treatments for the porous nanocomposite fabrications.

2.2. Methods

2.2.1. Step 1: Composite Powder Preparation

When polymers are nonconductive, carbon particles are added to achieve rapid heat transfer or dissipation of heat properties. The carbon particles can include MWCNT, graphene, and carbon black nanofillers which also have high electrical conductivity. These carbon fillers cannot be dissolved in water but can be dispersed easily in acids (H_2SO_4 and HNO_3), where the process increases the electrical and thermal conductivity within the composite structures and enhances the noise absorption coefficient. It also depends on frequencies, thickness, and surface morphologies. In these studies, these fillers were used at different concentrations (2:4, 3:6, 4:8, and 5:10) to improve the conductivity and stiffness values. Figure 2 shows the step-by-step dispersion and fabrication procedures.

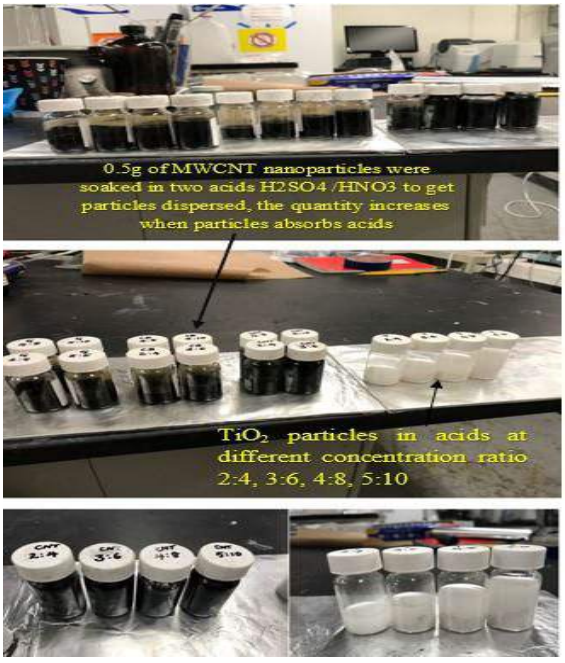

Figure 2. The preparation steps include various inclusions and dispersion in acidic (H_2SO_4/HNO_3) solution to form porous particulate composites.

2.2.2. Step 2: Nanocomposite Preparation

In the second step, carbon nanoparticles (0.5wt%, 0.05 wt.%, 1.5 wt.%) were dispersed in acids for a week to get particles completely soaked in an acidic solution (1:2 ratios of H_2SO_4/HNO_3). The soaked acidic mixture was mixed with other material compounds, such as polymers, sea salt, and ceramic nanoparticles, to form a viscous mixture solvent. Also, DMF solvent and epoxy resin 828 were used to create pore structures in the nanocomposites.

2.2.3. Step 3: Salt Leaching

The sea salt particles in the nanocomposite structures were dissolved in the hot DI water to create porous structures. In this study, the FIJI software was used to determine the level of the porosity of the nanocomposite materials.

2.3. Characterizations

To determine the properties of the prepared porous nanocomposite materials, several different characterization techniques were used. The characterization techniques include scanning electron microscopy (SEM), confocal laser microscope, differential scanning calorimeter (DSC), thermogravimetric analysis (TGA), FIJI software, and noise absorption and transmission losses.

3. Results and Discussion

3.1. 3.1 Nanocomposite Porosity Analysis

The microstructural images of the composites were captured using a laser confocal microscope for normal and acidic dispersed nanoparticles in the nanocomposites. The porosity percentages and shrinking of the pores were noticed with and without acidic composite samples. Figure 3 shows the porosity structures of the prepared nanocomposite materials obtained using the laser confocal microscope. The FIJI software also indicated the porose structure formations in the nanocomposite materials. The test results show that the prepared nanocomposites are highly porous (30-60%) and can be used for aircraft interior noise reductions.

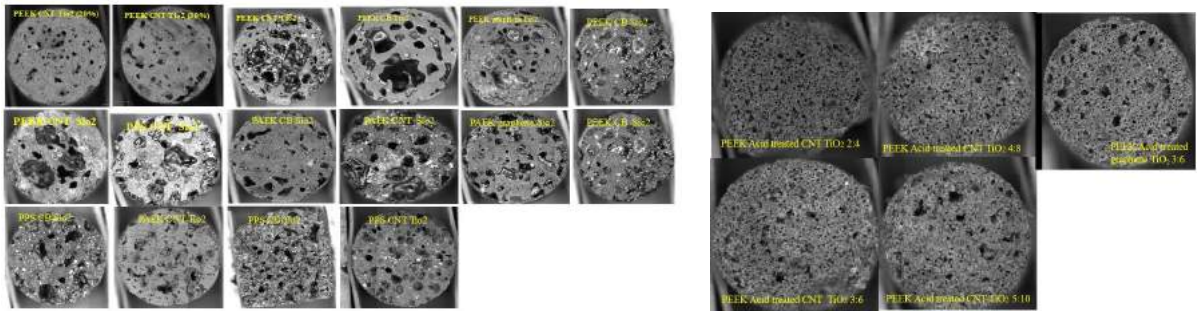

a) b)

Figure 3. (a) Microstructural images of laser confocal microscope showing pores and voids formed on the nanocomposites of different pore shapes and sizes captured during surface analysis and (b) microstructural images of acid (H_2SO_4/HNO_3) treated composites specifying different acid ratios (2:4, 3:6, 4:8, and 5:10).

3.2. SEM Analysis

The aromatic polymers were used in this research to increase the noise absorption rate with low transmission losses and high flame retardancy. Figure 4 shows the SEM images of the porous nanocomposite materials with various morphologies. During the dispersion of particles, the bonds between each particle were packed tightly due to filler concentrations and surface interactions. When ceramic particles are dispersed in polymers as they closely form strong bonds, polymer-particle structures, and dispersions were noticed during SEM imaging. When carbon nanoparticles are dispersed in ceramic and polymer particles, this will have higher heat dissipation and heat flow within the particle bonds. This lowers the frequency during noise tests, which is beneficial for noise absorption in polymer composites.

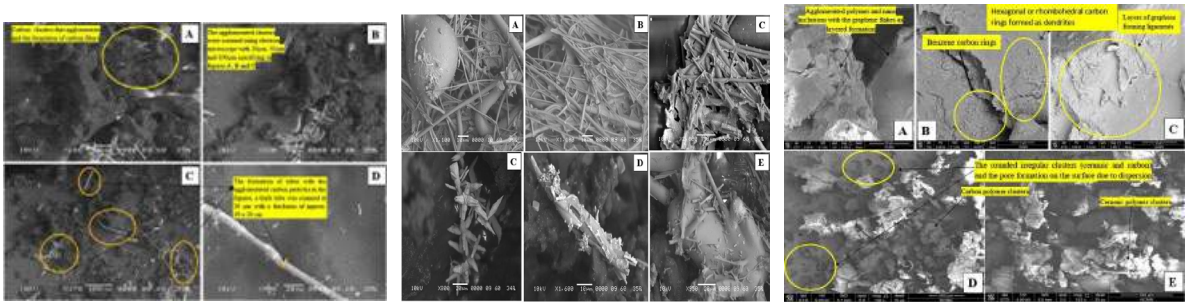

a) b) c)

Figure 4. The SEM images of (a) PEEK with TiO_2 and carbon blacks, (b) PEEK with TiO_2 and MWCNT, and (c) PEEK with TiO_2 and graphene inclusions.

The density of nanofillers is of great interest to study as the particles in composites interact with the waves and cause wave/mechanical losses which convert transmitted waves of mechanical energy into heat energy through sound attenuation. Dispersion of nanoparticles in the polymer matrix is necessary to avoid clusters and agglomeration that can affect wave propagation, surface density, surface misalignment, stiffness, strength, porosity, and dielectric permittivity values. The new studies investigated filler density and concentration percentages to test the variation in transmission losses as wave transmission increases through filler materials. This situation is also based on the particle's density over high and low-frequency ranges [13].

3.3. Sound Absorption and Transmission Losses

Studying sound absorption and transmission losses, analyzing the noise waves in polymeric nanocomposites through testing and modeling, and providing theoretical study with experimental data must be clearly understood to characterize the noise absorption coefficient values of the materials. Since sound absorption and transmission loss in polymeric nanoparticle composites are critical, properties of the materials with different geometries and structures need to be analyzed based on resonance and wave functions. Figure 5 shows the impedance results for the noise absorption coefficients of the porous nanocomposites at different frequencies. As can be seen, adding inclusions into the composite structures drastically changes the noise absorption coefficients and transmission losses [14-16].

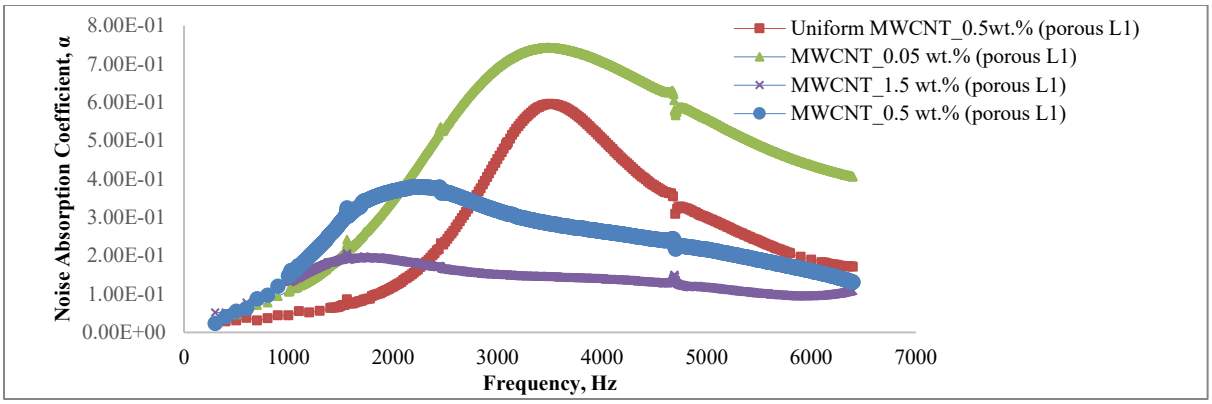
Noise Absorption Coefficient, α
8.00E-01
7.00E-01
6.00E-01
5.00E-01
4.00E-01
3.00E-01
2.00E-01
1.00E-01
0.00E+00
0
1000
2000
3000
4000
5000
6000
7000
Frequency, Hz
Uniform MWCNT_0.5wt.% (porous L1)
MWCNT_0.05 wt.% (porous L1)
MWCNT_1.5 wt.% (porous L1)
MWCNT_0.5 wt.% (porous L1)

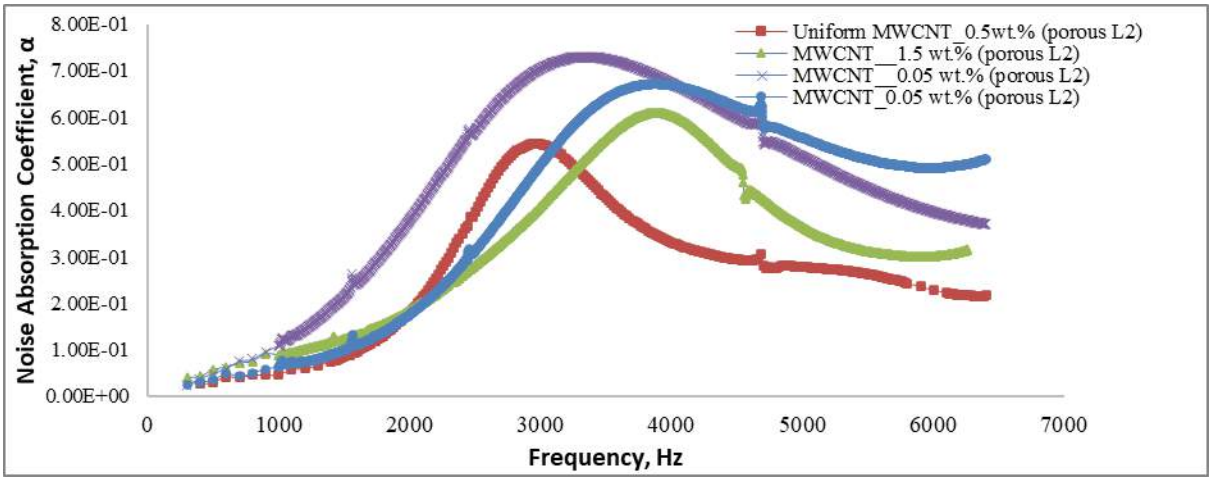
Noise Absorption Coefficient, α
8.00E-01
7.00E-01
6.00E-01
5.00E-01
4.00E-01
3.00E-01
2.00E-01
1.00E-01
0.00E+00
0
1000
2000
3000
4000
5000
6000
7000
Frequency, Hz
Uniform MWCNT_0.5wt.% (porous L2)
MWCNT__1.5 wt.% (porous L2)
MWCNT__0.05 wt.% (porous L2)
MWCNT_0.05 wt.% (porous L2)

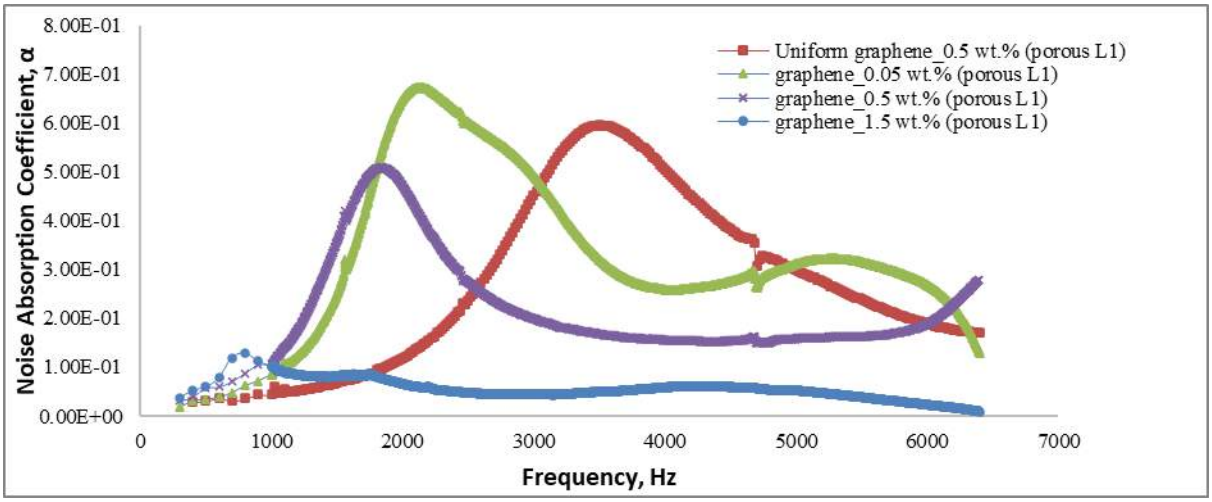
Noise Absorption Coefficient, α
8.00E-01
7.00E-01
6.00E-01
5.00E-01
4.00E-01
3.00E-01
2.00E-01
1.00E-01
0.00E+00
0
1000
2000
3000
4000
5000
6000
7000
Frequency, Hz
Uniform graphene_0.5 wt.% (porous L1)
graphene_0.05 wt.% (porous L1)
graphene_0.5 wt.% (porous L1)
graphene_1.5 wt.% (porous L1)

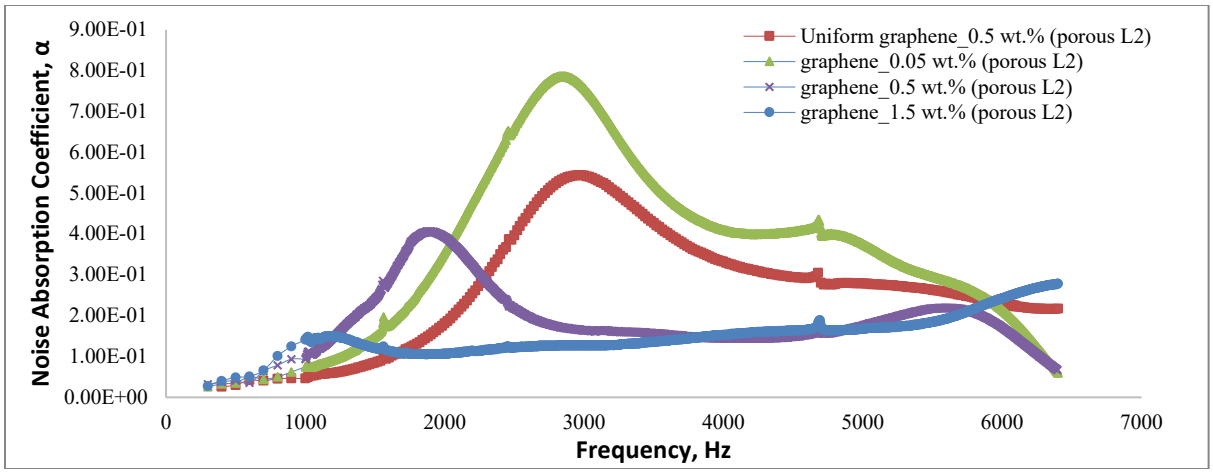

Figure 5. Images showing the noise absorption coefficients of the porous nanocomposite structures at different frequencies significantly affect the transmission losses.

3.4. DSC and TGA Analysis

The temperature variations of the polymeric structures in DSC and TGA results in the formations of the graphical representations for the thermal analysis. The formed curves are denoted as upper Ti and lower Tf. The convex and concave shapes in a TGA graph indicate the change in weight percentages as a function of the temperature. During the heating of the nanocomposite structures, the epoxy resin, volatility, and moisture evaporate and leave the structures, and the remaining unburnt materials (or oxidized substances). The TGA tests showed that up to 80wt% of the materials left the system during the burning. In the DSC analysis, exothermic and endothermic heat flows provide the important glass transition (Tg), crystallization temperature (Tc), and melting temperature (Tm) values. The test results confirmed that these Tg, Tc and Tm values of the polymeric structures were slightly changed by adding different inclusions in the polymers. Various other nanocomposite studies also confirmed that adding nanoscale inclusions in polymeric structures considerably changes many thermal, electrical, and mechanical properties of those polymeric materials [16-21].

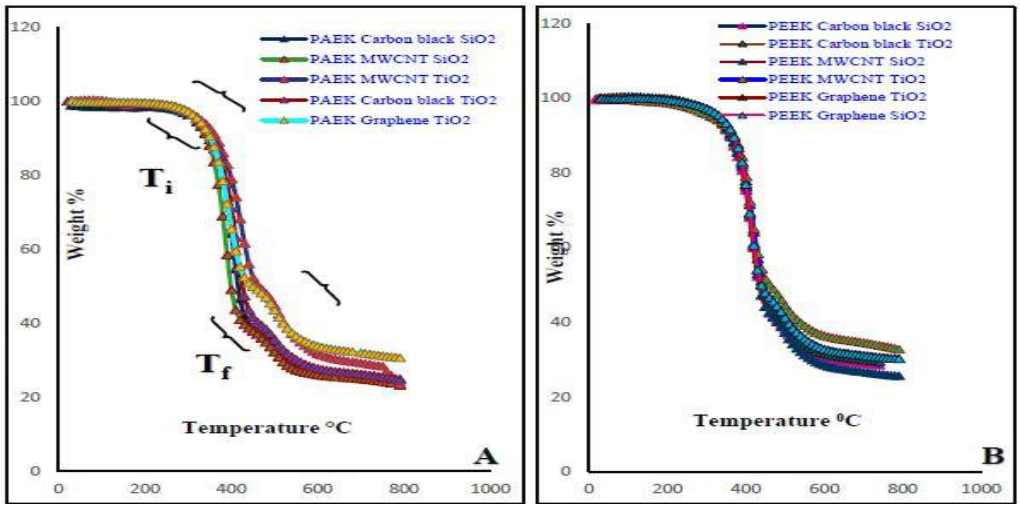

a)

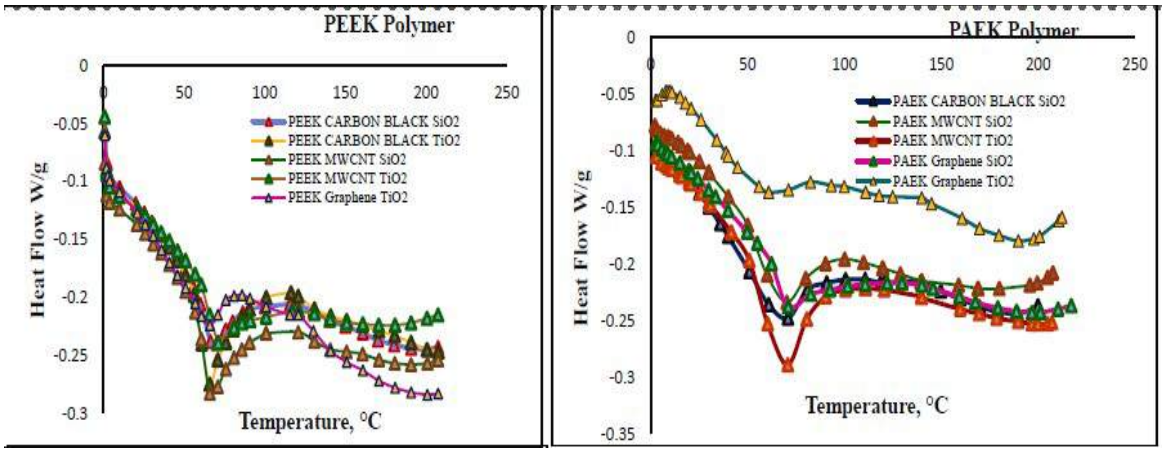

b)

Figure 6. The graphical representations of a) TGA and b) DCS of PEEK and PAEK nanocomposites with different carbon nanofillers and ceramic nanoparticles (TiO_2 and SiO_2) concentrations.

4. Conclusions

Polymeric nanocomposites were fabricated and tested for the sound absorption of the aircraft interior noise. Prepared nanomaterials were characterized using various techniques, including confocal laser microscope, SEM, TGA, DSC, FIJI software, and noise absorption and transmission loss units. The laser confocal microscopy and SEM studies indicated the well orders of inclusions and porous structures into the nanocomposites. The FIJI software provided detailed information about the porosity values. The TGA and DSC studies confirmed the organic and inorganic parts of the nanocomposites and their Tg, Tc, and Tm values. The noise absorption and transmission loss studies showed that adding inclusions and porous structures drastically affects the sound absorption capabilities of the nanocomposite structures with appropriate transmission losses. This study reveals that the prepared-purpose nanocomposite materials can be used in the noise reduction of aircraft and other transportation and defense systems.

5. References

[1] Guo, Q., Xue, Q., Sun, J., Dong, M., Xia, F., & Zhang, Z. (2015). Gigantic enhancement in the dielectric properties of polymer-based composites using core/shell MWCNT/amorphous carbon nanohybrids, *Nanoscale*, 7(8), 3660–3667.

[2] Cao, L., Fu, Q., Si, Y., Ding, B., & Yu, J. (2018). Porous materials for sound absorption. *Composites Communications*, 10, 25–35.

[3] G. Tsagaparopoulos, A., Eisenberg. (1995). Dynamic mechanical study of the factors affecting the two-glass transition behavior of filled polymers: Similarities and differences with random ionomers. *Macromolecules*, 28, 6067–6077.

[4] Hu, P., Jia, Z., Shen, Z., Wang, P., & Liu, X. (2018). High dielectric constant and energy density induced by the tunable TiO 2 interfacial buffer layer in PVDF nanocomposite contained with core–shell structured TiO2 @BaTiO3 nanoparticles. *Applied Surface Science*, 441, 824–831.

[5] Osorio-Vargas, P. A., Pulgarin, C., Sienkiewicz, A., Pizzio, L. R., Blanco, M. N., Torres-Palma, R. A., Rengifo-Herrera, J. A. (2012). Low-frequency ultrasound induces oxygen vacan-cies formation and visible light absorption in TiO_2 P-25 nanoparticles. *Ultrasonics Sonochemistry*, 19(3), 383–386.

[6] Choi, H. C., Jung, Y. M., & Kim, S. B. (2005). Size effects in the Raman spectra of TiO2 nanoparticles. *Vibrational Spectroscopy*, 37(1), 33–38.

[7] Tang, Y., Ao, D., Li, W., Zu, X., Li, S., & Fu, Y. Q. (2018). NH 3 sensing property and mechanisms of quartz surface acoustic wave sensors deposited with SiO2, TiO 2, and SiO 2 -TiO2 composite films. *Sensors and Actuators B: Chemical*, 254, 1165–1173.

[8] Breuer, O., & Sundararaj, U. (2004). Big returns from small fibers: A review of polymer/carbon nanotube composites. *Polymer Composites*, 25(6), 630–645.

[9] Nieto, A., Bisht, A., Lahiri, D., Zhang, C., & Agarwal, A. (2016). Graphene reinforced metal and ceramic matrix composites: a review. *International Materials Reviews*, 62(5), 241–302

[10] Rao, M. (2003). Recent applications of viscoelastic damping for noise control in automobiles and commercial airplanes. *Journal of Sound and Vibration*, 262(3), 457–474

[11] T. Tanigawa, E. Mizushima, M. Shimada, K. Morita, M. Kakitani and S. Takanezawa. (2018). Low Transmission Loss Film Material for High-Speed High-Frequency Devices. 2018 IEEE 68th Electronic Components and Technology Conference (ECTC), pp. 1757-1761.

[12] Li, X., Yu, K., Zhao, R., Han, J., & Song, H. (2018). Sound transmission loss of composite and sandwich panels in a thermal environment. *Composites Part B: Engineering*, 133, 1–14.

[13] Ahmadi, Saeid, Parvin Nassiri, Ismaeil Ghasemi, and Mohamma Reza Monazzam Esmaeilpoor. (2015). Sound transmission loss through nanoclay-reinforced polymers." *Iranian Polymer Journal,* 24, 641-649.

[14] Hedayati, A. Arefazar (2009). Effects of Filler Characteristics on the Acoustic Absorption of EPDM-based Highly Filled Particulate Composite. *Journal of Reinforced Plastics and Composites*, 28 (18), 2241-2249.

[15] Allan, P.S., Ahmadnia, A., Withnall, R. and Silver, J. (2012). Sound transmission testing of polymer compounds. *Polymer Testing*, 31(2),312-321.

[16] Khan, W.S., Asmatulu, R., and Yildirim, M.B. (2012). Acoustical Properties of Electrospun Fibers for Aircraft Interior Noise Reduction. *Journal of Aerospace Engineering*, 25, No. 3, pp. 376-382.

[17] Chillakuru, T.R., Khan, W.S., Uddin, M.N., Alarifi, I.M., and Asmatulu, R. (2021). Study on Epoxy Nanocomposites Viscoelastic Properties through Dynamic Shear Rheological Analysis Method. *Academic Journal of Polymer Science,* 5(2),1-10.

[18] Dhanasekaran, P.S., Uddin, M.N., Wooley, P., and Asmatulu, R. (2020). Fabrication and Biological Analysis of Highly Porous PEEK Bionanocomposites Incorporated with Carbon and Hydroxyapatite Nanoparticles for Biological Applications. *Molecules*, 25, 3572-3584.

[19] Soltani, S., Razinobakht, S.A., and Asmatulu, R. (2020). Effects of Carbon Black Silanization on Isothermal Curing Kinetics of Epoxy Nanocomposites," *Journal of Applied Polymer Science*, e49106,1-13.

[20] Swarna, V.S., Alarifi, I.M., Khan, W.A., and Asmatulu, R. (2019). Enhancing Fire and Mechanical Strengths of Epoxy Nanocomposites for Metal/Metal Bonding of Aircraft Aluminum Alloys. *Polymer Composites*, 40, 3691-3702.

[21] Ghazinezami, A., Khan, W. S., Jabbarnia, A., and Asmatulu, R. (2017). Impacts of Nanoscale Inclusions on Fire Retardancy, Thermal Stability, and Mechanical Properties of Polymeric PVC Nanocomposites. *Journal of Thermal Engineering*, 3, 1308-1318.

WE'D LIKE TO THANK OUR SPONSORS

BECOME A SPONSOR.
CONTACT US.

INFO@IEMSCONFERENCE.COM

INDUSTRY ENGINEERING & MANAGEMENT SYSTEMS CONFERENCE

IEMS 2023

THE 29TH CONFERENCE

WICHITA STATE UNIVERSITY

College of Engineering

Since 1928, Wichita State's College of Engineering has built a reputation for equipping engineering and computing students with the most complete education possible. Shocker engineering boasts hands-on research using the latest technology, Kansas' center of industry, applied learning and professional connections.

ASQ

Committed to providing enhanced expertise, professional networks, tools, and solutions to help our members advance their products, services, and industries.

TOOLINGU | sme

With nearly 90 years of experience, Tooling U-SME partners with educators, workforce organizations and the manufacturing industry to build capacity, and to provide training and development workforce education solutions that will help narrow the skills gap within manufacturing communities.

SHUTTLE AEROSPACE

We specialize in manufacturing of parts and assemblies for the Aerospace Industry. Shuttle Aerospace is specialized in metallic and non-metallic machined components: heat treatment, surface finishing, and welding.

CYBERTRON PC

Cybertron PC debuts the new CLX brand: the Cybertron Luxury Experience. After 19 years of PC building and custom requests, CLX was created for the discerning gamers who demand the best.